HIGHLY DURABLE HYDROPHOBIC THIN FILMS FOR MOISTURE PREVENTION OF COMPOSITE STRUCTURES FOR AEROSPACE APPLICATIONS

A Dissertation by

Erkan Kececi

Master of Science, Wichita State University, 1995

Bachelor of Science, Yildiz Teknik Universitesi, 1990

Submitted to the Department of Mechanical Engineering
and the faculty of the Graduate School of
Wichita State University
in partial fulfillment of
the requirements for the degree of
Doctor of Philosophy

May 2012

© Copyright 2011 by Erkan Kececi

All Rights Reserved

Note that dissertation work is protected by copyright, with all rights reserved. Only the author has the legal right to publish, produce, sell, or distribute this work. Author permission is needed for others to directly quote significant amounts of information in their own work or to summarize substantial amounts of information in their own work. Limited amounts of information cited, paraphrased, or summarized from the work may be used with proper citation of where to find the original work.

HIGHLY DURABLE HYDROPHOBIC THIN FILMS FOR MOISTURE PREVENTION OF COMPOSITE STRUCTURES FOR AEROSPACE APPLICATIONS

The following faculty members have examined the final copy of this dissertation for form and content, and recommended that it be accepted in partial fulfillment of the requirement for the degree of Doctor of Philosophy, with a major in Mechanical Engineering.

_____
Ramazan Asmatulu, Committee Chair

_____
Brian Driessen, Committee Member

_____
Hamid Lankarani, Committee Member

_____
Krishna Krishnan, Outside Committee Member

_____
T.S. Ravigururajan, Committee Member

Accepted for the College of Engineering

_____
Zulma Toro-Ramos, Dean

Accepted for the Graduate School

_____
J. David McDonald, Dean

DEDICATION

To my parents

ACKNOWLEDGEMENTS

I would like to gratefully and sincerely thank my advisor Dr. R. Asmatulu for his guidance, understanding, patience, encouragement, and support during my graduate studies at Wichita State University.

I also thank my friends, co-workers, and committee members for their support and advices. Finally, I would like to thank to my family for their patient and continuous support.

ABSTRACT

Advanced polymeric composites are widely used in aerospace industry because of the high strength-to-weight ratio, manufacturability and other distinctive advantages. These polymeric composites are usually subjected to wide ranges of environmental conditions where they can absorb a significant amount of moisture or solvents from the environment and reduce their mechanical, thermal, and other physical properties and service times.

In the present work, four different hydrophobic thin barrier films were co-bonded to the surfaces of composite structures to investigate mechanical properties, moisture prevention and absorption characteristics, and other physical behaviors of these materials. These hydrophobic films include polyvinyl fluoride (PVF), polyether ether ketones (12.5 mμ and 25 mμ), polyimide, and polytetrafluoroethylene. Eight different tests were conducted on the coupons for comparison and evaluation purposes, which consisted of short beam shear, sandwich flexure, compression, paint tape test, moisture absorption and ingression, UV light and water contact angle, shrinkage, and bonding. In addition to these tests, finite element analysis (FEA) modeling was used to predict the stiffness of the conditioned coupons.

Conditioning performed by fully immersing coupons in water at 22 ±2°C for 14 and 29 days, and in Skydrol for 7 days prior to the testings. The duration of the water exposure was determined based on the equilibrium time of the coupons which had no barrier film.

The test results confirmed that using the barrier films as the outermost ply on the composite significantly increased the mechanical and physical properties of the composite coupons, which will be a drastic improvement for aerospace applications. Finally, the FEA model was developed to predict the mechanical behavior of the composites associated with barrier films. The test results of the FEA are closely related to the experimental results.

TABLE OF CONTENTS

TABLE OF CONTENTS (Continued)

Chapter Page

LIST OF TABLES

LIST OF FIGURES

LIST OF FIGURES (Continued)

LIST OF FIGURES (Continued)

LIST OF FIGURES (Continued)

LIST OF FIGURES (Continued)

LIST OF ABBREVIATIONS / NOMENCLATURE

AM	Additive Models
ASTM	American Society of Testing Material
CD	Cumulative Damage
CTE	Coefficient of Thermal Expansions
DSC	Differential Scanning Calorimeter
DMA	Dynamic Mechanical Analysis
ECD	Exponential Cumulative Damage
FEP	Fluorinated Ethylene Propylene
KPa	Kilo Pascal
MPa	Mega Pascal
MSE	Mean Squared Error
UV	Ultra Violet
PEEK	Polyether Ether Ketone
PCNC	Polymer Clay Nano Composites
PTFE	Polytetrafluoroethylene
PVF	Poly Vinyl Fluoride
RH	Relative Humidity
RT	Room Temperature
SBS	Short Beam Shear
TFE	Tetrafluoroethylene
TGA	Thermogravimetric Analysis
TGA	Thermogravimetric Analysis

VDF	Vinylidene Fluoride
VF	Vinyl Fluoride
WTR	Water Transmission Rate

LIST OF SYMBOLS

A	Area
C	Moisture Weight Fraction Content
°C	Celsius
C_C	Constant of Proportionality
C_T	Thermometric Conductivity
C_S	Saturated Moisture Content of Medium
D	Diffusity
D_{IJ}	Mass Diffusion Tensor
D_L	Diffusion for Longitudinal Direction
D_0	Pre-exponential Factor
D_T	Diffusion for Transverse Direction
Dz	Diffusion Coefficient
E	Modulus
E_A	Diffusion Activation Energy
f	Volume Fraction of Particles in the Composites
°F	Fahrenheit
h	Thickness
h(u)	Assumed Damage Model Function
I	Moment of Inertia
J_I	Moisture Flux
L	Support Span

m	Saturation Level
M_∞, Ms	Equilibrium or Saturation Mass
M(%)	Relative Mass Gain
M_0	Initial Moisture Concentration
M_n	Moisture Content at Time t (%)
n	An Index
N	Newton
ρ_c , ρ_w	Water Density and Dry Composite Density
P	Load
R	Molar Gas Constant, 8.314 J Mol^{-1} K^{-1}
t	Time
t_D	Diffusion Time, hr
t_1 , t_2	1 and 2 are Discrete Times (t) in the Sorption Process
T	Material Temperature
Tg	Glass Transition Temperature
V_w , V_c	Volumes of Water and Dry Composite
W	Initial Strength of Material
W_b	Baseline Weight Prior to Conditioning
W_i	Weight at Current Time
W_{i-1}	Weight at Previous Time
Ψ	Theoretical Strength
X_0	Reduction of Theoretical Strength by a Random Amount

LIST OF SYMBOLS (Continued)

φ	Theoretical Strength of Composite Specimen
σ_{sc}	Stress in Composite
σ_{sf}	Stress in Fiber
σ_{sm}	Stress in Matrix
ε	Hygric Strain
ε_{∞}	Saturated Hygric Strain
τ_f	Shear Stress Mid-plane of the Beam
σ	Stress
δ	Displacement

CHAPTER 1

INTRODUCTION

In this dissertation, moisture prevention and absorption characteristics of a variety of hydrophobic thin barrier films, including polyvinyl fluoride (PVF, Tedlar), polyether ether ketones (PEEKs) (12.5 mμ and 25 mμ), polyimide (Kapton), and polytetrafluoroethylene (PTFE, Teflon) were investigated by evaluating mechanical and other physical properties. Hydrophobic films were co-bonded to polymeric composite laminates and sandwich articles, and then a variety of tests were conducted on the composite coupons to verify the moisture prevention characteristics.

1.1 Composite and Moisture Interaction

The word composite is defined as a combination of two or more materials created through a process to form a new engineered material. Two primary constituents that make up composites are a matrix and reinforcement [1]. Since the last decade, composites use has been significantly increased in the aerospace industry due to the composite's higher strength to weight ratio, and other distinctive advantages such as low coefficient of thermal expansion (CTE), corrosion resistance, ease of manufacturing, part consolidation (ability to fabricate complex parts in one step), design flexibility (be ability to fabricate different thickness dimensions within the same structure), fatigue resistance, and high temperature resistance.

Fiber reinforced polymer composites are subjected to a wide range of mechanical loads and environmental conditions, such as high and low temperatures, moisture, aggressive solvents, etc. Compared to other structural materials, polymers can absorb more moisture or solvents from outside environments. Those liquids can affect their mechanical, thermal, and other physical properties and their service life. With the absorption of water into the composite structures, the

polymer matrix goes through a plastification phase, or physical aging, as water molecules move through the matrix. During the transport hydrolysis, or chemical aging, the polymer can be damaged or degraded by osmotic fissuring [2]. To understand the moisture absorption process, composition of the polymeric matrices must be known.

For the structural fiber reinforced composite materials, the matrix is either thermoplastic or thermoset polymer. The main functions of matrix materials are to transfer stress between reinforcements, hold fibers together, and protect the reinforcements from environmental effects. Polymer thermoset resin is the most common matrix for aerospace applications due to its high mechanical properties, chemical resistance to the environment, low coefficient of thermal expansions (CTE), and excellent adhesion to mating materials [1,42].

Common reinforcements for the aerospace industry are carbon, glass, and Kevlar. The primary functions of the reinforcement are to provide strength and stiffness, and to improve the mechanical properties of the composite [3]. Processing of thermoset resin composites involves resin and a curing agent (hardener). With the required conditions, these two chemicals react with each other to form a chain of molecules. First monomers start to grow, called A-stage, and then these monomers grow through branching, called B-stage, prior to gelling. At this stage, monomers are connected via van der Waals bonds. As the process continues, a network of chains is created to form cross links between monomer chains with covalent bonds. This process creates a non-reversible chemical bond [3]. Figure 1.1 shows the epoxy chemical reaction formed during the curing process [3].

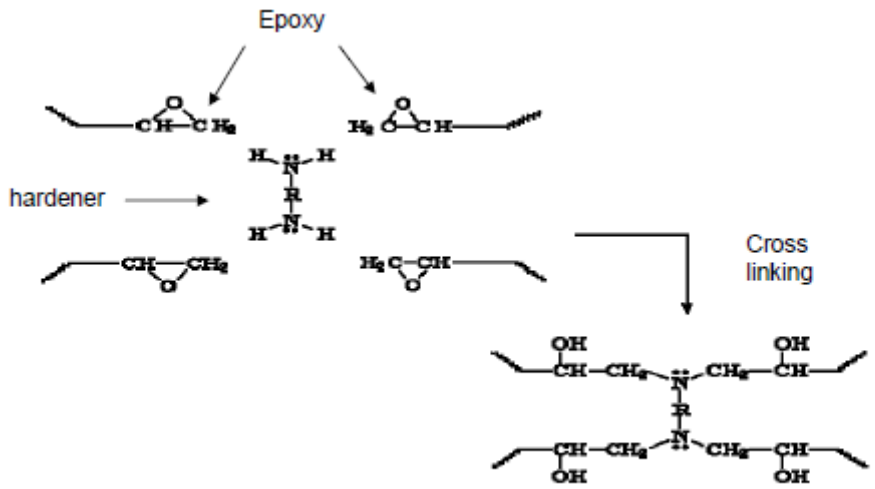

Figure 1.1 Epoxy chemical reaction formed during the curing process [3].

CHAPTER 2

LITERATURE REVIEW

2.1 Diffusion

In 1855, Fick stated that the flux of a liquid (or a solvent) is directly proportional to the negative concentration gradients. The constant of proportionality is known as moisture diffusivity constant, D, defined as the rate or speed at which the material absorbs, desorbs, or transports moisture [4,5]. Diffusion is defined as a transport rate of a fluid through material per unit time, (mm^2/s) [6], or the amount of a particular substance that diffuses across a unit area in a unit of time [7]. Moisture diffusivity is defined as the liquid that diffused and dispersed through a gas as a vapor, condensed on a surface as dew, or was transported into material which can be quantified [7]. Diffusion coefficient, D, can be calculated by exposing a material to a known solvent at a certain temperature while monitoring weight gain as a function of time. To establish D precisely, a material has to be exposed until it reaches a condition, moisture equilibrium, such that it is not able to absorb any more moisture from the surrounding environment [22].

A common method for water absorption into polymers is the activated absorption model that can be explained in three steps [6]:

1. Bulk dissolution of water in the polymer
2. Moisture absorption into surfaces of the excess free volume elements
3. Hydrogen bonding between polymer hydrophilic groups and water

To characterize composite affinity to water, the steps below shall be done prior to the study of the effects of water intake [6]:

1. Define reversible and irreversible mechanism through analytical testing
2. Create a kinetic model based on established formulas, diffusion law, chemistry, etc.

3. Establish properties of materials based on physics laws.

Diffusion occurs when there is porosity, voids and vacancies within molecules. Hygrothermal exposure causes molecules (liquid or gas) to diffuse into the polymer and occupy positions within molecules. Rate is controlled by the amount of free volume in the polymer. Having high level cross-linking or densely-packed molecules causes a slow sorption rate in the structure. Water molecules can move into the polymer in the x, y or z direction, which are formed by adjacent parallel polymer chains. When two adjacent polymers separate, a space is created which allows water molecules to go between them. Water molecules are attracted to polar sites and are absorbed by forming hydrogen bonds. With an increase of polar groups, higher sorption rates happen in the composite structures [8].

2.1.1 Moisture Diffusion Models for Composite Laminates

Diffusion rate depends on the chemical and physical structure of a material, liquid solubility and type, humidity, and temperature conditions. Depending on the hygroscopic level of a material, the natural moisture absorption rate can significantly change. For a theoretical calculation, diffusion rate follows Fick's second law in most cases. However, when the polymer structure has more than one type of material, the theoretical Fick's law calculation shows a significant difference from the experimental results. In that case, more analysis is required to find the diffusion rate [9]. Many moisture diffusion models have been developed for laminate structures, as discussed in the following sections.

Abot, et al. [6] stated that saturation water mass, Ms (constant) can be achieved only if the interaction between fluid and composite is reversible. They investigated this water sorption model by immersing carbon epoxy laminates with different fiber angles in water and finding moisture absorption rates, equilibrium or saturation mass are calculated using equations (2.1) and (2.2),

$$M(\%) = \frac{mass\ of\ wet\ specimen - mass\ of\ dry\ specimen}{mass\ of\ dry\ specimen} x\ 100 \tag{2.1}$$

$$M_\infty = \frac{asymtatic\ mass\ of\ wet\ specimen - mass\ of\ dry\ specimen}{mass\ of\ dry\ specimen} x\ 100 \tag{2.2}$$

where M(%) is relative mass gain [49] and M_∞ is the equilibrium or saturation mass, which characterizes composite affinity for water (hydrophilicity). The average moisture concentration, -c-bar, is given by equation (2.3),

$$\bar{c} = \frac{V_W}{V_C} = \frac{M_W/\rho_W}{M_C/\rho_C} = \frac{\rho_C}{\rho_W} M \tag{2.3}$$

where M_w and M_c are water mass and dry composite mass, V_w and V_c are volumes of water and dry composite, and ρ_c and ρ_w are water density and dry composite density. Abot, et al. [6] also explain the moisture transport into the matrix in two steps:

Step 1. Solvent dissolution on polymer surface which creates a concentration gradient.

Step 2. Diffusion of solvent in concentration gradient direction through Fick's second law of diffusion.

Fick's second law is giving at equation (2.4) and diffusion time can be calculated using equation (2.5),

$$D = \frac{\pi}{16} h^2 \left[\frac{M}{M_\infty \sqrt{t}}\right]^2 \tag{2.4}$$

$$t_D = \frac{\pi h^2}{16D} \tag{2.5}$$

where D is diffusity, amount of water passing per second through a unit area, h is thickness, t is time, t_D is diffusion time in hours, Dz is diffusion coefficient, amount of water passes per unit, Z

is the coordinate along the sample thickness, M_0 is initial moisture concentration and M_∞ is saturation moisture concentration. The researchers concluded that:

- water sorption follows a dual sorption-diffusion process, first apparent moisture equilibrium reached by Fick's law and second a slow relaxation process allows to reach through thermodynamic equilibrium.
- the moisture absorption rate is similar in x and y directions and slower in z direction.
- fabric laminates absorb more moisture compared to uni-directional laminates.
- If the equilibrium point has not being reached, composite mass can increase or decrease.

Pilli, et al. [5] stated that the moisture diffusion coefficient can be determined through equation 2.6 for an accelerated moisture absorption by increasing pressure in the conditioning chamber. They used a quasi-isotropic laminate and chopped fiber composite laminates to determine the moisture diffusion coefficient. Figure 2.1 shows the change of moisture content with the square root of time for Fickian materials [5].

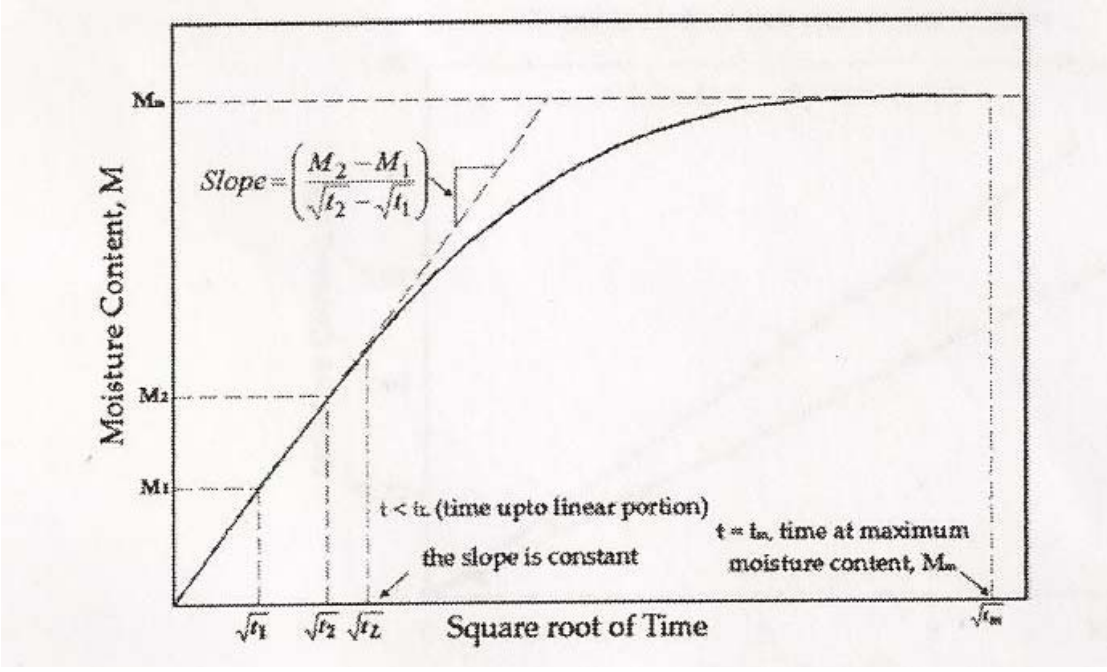

Figure 2.1 Change of moisture content with the square root of time for Fickian materials [5].

$$D = \pi \left[\frac{h}{4M_m}\right]^2 \left[\frac{(M_2 - M_1)}{(\sqrt{t_2} \quad \sqrt{t_1})}\right]^2 \tag{2.6}$$

$$M(\%) = \frac{mass\ of\ wet\ specimen - mass\ of\ dry\ specimen}{mass\ of\ dry\ specimen}\ x\ 100 \tag{2.7}$$

In equation (2.6), D is the diffusion coefficient, h is thickness, M_m is moisture content at equilibrium, M is moisture content at t_1 or t_2, m is saturation level, and t_1 and t_2 are discrete times (t) in the sorption process.

Shi et al. [10] explained the diffusion coefficient with Arrhennius equation. Glass laminates were coated with 150 micrometer thick Epon 828 resin, and samples were conditioned through accelerated conditioning and water bath immersion. The diffusion coefficient is determined with equation (2.8),

$$D = \frac{D_0 \exp(-E_A)}{RT} \tag{2.8}$$

where D is the diffusion coefficient, D_0 is a pre-exponential factor, E_A is diffusion activation energy, and R is the molar gas constant, 8.314 J Mol^{-1} K^{-1}. Activation energy E_A is determined using equation (2.9).

$$\ln D = -\left(\frac{E_A}{R}\right)\frac{1}{T} + \ln D_0 \tag{2.9}$$

To verify this theory, temperature dependence was modeled using the Arrhenius Equation. The experimental test results indicated that the diffusion coefficient was very similar to Arrhenius fitting in which D was 5.1 ± 0.6 x 10^{-10} cm^2/s. Figure 2.2 shows how experimental data fitted to the Arrhenius equation [10].

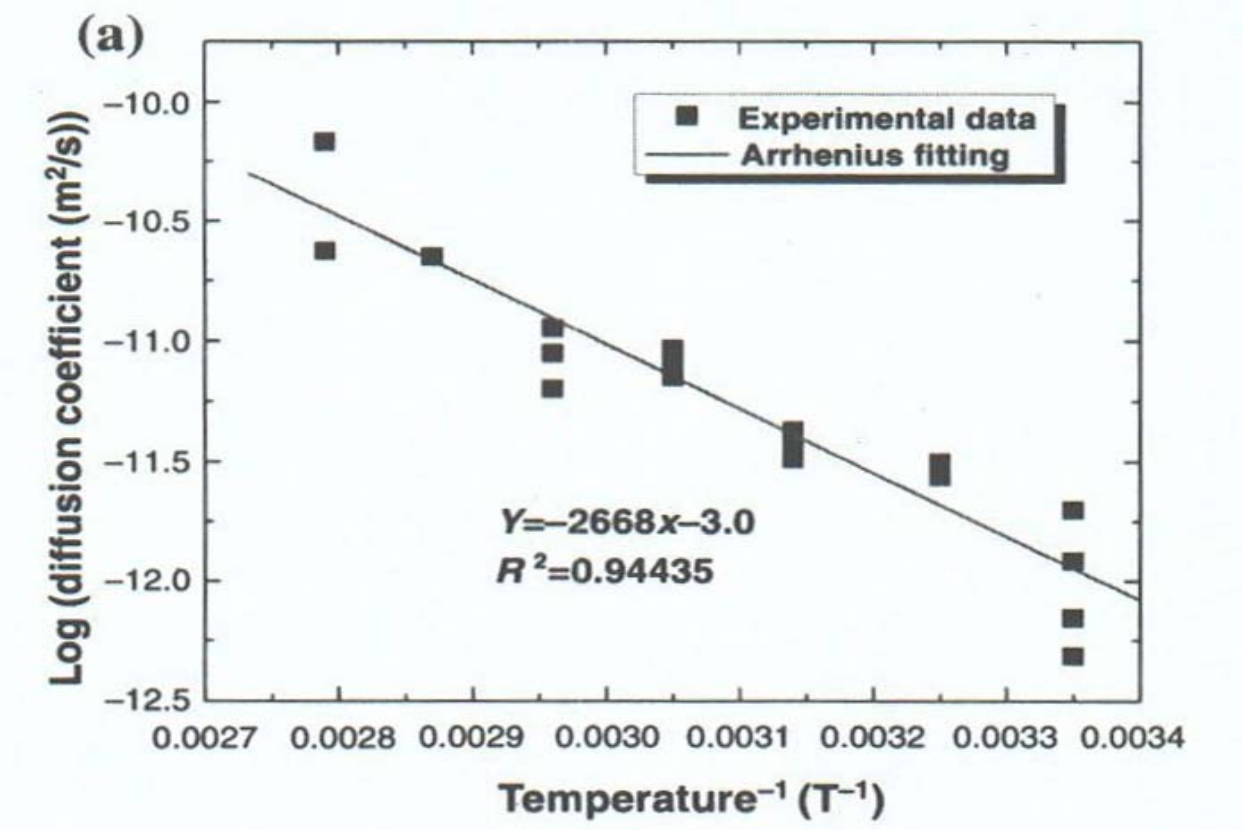

Figure 2.2 Diffusion coefficients of saturated epoxy specimens and fitting to Arrhenius equation [10].

Wang et al. [11] explained moisture diffusion in thickness direction with equation (2.10) and equation (2.11)

$$D_M = 0.0016e^{\frac{604}{T+90}} \tag{2.10}$$

$$T = T_1 0 + (T_1 1 - T_1 0\,[1 - 4\Sigma_1(n = 1,3,5)^{\top}\infty \blacksquare\, [1/n\pi\,(-1)^{\dagger}((n-1)/2)\,]\;\; e^{\dagger}(-\;[nh/h^{\dagger}2\,]\;\; {}^{\dagger}2\; C_1 T\; t)\;\; \cos(n\pi/h\; x)]$$

Equation (2.11) is shown above.

where D_M is moisture diffusity, cm^2/day, T is temperature of medium material, T_0 and T_1 are environmental temperatures at time t=0 and $t=t_1$, n is index, h is thickness of laminate in centimeters, x is the coordinate in the direction of thermal conduction and moisture diffusion, and C_T is thermometric conductivity, which is derived by fitting the equation for temperature

data at the center of each specimen. The C_T value is calculated as 1.87 x 10^{-5} cm^2/s. The saturated moisture content is calculated using equation (2.12).

$$c_s = C_c \frac{R}{T + 273} \tag{2.12}$$

where c_S is the saturated moisture content of medium, C_C is constant of proportionality, R is relative humidity of the environment, and T is material temperature.

To verify this theory, Wang et al. [11] conducted an experiment on 0.114 cm thick laminate. Samples that had embedded thermocouples placed in mid-plane were conditioned in the chamber. Specimen temperatures were recorded in a variety of environments as shown in Figure 2.3 [11].

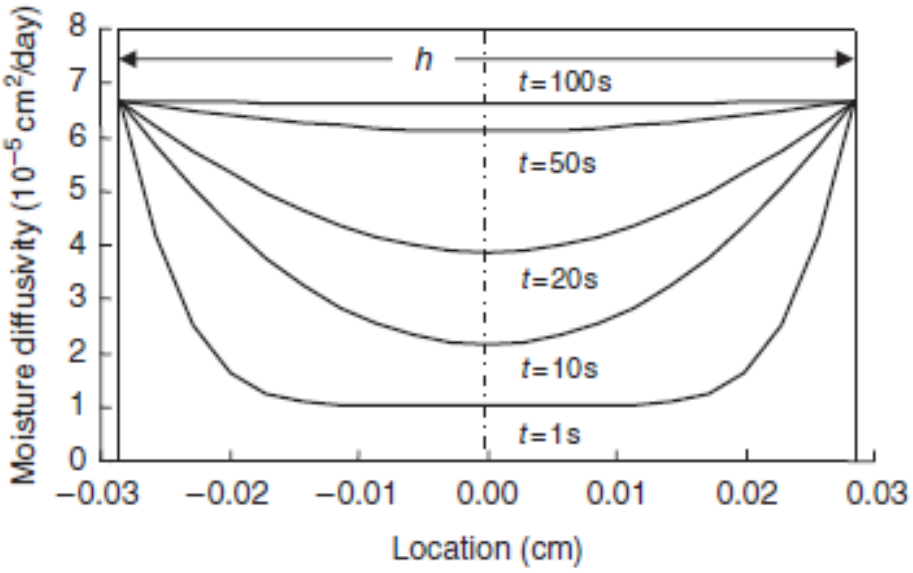

Figure 2.3 Moisture diffusivity in a 4 ply uni-directional carbon/epoxy laminate undertaking an environmental temperature change from 20°C to 96°C [11].

Basf et al. [12] stated that the amount of moisture absorption was dependent on three parameters: fiber volume fraction, diffusion coefficient and temperature. During the tests, injection molded Nylon 6 tensile coupons were used for moisture absorption determination. Weight gain and a Karl-Fisher moisture analyzer were used for the moisture gain verification. It

is stated that moisture absorption correlated with the Fick's laws. The moisture flux per Fick's first law is giving in equation (2.13),

$$J_i = -D_{ij}\frac{\partial C}{\partial x_i} \tag{2.13}$$

where J_I is moisture flux, D_{IJ} is the mass diffusion tensor, C is the moisture weight fraction content, and x_i is the spatial coordinate. From equation (2.13), change of moisture content with time t and Fick's second law can be derived from equation (2.14),

$$\frac{\partial C}{\partial t} = \frac{\partial}{\partial x_i}\left\{D_{ij}\frac{\partial C}{\partial x_j}\right\} \tag{2.14}$$

For the unidirectional fiber composites, diffusion coefficient, D, can be stated in terms of fiber and matrix volume. Diffusion determined for the longitudinal direction, D_L, using equation (2.15) and for transverse direction, D_T, using equation (2.16),

$$D_L = V_f D_f + D_m (1\text{-}V_f) \tag{2.15}$$

$$D_T = D_m f (V_f, D_f, D_m) \tag{2.16}$$

where, f and m stand for fiber and matrix.

Earl et al. [8] evaluated the moisture absorption characteristics of PVC films. Test coupons were exposed to water in two ways: immersion into water and conditioning at 95% RH at 40°C. Absorption was observed in 2 stages: cell wall and cell cavities. Weight gain increased with respect to the square root of conditioning time. They stated that moisture absorbed into the laminate is diffusion driven. Per Fick's law, the percent moisture content at time t (Mt) giving at equation (2.17) and diffusivity can be calculated by equation (2.18) when M_∞ is moisture content at equilibrium known.

$$M_t = M_\infty\left[1 - \frac{8}{\pi^2}\sum_{n=0}^{\infty}(2n+1)^{-2}e\left[\frac{-D(2n+1)^2\pi^2 t}{l^2}\right]\right] \tag{2.17}$$

$$D = \pi \left[\frac{I}{4M_{\infty}}\right]^2 \left[\frac{(M_2 - M_1)}{(\sqrt{t_2} - \sqrt{t_1})}\right]^2 \tag{2.18}$$

where D is diffusivity constant, M_∞ is moisture content at equilibrium (%), M_t is moisture content at time t (%), n is integer, t is time and I is material thickness. Figure 2.4 is shows how experimental test data fits to the Fickian model.

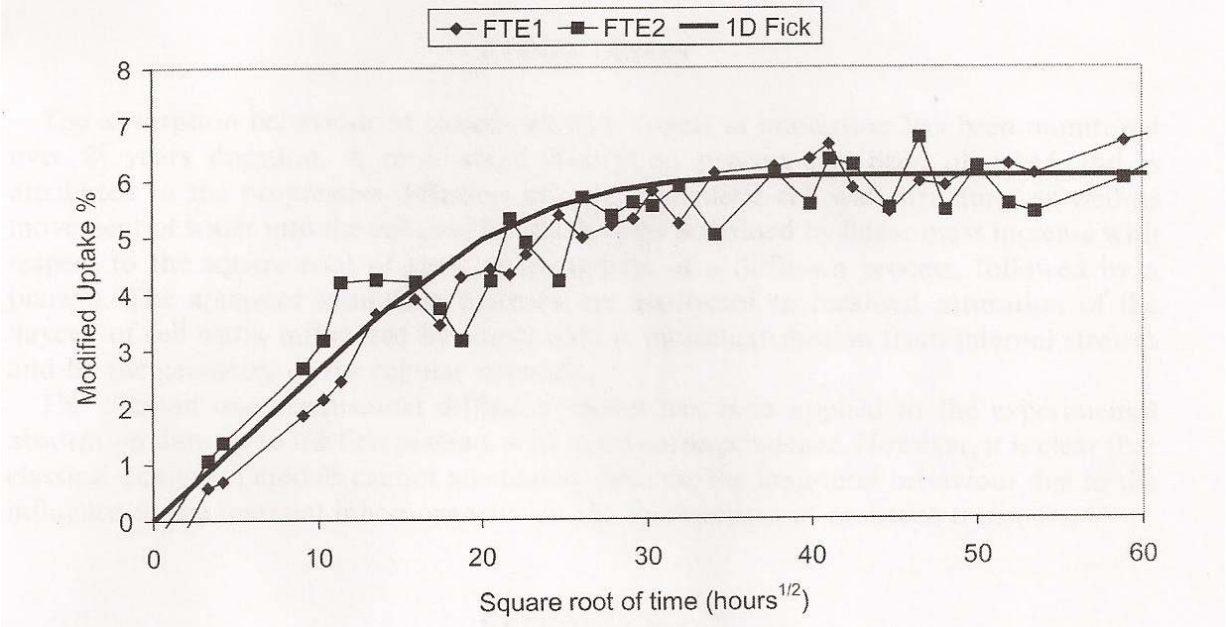

Figure 2.4 One dimensional moisture uptake with fit of one-dimensional Fickian model [8].

2.2 Moisture Absorption

Moisture absorption can be defined as dissolution, diffusion, swelling, relaxation, deformation, and pressure stress formed in the matrix materials. Polymers are very sensitive to moisture due to the interactions between high polar groups of resin and water molecules. Water/liquid uptake mostly happens in the matrix or at matrix-fiber interfaces, and is absorbed into the polymer through a diffusion mechanism. Moisture absorption is a mostly irreversible process and causes degradation of the material, resulting in chemical or physical aging [6].

2.2.1 Factors Affecting Moisture Absorption

Material properties, degree of cure, polarity, homogeneity of material, environment and material conditions, temperature, relative humidity, pressure, thickness, and design are the most critical factors affecting moisture absorption [13]. For example, high fiber volume laminates absorb less moisture compared to resin dominated ones due to the higher sensitivity of resin to a liquid penetration [29]. Another factor is the composite surface morphology, such as voids, pin holes and matrix cracks that allow moisture to be absorbed easily, which detrimentally affects moisture diffusion rate. Processing of composites is another key factor that dominates moisture absorption. Differences in crosslink densities can cause solvent-polymer crazing, which changes water solubility in the polymer structure [14,23]. Water absorption is also affected by degree of crystallinity, number of polar groups, and the bond strength between water molecules and polymer molecules. Due to the above mentioned characteristics, the hygrostrain effect can be tailored based on polymer material properties and service environment [6,15].

Part geometry can also affect moisture uptake rate and amount. Studies verified that ply stack change and fabric type can change moisture uptake or diffusion rate as well. It has been proven that unidirectional composite laminates absorbs less moisture than fabric ones although they both have the same resin volume ratio [16].

2.2.2 Moisture Effect on Mechanical and Other Physical Properties

Moisture can cause changes in a polymer matrix due to the high polar interactions of water molecules with polymer chains, and within a matrix and fiber interface due to the coupling with internal stresses. Distribution of water in a polymer composite either in the matrix or at a matrix-fiber interface might cause material degradation, changing physical, chemical, and mechanical properties. Hydrolysis, or chemical aging, happens at the micromoleculer chain level, which eventually alters material characteristics [2]. Moisture absorption can cause

hygrothermal expansion, cracking of the matrix, or delamination, which may reduce mechanical and physical properties such as glass transition temperature, Tg.

Thellen et al. [17] conducted a study to verify the effect of moisture on the mechanical and barrier properties. Tests were conducted on multilayer Nylon MXD6 films (m-xylylene adipamide), an aromatic polyamide that is proven as a gas barrier film for uses such as drink bottles. Five layer samples including a barrier film in the middle were fabricated and placed in the condition chamber at 140°C for 120 hours. Coupons were tested after elevated temperature conditioning to compare to the control condition (environmental) for tension, glass transition temperature, water vapor transmission, and oxygen transmission test [17].

Tension tests were carried out per ASTM D 882. The test results indicated that the strain decreased due to the brittleness of the coupons after drying at elevated temperature. Differential scanning calorimeter (DSC) test results also showed that after the loss of moisture, nylon's glass transition temperature increased about 20-40°C due to the lower moisture in the structure, which caused a stiffer polymer.

Basf Corp. [12] conducted research to determine the effects of moisture on unfilled Nylon 6 material. Experimental data showed that absorbed moisture/water acts like a plasticizer and change strength, stiffness, flexure, and Tg properties. In this study, a specimen was exposed to moisture with two methods.

- Immersion in water (room temperature and 100°C)
- Conditioning (23-70°C with 50-100 %RH)

Results showed that strength and flexural properties decreased about 50%. Tg was indicated to be 80% lower due to moisture absorption in the polymeric structure. Figure 2.5 shows the effects of conditioning methods on flexural stress [12].

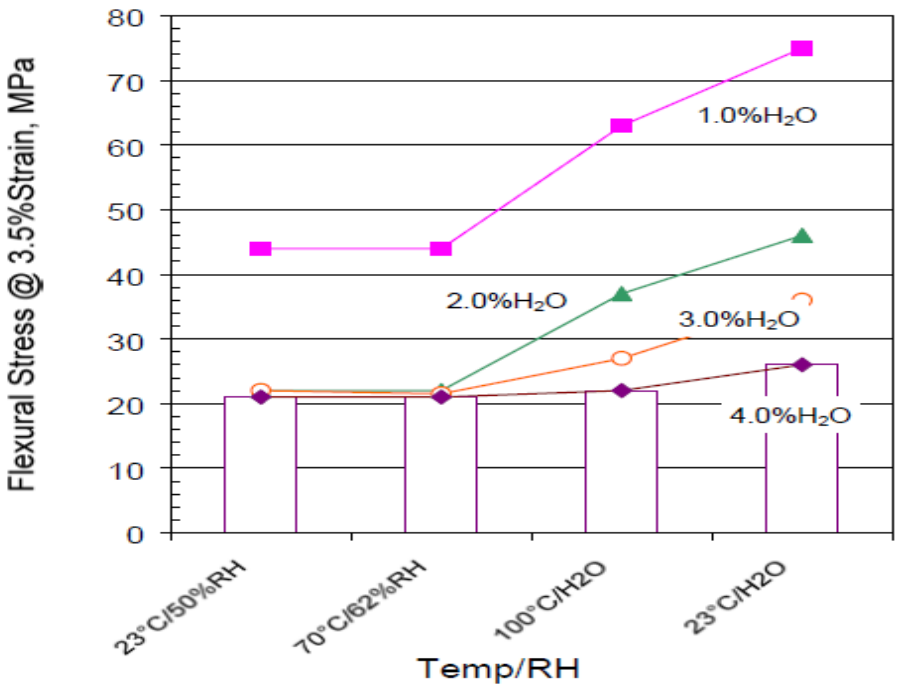

Figure 2.5 Effects of conditioning methods on flexural stress [12].

Menail et al. [2] conducted a study to estimate the effect of water absorption on Kevlar and glass fiber reinforced epoxy laminates after the material was damaged through fatigue testing at 100, 1000, and 50000 cycles. After the cyclic loadings, the samples were immersed in water for three different time durations: 100 hr, 500 hr, and 1000 hr. Static testing was conducted at three different conditions:

- After fabrication
- After fatigue testing
- After fatigue testing and water immersions.

Menail et al. claimed that internal damage happens due to the osmotic cracking related to the amount of water absorption. Test results showed that water absorption increased with increase of fatigue cycles, while the strength and stiffness decreased after fatigue testing and increased cycle number. It is concluded that material degradation mostly depends on fatigue cycle number and water absorption, which are a function of immersion time, along with internal

damage rate within the matrix, and at the matrix-fiber interface. Figures 2.6 and 2.7 show the effect of fatigue cycle and water immersion time for the static strengths of glass fiber laminates [2].

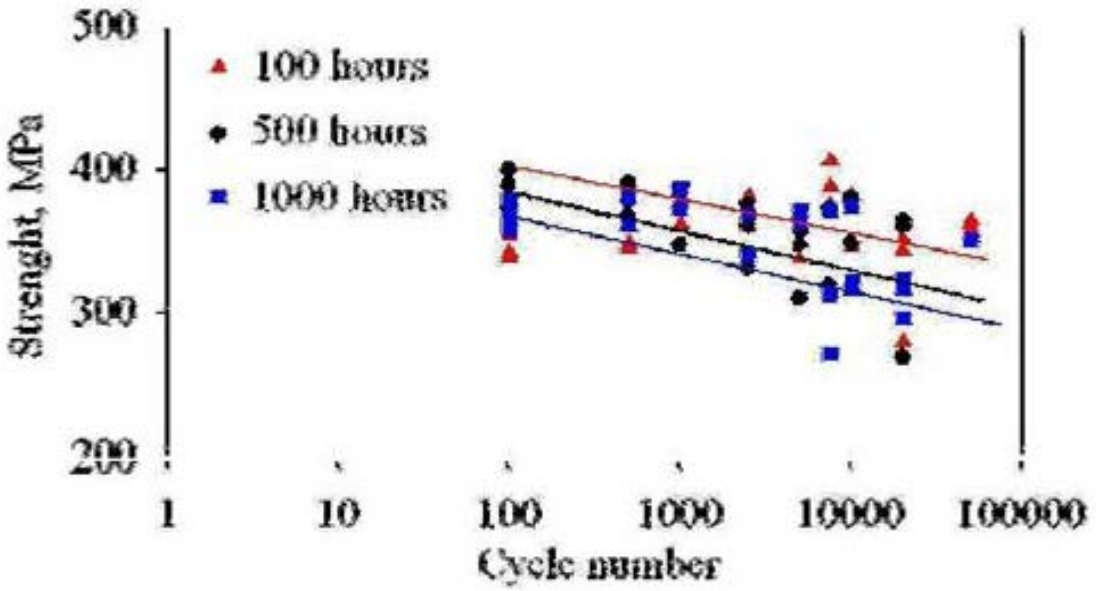

Figure 2.6 Effect of fatigue cycle and water immersion time for the static strengths of glass fiber laminates [2].

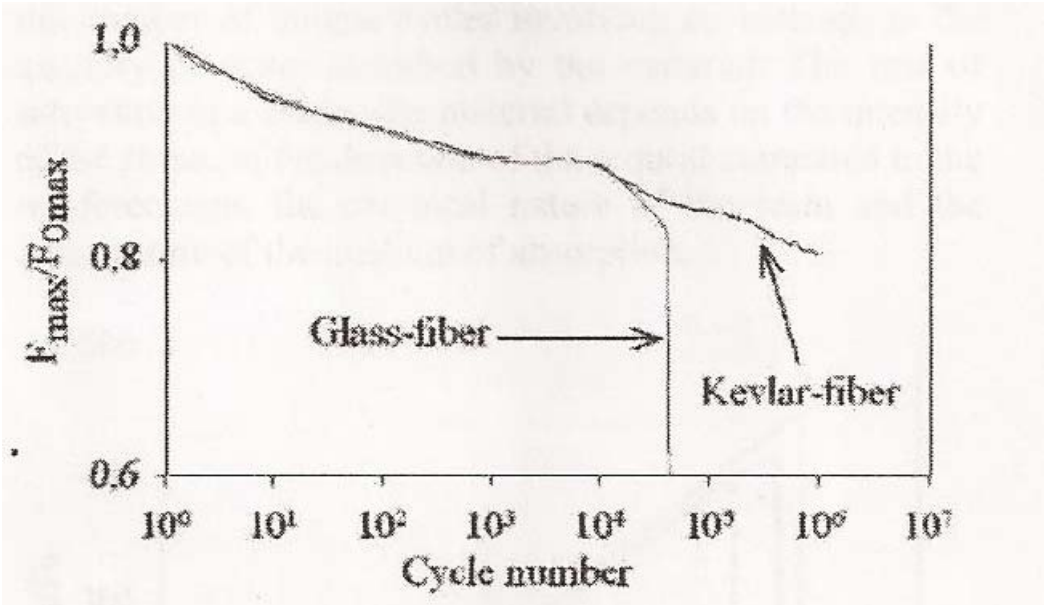

Figure 2.7 Hygrothermal fatigue results [2].

Abot, et al. [6] conducted research on plain weave epoxy carbon laminates conditioned in water. Results indicated that storage modulus (stiffness), tan δ and glass transition temperature Tg were significantly reduced. Figure 2.8 shows the storage modulus and glass transition temperature for dry and wet samples [6].

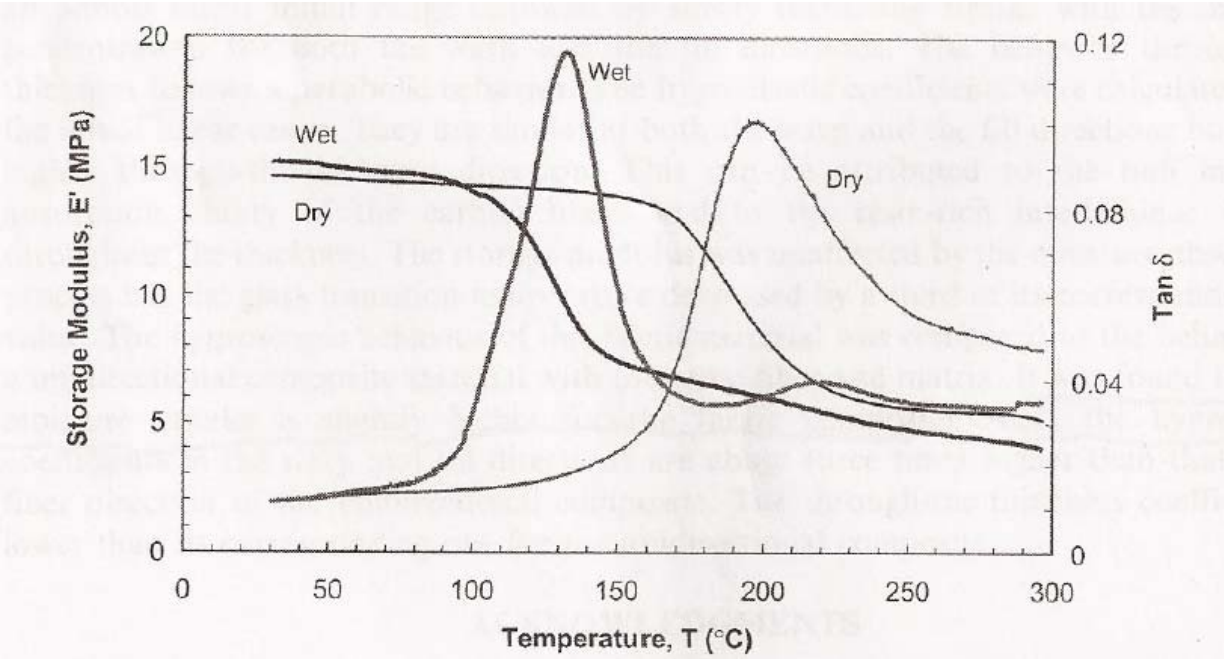

Figure 2.8 Storage modulus and glass transition temperature for dry and wet samples [6].

Shi et al. [10] conducted research to find out the effect of moisture on resin coated glass laminates with 150 micrometer thick Epon 828 resin. After the curing process, samples were conditioned through accelerated conditioning and in water bath immersion. Surface resin characteristics were studied for pristine and conditioned samples. The diffusion coefficient was calculated using the Arrhenius equation. Glass transition (Tg), surface modulus and hardness, moisture content, and degradation tests were conducted. Moisture content for pristine samples was found to be about 7% using the TGA analysis. DMA test results showed that Tg decreased from 77 to 49°C. Elasticity and hardness of the coating was decreased with increasing moisture

uptake. Hardness tests were conducted using a Berkovich nano-indentor. Figure 2.9 shows the water distributions for wet and dry samples [10].

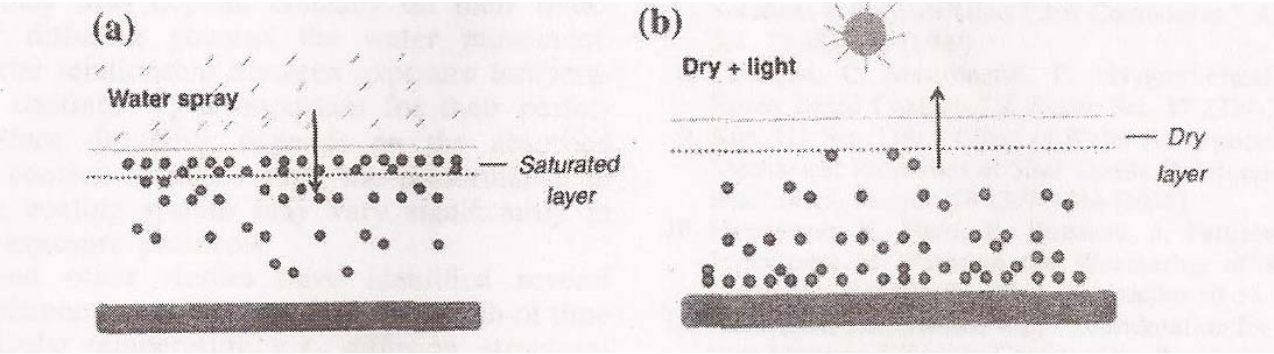

Figure 2.9 Water distributions in the structures for wet (a) and dry (b) samples [10].

Basf et al. [12] conducted a study on injection molded Nylon 6 tensile coupons used for moisture absorption determination. Moisture content was measured by weight gain and Karl-Fisher moisture analyzer. Conditioning was conducted in two ways:

- Immersion into water: RT immersion or boiled water immersion
- Conditioning chamber: - 23°C to 70°C with 50% RH to 100% RH

The following are conclusions from these tests:

1. material anomalies such as voids, porosity and damage can affect diffusion coefficient.
2. moisture equilibrium depends on temperature and relative humidity
3. direct water immersion might cause material degradation
4. with increased moisture absorption from 0.15% to 1.36%, Tg decreased from 47°C to 8°C.
5. tensile strength dropped from 80 to 20 MPa when moisture gain reached 10%.

It is concluded that Nylon 6 was very sensitive to the moisture absorption as indicated in Figures 2.10 and 2.11.

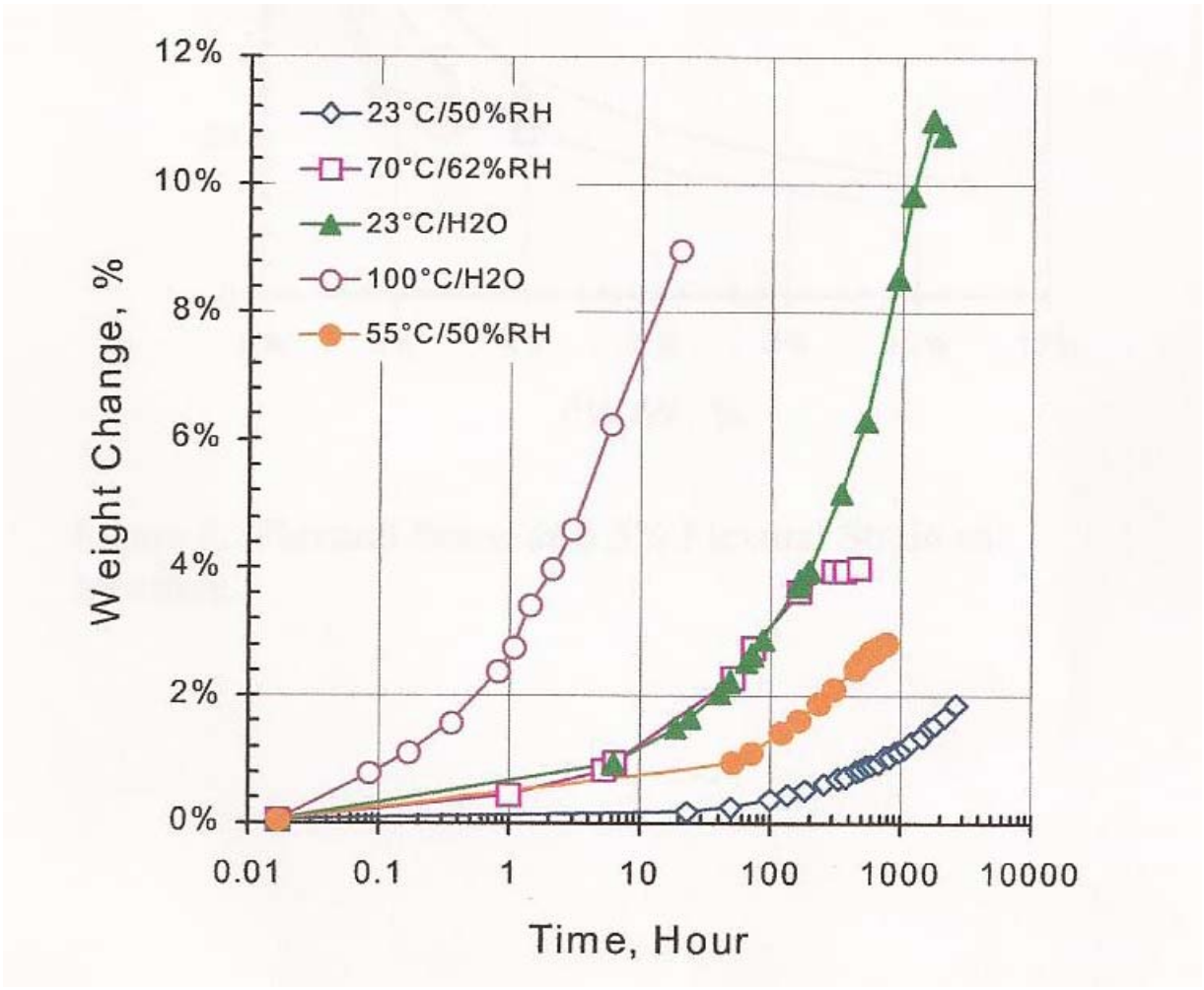

Figure 2.10 Moisture gain vs. time and temperature [12].

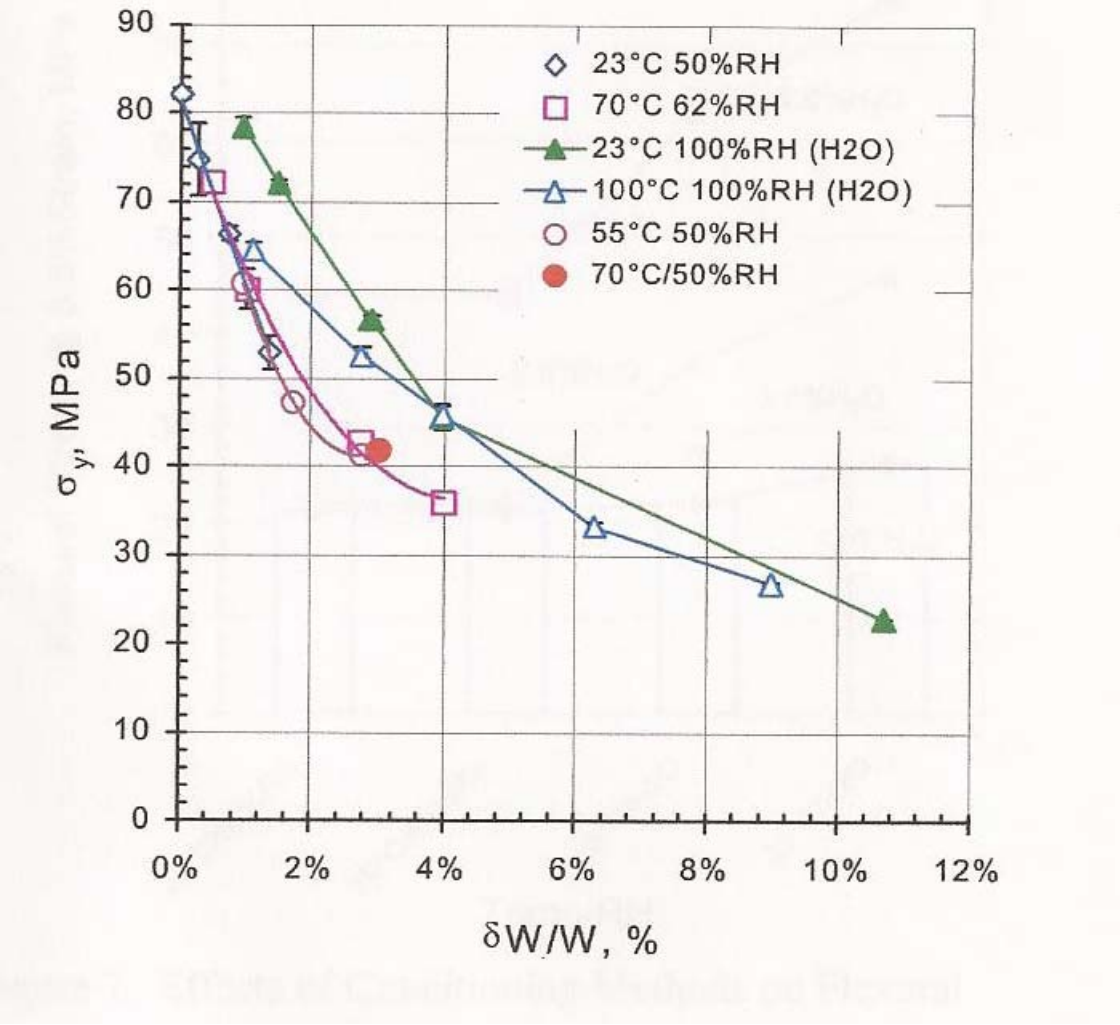

Figure 2.11 Tensile strength relative to moisture gain [12].

2.2.3 Accelerated Moisture Absorption Tests

Depending on the material properties, equilibrium moisture conditioning can take longer times (months and years) at normal conditions. During this time, material chemistry may change due to the aging process, resulting in material degradation and reduced life span. To eliminate these concerns, accelerated conditioning is chosen as a method to find the lifetime of polymeric materials. With the accelerated conditioning method, reaching moisture equilibrium can be up to sixty times faster compared to in-service conditions. The most common method for accelerated conditioning is the variable conditioning method. In this method, two conditioning steps are

used. Specimens are conditioned at higher temperature and relative humidity (RH) followed by lower temperature and RH to reach a full moisture equilibrium condition [5]. However, it is known that accelerated conditioning can increase hygrothermal fatigue and decrease mechanical properties. For example, Jedidi et al. [16] showed that accelerated moisture absorption could decrease Tg about 20°C for 90° and 45° ply stack laminates.

Menail et al. [2] studied to verify the effects of different moisture uptake methods on the fatigue behavior of glass and Kevlar fibers with epoxy matrix. Two moisture absorption methods were used: immersing in water and conditioning in the chamber. It is concluded that the influence of water can cause more degradation in wet state (immersed in the tap water), than in humid state of the chamber.

Pilli et al. [5] used Fick's law to find the diffusion coefficient, and conducted a study to achieve saturation levels at lower temperatures, but in an accelerated way by inducing a hydrostatic pressure of 0.45 MPa. Two methods were used for the accelerated moisture conditioning, an initial high humidity step (> 95% RH) followed by a lower one (> 85% RH) with high temperature as indicated at Figure 2.12.

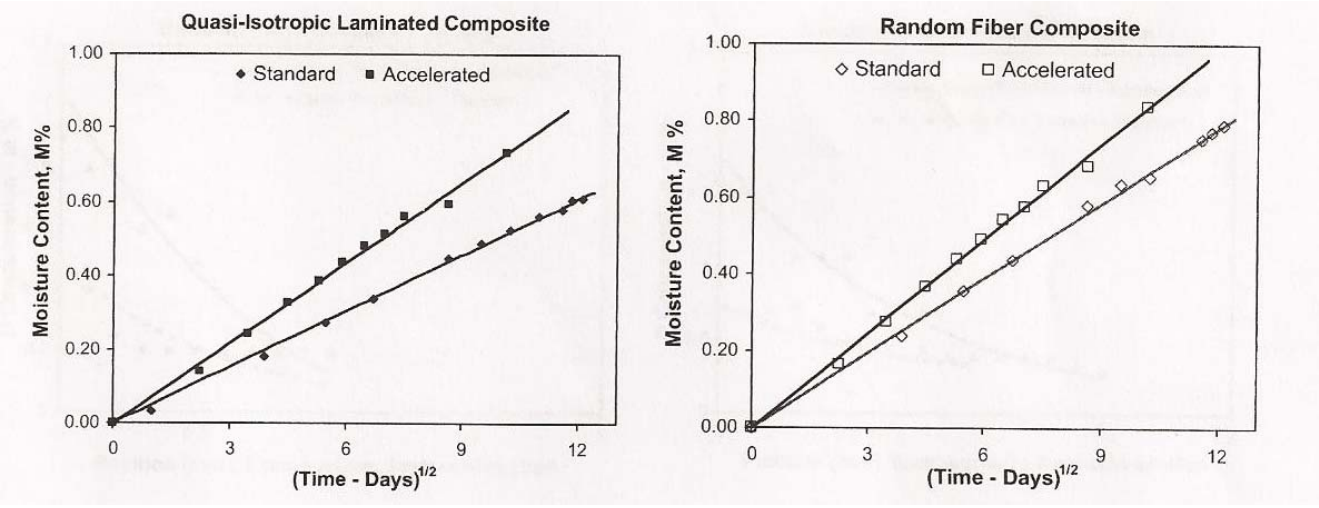

Figure 2.12 Change of moisture content for accelerated and standard conditioning [5].

The experimental results showed that by accelerating moisture absorption, saturation time was significantly reduced. Pilli used Fick's law equation (2.19) to find the diffusion coefficient,

$$D = \pi \left(\frac{h}{4M_m}\right)^2 ((M_1 2 - M_1 1)/(\sqrt{t_1 2} - \sqrt{t_1 1}))^2 \quad (2.19)$$

where D is diffusion coefficient, h is thickness, M_m is mass moisture concentration, m is saturation level, t_1 and t_2 are discrete times in the sorption process. Table 2.1 gives the comparisons of the projected time for two composite systems [5].

TABLE 2.1

A COMPARISON OF THE PROJECTED TIME FOR TWO COMPOSITE SYSTEMS [5]

Time to saturation, years	**Standard conditioning**	**Accelerated**
Oriented fiber composite	7	3.9
Random fiber composite	4.2	2.4

2.3 Moisture Prevention Methods

Paint is the most common moisture barrier film for aerospace composite applications. However, due to the application, service environment, cost, weight increase, reliability, and engineering requirements, barrier films are chosen as an alternative method in addition to paint.

2.3.1 Barrier Films

The barrier film approach uses moisture-proof materials to eliminate hygrostrain problems. Among a variety of options, polymer based poly vinyl fluoride (PVF) is the only barrier film used extensively in aerospace applications. PVF is a thermoplastic fluoropolymer with the repeating vinyl fluoride unit. PVF has low permeability for vapors, burns very slowly, has excellent resistance to weathering and staining, and is resistant to most chemicals, except ketones and esters. It is available in the form of film in a variety of colors and formulations for

various end uses, and as a resin for special coatings [5]. The industry brand of PVF film is Tedlar, which is a trade mark of DuPont, and has a surface plasma treatment for a better bonding.

Another barrier film is a coating developed using polymer clay nanocomposites (PCNC) [18,19]. Nanoclay and polymer latexes are mixed well to make PCNC suspensions in aqueous solutions with ultrasonification. X-ray Diffraction, XRD, and differential scanning calorimeter (DSC) test results indicated that PCNC suspensions can be ideal water or vapor barriers because of the high surface-to-volume ratio of the nanofiller and the increased tortuosity of the diffusion path against the moisture. This high molecular density organic polyimide film is used to prevent moisture especially in electronic devices such as photoresists, encapsulants, and insulators. A PCNC barrier film is fabricated with Langmuir-Blodgett (LB) technique in three steps as it shown at Figure 2.13,

- Spreading solution of amphiphilic molecules
- Compressing monolayer after evaporation
- Depositing monolayer on substrate

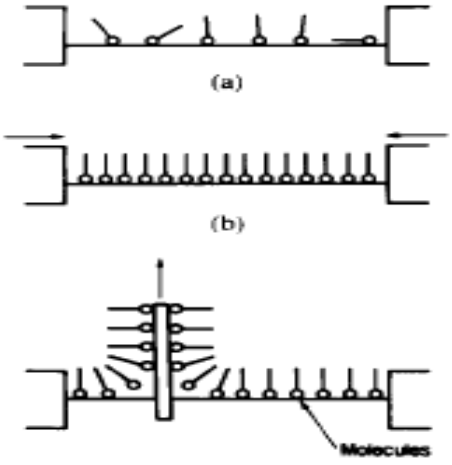

Figure 2.13 Protective film fabrication through LB process [20].

It is also verified through ultraviolet (UV) spectrum tests that moisture exposed and water immersed LB film coated substrates did not take up much moisture, and were an effective method to prevent water vapor from entering into the polymeric structure. Figure 2.14 shows the effects of moisture barriers at 50ºC and 95%RH [15]. Test results revealed that the bare surface gained more moisture in a shorter time.

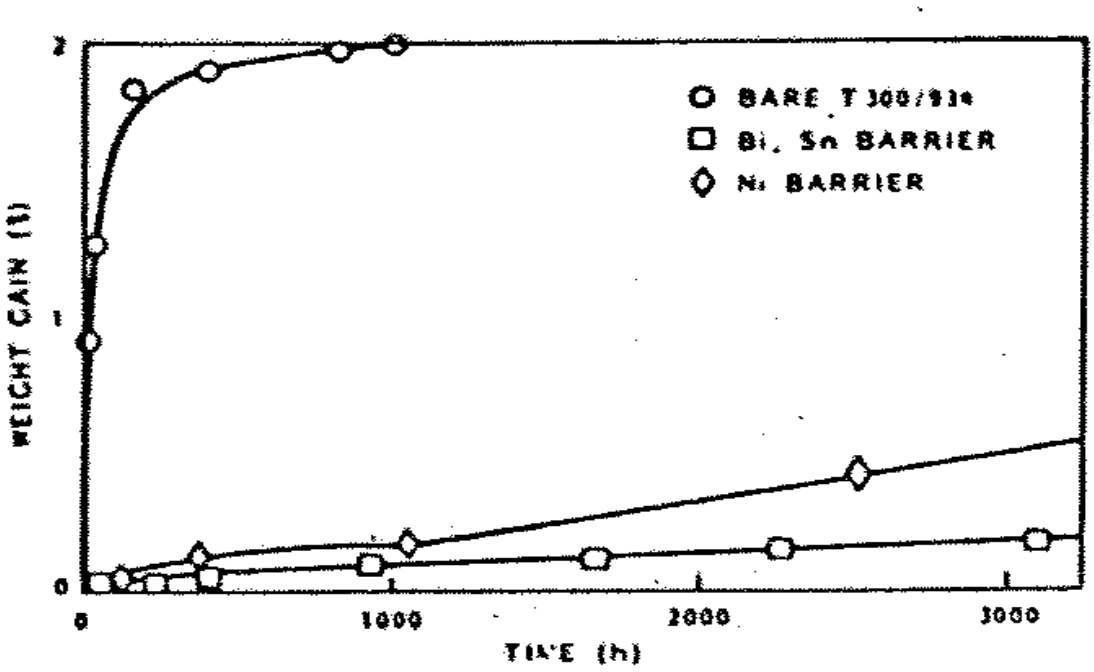

Figure 2.14 Effects of moisture barriers (bare, BiSn and Ni films) at 50 ºC at 95 %RH [15].

In addition to moisture prevention characteristics, moisture barriers are designed to meet functional integrity of the application, and environmental conditions such as high/low temperature, pressure, humidity, and chemical gasses. For example, liquid resistant gloves are used to protect surfaces from chemicals, solvents, toxic materials, and retention of air or gasses. On the other hand, there are also constraints that affect barriers applications, such as temperature, weight, forming to part shape, service life, etc [15].

2.2.3 Methods of Measuring Moisture Content

Barrier films are expected to withstand all matter without changing material properties. These tests are conducted to find out the effectiveness of the barrier films for environmental and service conditions. Abot et al. [6] measured moisture gain for 26 mm thick carbon epoxy composite laminates under three categories: weight gain, moisture expansion, and viscoelastic properties. In these experiments, specimens are first dried at 75°C until the weight loss is stabilized, and then immersed into a water bath until the moisture equilibrium point. The coupons are weighed in a digital scale until the moisture equilibrium is reached. Moisture expansion is measured with a precision micrometer (1.3 μm). A dynamic mechanical analyzer (DMA) is also used to measure viscoelastic behavior (1 Hz and 5°C/min).

Menail et al. [2] quantified moisture barrier properties for polyimide films in three steps. Langmuir-Blodgett (LB) coated specimens were conditioned through a steam chamber at 127◦C and immersed in ionized water prior to the testing for 20 hr at room temperature. After exposure to moisture, the samples were subjected to three tests:

- Water steam
- Tape test
- UV light tests

  UV light tests were conducted before and after the tape test to detect any moisture throughout the spectrum change. Measurement was usually made by using Perkin-Elmer 33.

2.4 Modeling

Statistical distributions are used to describe real composite strength data, such as Weibull and lognormal. However, because of the heterogeneity and structure of composites,

experimental data may not fit well on these distributions. Because of this discrepancy, cumulative damage models are created for a better data reduction.

When there are many independent variables for the process, modeling does not perform well for the wide distribution of data. Having large standard deviation makes the estimation more difficult during the modeling. For a better solution, Stone et al. [21] came up with an additive model (AM) - nonparametric regression. AM uses one dimensional smoother lines to create a restricted class of nonparametric regression. This modeling method estimates an additive guess to the multivariate regression function. There are two advantages of the additive modeling. First, the problem of increasing variance for increasing dimensionality is avoided since each additive is estimated. Second, the estimation of individual parameters gives sufficient information. Later, more generalized additive models developed by Hastie and Tibshirani (1990) allowed response probability to be any member of the exponential family distribution. Some of the common statistical models use this model such as additive models for Gaussian data.

Owen et al. [43] developed a model to predict the tensile strength of a composite based on an exponential cumulative damage (ECD) approach. Table 2.2 gives the expressions for the initial damage and damage model functions for three C-D models.

TABLE 2.2

EXPRESSIONS FOR THE INITIAL DAMAGE AND DAMAGE MODEL FUNCTIONS FOR THREE C-D MODELS

Damage Model	**Initial Damage Expression**	**Damage Model Function**
Additive (C-D)	$W = \Psi - X_0$	$h(u) = 1$
Multiplicative (C-D)	$W = \Psi / X_0$	$h(u) = u$
ECD	$W = \Psi^{(1/\ln(X0))}$	$h(u) = u\ln(u)$

Where W is initial strength of material, Ψ is theoretical strength, X_0 is reduction of theoretical strength by a random amount, and h(u) is assumed damage model function. ECD model is calculated using equation (2.20),

$$Fs(s;L) = P(S \le s) = gauf\left\{ \frac{\mu\sqrt{s}}{\sigma} - \frac{\ln[\ln(\varphi)] - \frac{\sqrt{2L}}{\sqrt{\pi}\,\varphi\ln(\varphi)} - \frac{L\,[\ln(\varphi+1)}{2\,[\varphi\ln(\varphi)]^2}}{\sigma\sqrt{s}} \right\}, s > 0 \quad (2.20)$$

where D is amount of damage at a stress increment, μ and σ are mean and standard deviation of D, φ is theoretical strength of composite specimen and gauf is s-normal Cdf.

Owen used the ECD model to fit two different data sets. The first set of data came from experiments involving strength measurements for coupons based on composite length. The second data set is based on the individual fiber used to evaluate their tensile strengths. For the first set of data, the ECD model's mean squared error (MSE) was much closer to multiplicative Gauss-Gauss model results (Table 2.3). However, for the second set of data, the ECD model's MSE was closer to other models used to fit the data as it seen at Table 2.4 [43].

TABLE 2.3

MSE MEASUREMENT FOR VARIOUS MODELS USING COMPOSITE STRENGTH DATA

Additive Gauss-Gauss	**Multiplicative Gauss-Gauss**	**Power-law Weibull**	**ECD**
0.004983	0.004196	0.008440	0.004252

TABLE 2.4

MSE MEASUREMENT FOR VARIOUS MODELS USING FIBER STRENGTH DATA

Additive Gauss-Gauss	**Multiplicative Gauss-Gauss**	**Power-law Weibull**	**ECD**
0.008108	0.008286	0.008324	0.008464

Owen's model is similar to the cumulative damage (C-D) models (additive Gauss-Gauss, and multiplicative Gauss-Gauss), so the C-D model theory is utilized to find ECD parameters. Owens [43] claims that the ECD model depends more on existing damage parameters than the C-D model functions, and its strength distribution is also tractable.

Li et al. [44] developed a two layer model to predict the tensile strength of particulate filled composites which considered particle size, size distribution, and particle clustering. Li created two layer models by modifying Christensen et al.'s 3 layer model and using the rule of mixture approach. This model includes three phases: particle, matrix, and equivalent medium phase (outside). Uniform matrix layer coated particles are embedded into an infinite equivalent medium as is seen in Figure 2.15.

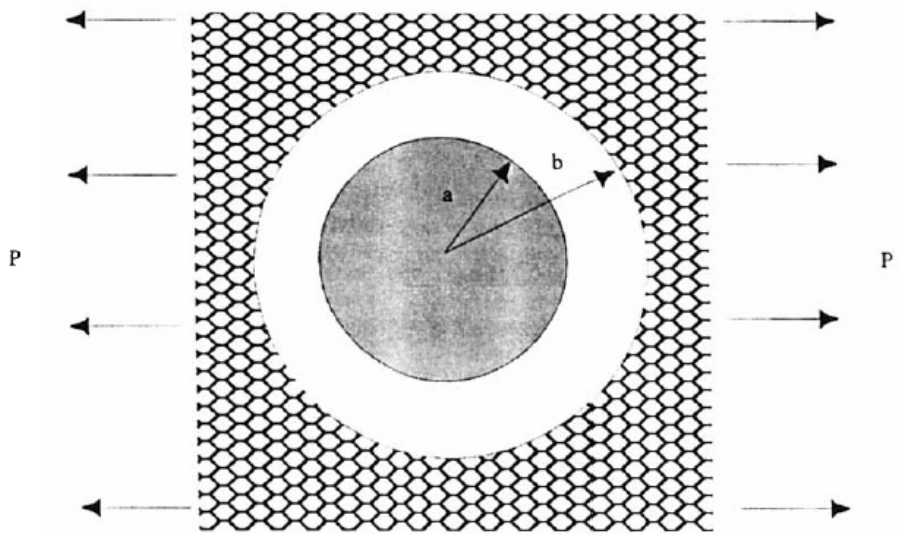

Figure 2.15 Two-layer built-in model [44].

where, a is radius of the particle, b-a is thickness of layer, P is load. Li et al. calculated stress in composite by using equation (2.21),

$$\sigma_{sc} = mf\sigma_{sf} + (1 - f^n)\,\sigma_{sm} \tag{2.21}$$

where σ_{sc} is stress in composite, σ_{sf} is stress in fiber, f is volume fraction of particles in the composites, σ_{sm} is stress in matrix, m : m ε [0, 1] is a parameter that depends on effective

fractions of inclusions, such as number of particles that bonded well on the matrix, and n : n ε [0, 1] is a parameter that depends on degradation of matrix. The model results from literature are compared to experimental results, and they are similar in both cases. Figure 2.16 shows the comparison of the Li et al. model with experimental test results and reference model results from literature [44].

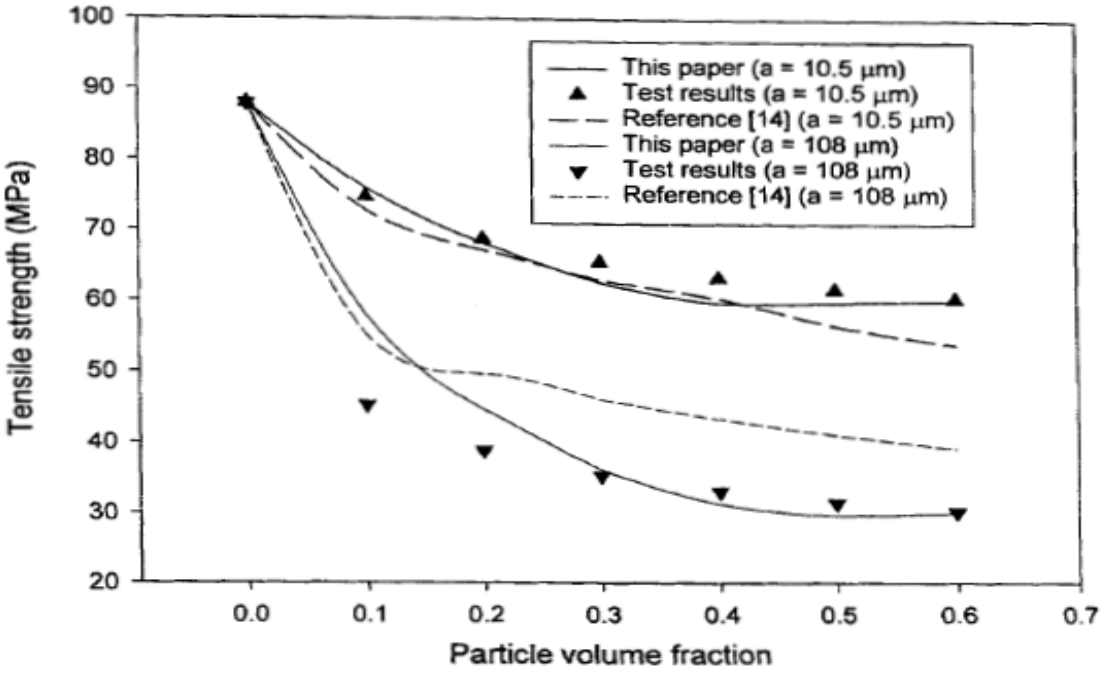

Figure 2.16 Comparison of Li et al. model with experimental test results and reference model results from literature [44].

Chang et al. [24] studied moisture diffusion for finite thickness composite laminates. He modified Fick's first law (Eq.2.22) and calculated moisture content and diffusion depth based on strain. Moisture content was calculated using induced real-time hygric strain with equation (2.22),

$$\frac{\partial c}{\partial t} = D\frac{\partial^2 c}{\partial x^2} \tag{2.22}$$

where D is diffusity constant, t is duration of diffusion, x is the coordinate in the diffusion duration, and c is the weight of the diffusing substance per unit volume of the medium. The relationship c=c(x,t) is a function of x and t, n is an index for a finite thickness composite laminate in which diffusing substances diffuse through both surfaces. Boundary conditions for a plate (h) can be defined through equation (2.23) and equation (2.24)

$$c(-h/2;\ t) = c_{\infty} \tag{2.23}$$

$$c(h/2;\ t) = c_{\infty} \tag{2.24}$$

where c_{∞} is saturated c, and h is the thickness of medium/plate. A gradient dependent model is created, which depends on diffusion process as shown at Figure 2.17.

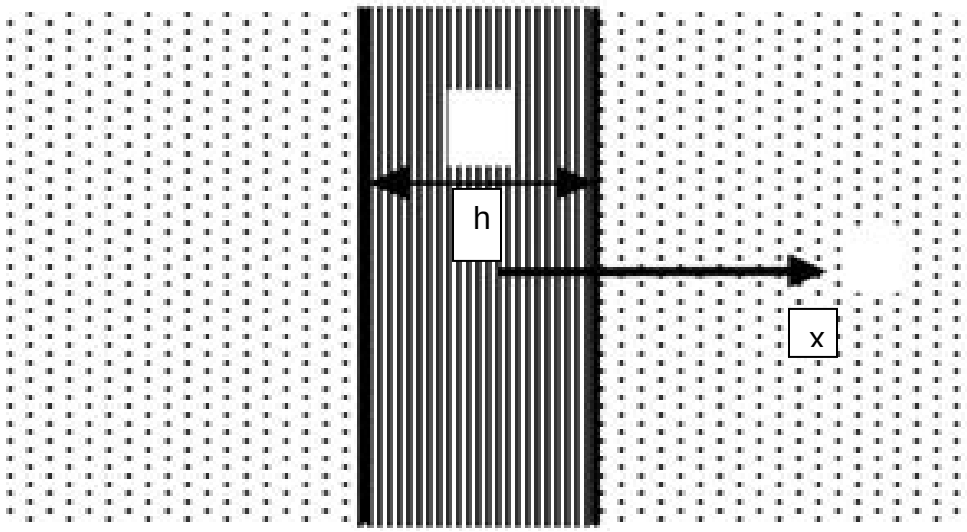

Figure 2.17 Diffusing substances diffusing through both surfaces [24].

The variable c can be derived from Eq. 2.25:

$$c(x,t) = c_{\infty}\left[1 - \frac{2}{\sqrt{\pi}} \sum_{n=1,3,5..}^{\infty} \frac{1}{n}(-1)^{n-\frac{1}{2}} e^{-Dt\left(\frac{n\pi}{h}\right)^2} \cos\left(\frac{n\pi}{h}x\right)\right] \tag{2.25}$$

Experiments are conducted to create proportional hygric strain by diffusing moisture through both surfaces of the laminate. When moisture diffuses into a laminate, it introduces hygric strain which is proportional to the average moisture content (Eq. 2.22). When an advancing boundary is not considered, the hygric strain of the laminate, ε, can be calculated from Eq.2.26 by using Eq. 2.25. Then, hygric strain data, solution parameters, is used for theoretical formulations to obtain the hygric property of the material,

$$\varepsilon(t) = \varepsilon_{\infty}\{1 - \frac{8}{\pi^2} \sum_{n=1,3,5..}^{\infty} [\frac{1}{n^2} - \left(\frac{n\pi}{h}\right)^2 Dr]\} \quad (2.26)$$

where ε is hygric strain, ε_{∞} is saturated hygric strain and r is an index.

Chang et al. [24] conducted experimental diffusion tests on water immersed carbon epoxy composite laminates for hygric strain versus immersion duration. Moisture induced proportional hygric strain, and then hygric strain data was fitted by the theoretical solution to obtain the hygric property of the material, which was used to define the hygric behavior of composite (Figures 2.18). When the experimental data is plotted, it fits the theoretical calculations as it shown in Figure 2.19.

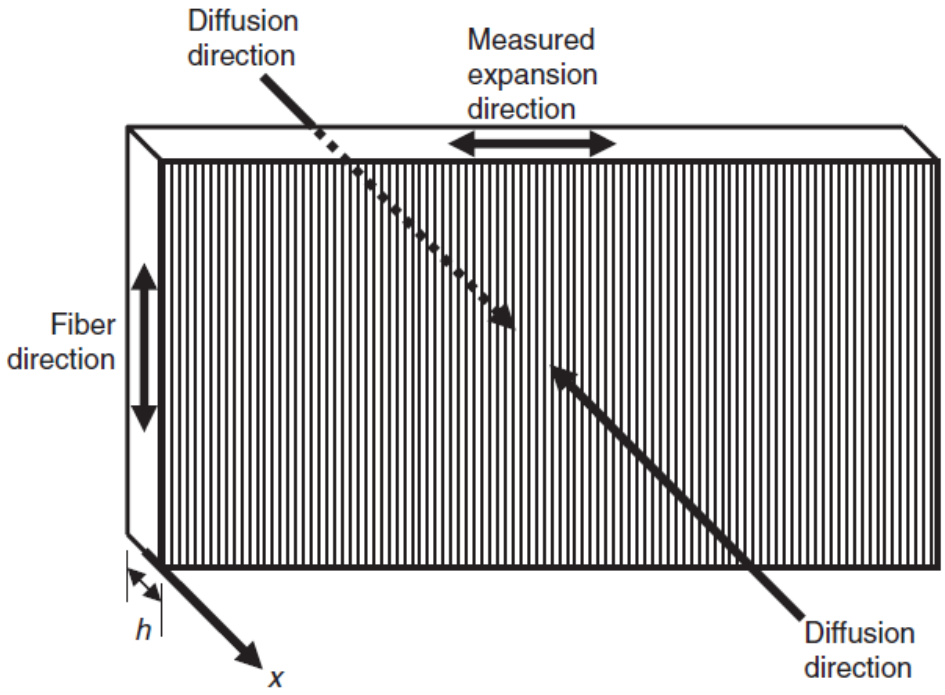

Figure 2.18 Substance diffusing through both surfaces and strain direction [24].

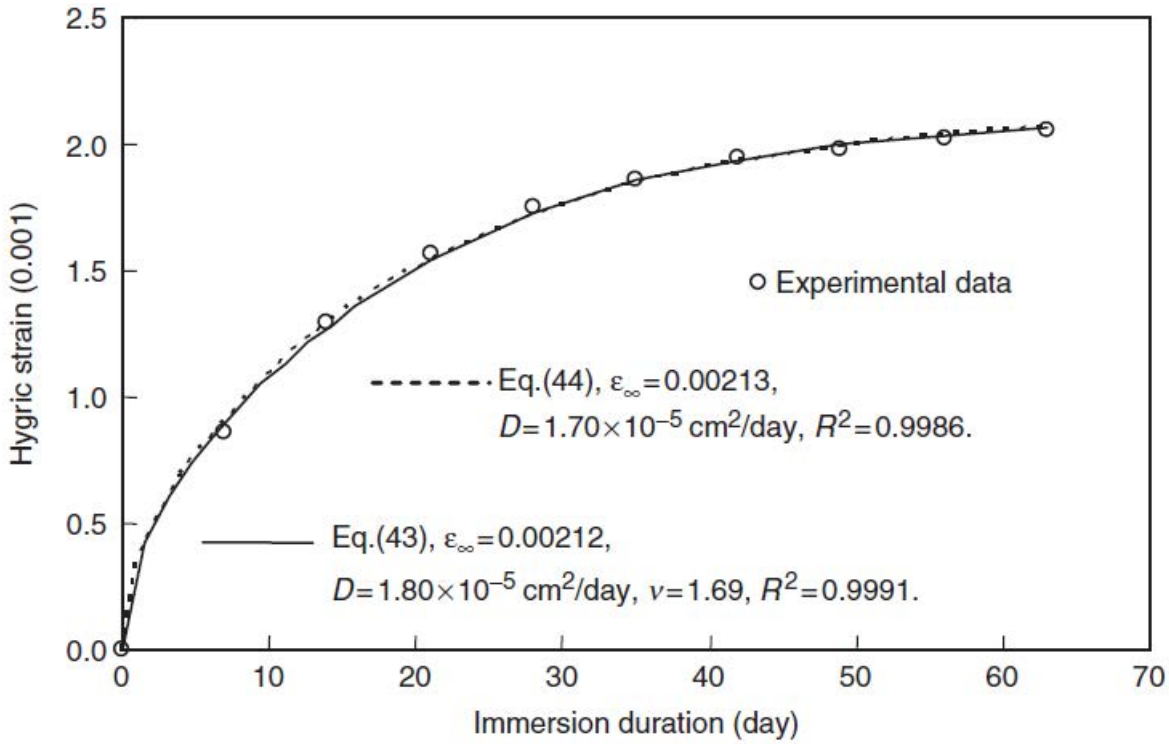

Figure 2.19 Hygric Strain data vs. immersion time test fitted by the theoretical solutions [24].

CHAPTER 3

TECHNICAL APPROACH

3.1 Proposed Approach

Tedlar is the only barrier film used as the outermost ply on aerospace composite laminate and sandwich assemblies. Tedlar is used to prevent water, moisture, chemical, and solvent ingression into the Nomex or metal core area due to its higher water contact angle and strong interfacial bonding properties on composite laminates. In this work, alternative barrier films are investigated. A polyether ether ketone (PEEK) based thermoplastic film, which claimed that has similar preventive properties as Tedlar, has been chosen as the primary alternative. In addition to PEEK film, Kapton and Teflon films are identified as secondary alternatives for Tedlar film replacement. Tedlar applied panel is shown at Figure 3.1.

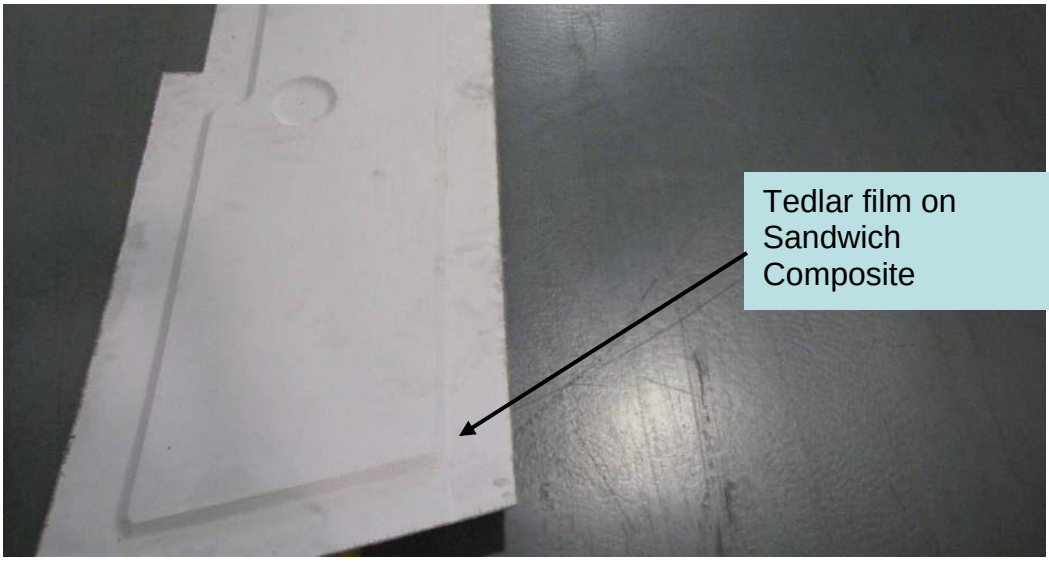

Figure 3.1 Tedlar applied honeycomb assembly with white film color.

3.2 Proposed Moisture Barrier Films

3.2.1 Tedlar

Tedlar is a registered trade mark of DuPont. Its chemical structure is poly vinyl fluoride (PVF) as is shown in Figure 3.2, a thermoplastic fluoropolymer with repeating vinyl fluoride unit, $(CH_2CHF)_n$

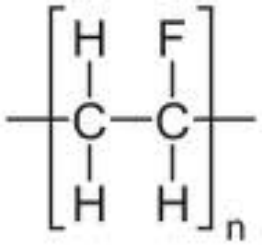

Figure 3.2 Chemical structure of poly vinyl fluoride [25].

A fluoropolymer is a fluorocarbon with multiple carbon-fluorine bonds. The carbon-fluorine bond isthe strongest bond in organic chemistry and it is very short due to its partial ionic character. When more fluorine is attracted to the same carbon element, bond strength increases drastically. A significant polarity/dipole moment is created due to fluorine's higher electro-negativity compared to carbon (4.0 for F vs. 2.5 C). Therefore, electron density is concentrated around the fluorine, leaving the carbon relatively electron poor. This causes an asymmetric distribution of electrons in chemical bonds, with partial charges.

Fluoropolymers can be homopolymers or copolymers. Some monomers used to prepare fluoropolymers are ethylene (E), propylene (P), vinyl fluoride (VF1), vinylidene fluoride (VDF or VF2), tetrafluoroethylene (TFE), hexafluoropropylene (HFP), perfluoropropylvinylether (PPVE), perfluoromethylvinylether (PMVE), and chlorotrifluoroethylene (CTFE). Table 3.1 give the various fluoropolymers, their names, monomers and melting points [25].

TABLE 3.1

VARIOUS FLUOROPOLYMERS AND CHARACTERISTICS

Fluoropolymer	**Trade Names**	**Monomers**	**Melting Point (°C)**
PVF (polyvinylfluoride)	Tedlar	VF1	200
PVDF (polyvinylidene fluoride)	Kynar, Solef Hylar	VF2	175
PTFE (polytetrafluoroethylene)	Teflon, Algoflon, and Polymist	TFE	327
PFA (perfluoroalkoxy polymer)	Teflon. Hyflon	PPVE + TFE	305
FEP (fluorinated ethylene-propylene)	Teflon	HFP + TFE	260
ETFE (polyethylenetetrafluoroethylene)	Tefzel, Fluon	TFE + E	265
FEP (fluorinated ethylene-propylene)	Teflon	HFP + TFE	260

Tedlar initially was produced for building siding as a barrier film for extreme weather conditions. Later, the properties were restructured to meet aerospace applications as a barrier for moisture prevention. Tedlar has excellent resistance to moisture, ultraviolet light (up to 350 nm UV), chemical solvents, acids and bases except ketones, and esters. It is non-staining material and is able to sustain its properties at higher temperatures. Tedlar is available in variety of thicknesses, and is available as film (transparent or pigmented) or powder resin for coating [25]. Some of characteristics of Tedlar are as follows;

- Thermal: Tedlar has a service temperature between -73ºC and 107ºC
- Electrical: It retains good dielectric properties and low dielectric constant

- Chemical: It resists chemicals, solvents, acids, and bases. Tedlar keeps its properties against high temperature solvents including oils, greases, hydrocarbons, and chlorinated solvents.
- Optical: transparent type Tedlar, unaffected by UV.

Table 3.2 shows some of physical properties of Tedlar.

TABLE 3.2

SOME OF THE PHYSICAL PROPERTIES OF TEDLAR (0.0254 MM THICK) [25]

Weight (g/m^2)	**Tensile Strength (MPa)**	**Elongation (%) at 170°C**	**Service Temp. (°C)**
35	41	200	-72 to 107

3.2.2 Polyether Ether Ketone

Polyether ether ketone (PEEK) is a thermoplastic polymer with semicrytalline properties. It is obtained with the step-growth polymerization (SGP) method. First, monomers become dimers, then trimmers, followed by longer oligomers, and then long chain polymers are created as is shown in Figure 3.3 [45].

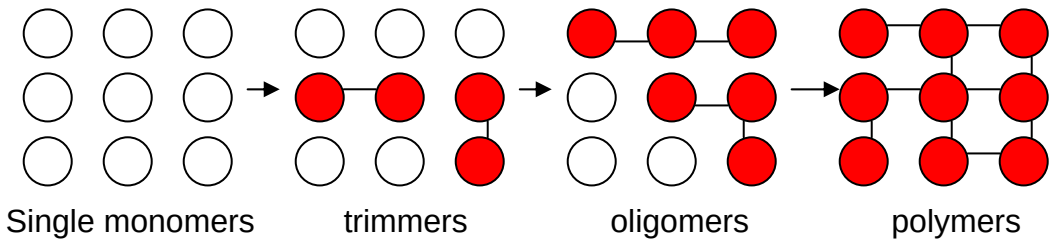

Figure 3.3 Step-growth polymerization (SGP) method [45].

PEEK is very resistant to high temperature and chemical solvents, has a good impact resistance, low coefficient of friction, and the ability to retain tensile and flexural mechanical properties at high temperatures. PEEK is available in many forms, and the most common ones are standard unfilled and fiber filled ones. Some key characteristics of PEEK are given below and shown at Table 3.3:

- Thermal: PEEK has high service temperature up to 143 to 260 ºC
- Electrical: It retains its dielectric properties up to 200 ºC
- Chemical: It has a resistance to organic and inorganic chemical solvents. It is degraded only by concentrated anhydrous or oxidizing agents

TABLE 3.3

SOME OF PHYSICAL PROPERTIES OF PEEK [25]

Density (kg/m^3)	**Tensile Strength (Mpa)**	**Young Modulus (GPa)**	**Elongation (%)**	**Glass Transition Temp (°C)**	**Melting Point (°C)**	**Thermal Conductivity (W/Mk)**
1320	90-100	3.6	50	143	343	0.25

PEEK has broad applications, especially where high temperature properties are in demand. The following are the most common applications:

- Engine components: piston, pump, compressor, and bearing components require good mechanical properties at high temperature service environment.
- Wire insulation: extremely high temperature applications, cable couplings, and connectors.
- Appliances: handles and cooking equipment.
- Medicine: PEEK is a biocompatible material and is used for prosthetics, instruments, and diagnostics.

For this study, PEEK based APTIV film was chosen, which was produced by VICTREX® PEEK™ polymer.

3.3.2 Kapton

Kapton is a polyimide polymer and is produced by condensation of pyromellitic dianhydride and 4.4’-oxydiphenylamine through a step polymerization process. The intermediate polymer, known as a "poly(amic acid)," is soluble. Figure 3.4 shows structure of Polyimide which is a polymer of imide monomers.

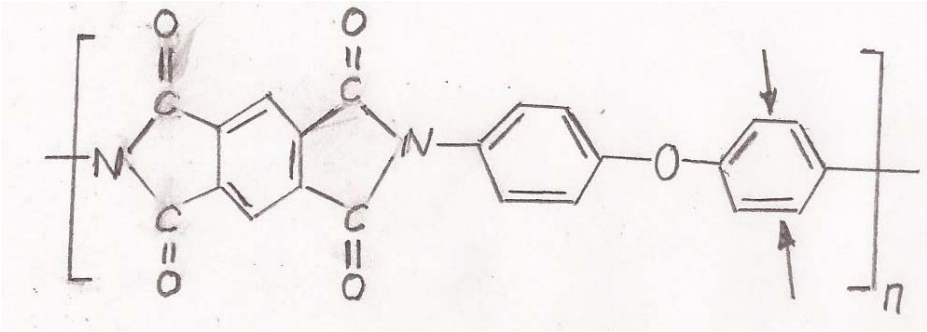

Figure 3.4 The structure poly-oxydiphenylene-pyromellitimide [53].

It has very high service temperature characteristics and isused mainly for;

- Electronics (printed circuits)
- Thermal garments (space suits)
- Electrical wiring (especially for aircraft)
- X-ray sources and detectors

Some key characteristics of Kapton are as follows:

- Thermal: high conductivity, $4.638\times10^{-3}\ T^{0.5678}\ \mathrm{W\cdot m^{-1}\cdot K^{-1}}$
- Electrical: good dielectric qualities
- Chemical: good chemical resistance to organic solvents.

In this study, Kapton samples produced by Du Pont were used as thin films.

3.2.4 Teflon

Teflon is polytetrafluoroethylene (PTFE), a fluorocarbon, which is a synthetic fluoropolymer of tetrafluoroethylene. Fluorocarbon has only carbon and fluorine atoms (Figure 3.5). PTFE is a super-hydrophobic material and it is non-polar. Molecules that are not attracted to water are called hydrophobic. In this study, thin Teflon samples produced by Du Pont were used. Table 3.4 gives some of the properties of Teflon.

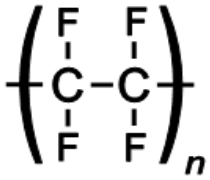

Figure 3.5 Teflon chemical structure [25].

TABLE 3.4

SOME OF THE PROPERTIES OF TEFLON [25]

Molecular Formula	**Density (kg/m^3)**	**Tensile Strength (MPa)**	**Elongation (%)**	**Glass Transition Temp. (°C)**	**Melting Point (°C)**	**Thermal Conductivity (W/Mk)**
$(C_2F_4)_n$	2200	31	450	160-240	327	0.25

3.3 Testing

To determine moisture barrier characteristics, a series of tests were conducted on test coupons that were subjected to moisture absorption through direct immersion in a variety of liquids. For comparative testing, three types of prepreg materials were used, including carbon, Kevlar, and glass with epoxy resins. Characteristics of prepreg raw materials are given in Table 3.5. Evaluation was conducted by comparative analysis of the panels fabricated with Tedlar,

alternative barrier films, and without any barrier film. Test panel types and matrixes are also shown in Table 3.6.

TABLE 3.5

MATERIALS USED FOR THE TEST PANEL FABRICATION

Materials	**Manufacturers**
Carbon prepreg	Cytec E7K8 PW-3K-193 Epoxy Prepreg
Kevlar prepreg	Hexcel F161 Epoxy with 285K Aramid Fiber
Glass prepreg	JD Lincoln L552FR Epoxy with 1581 Glass Fiber
Honey Comb Core	Hexcel 3.0 lb/ft^2, 0.375 inch thick core
Film Adhesive	Cytec FM 300 GR 50
Tedlar	Du Pont, 0.025 mm thick (both surfaces plasma treated)
PEEK-1	APTIV film , by VICTREX® PEEK™, 0.025 mm thick (surface plasma treated)
PEEK-0.5	APTIV film , by VICTREX® PEEK™, 0.0125 mm Thick (surface plasma treated)
Teflon	Dupont, 0.025 mm thick (no surface treatment)
Kapton	Dupont, 0.025 mm thick (both surfaces plasma treated)

TABLE 3.6

TEST TYPES, CONDITIONS, AND METHODS

Test #	Test Type	Test Method	Conditioned	# of Coupons	Testing Environment
1	3-point Bend	ASTM D2344	Water	4	RT
2	4-point Bend	ASTM D7249	Water/fuel	4	RT
3	Compression	ASTM D695	Water/fuel	4	RT
4	Paint Tape Test	ASTM D3359	RT	3	RT
5	Moisture	ASTM D5229	Water 82°C /95%	2	RT
6	Contact Angle	ASTM D7490	NA	1	RT
7	Shrinkage	NA	NA	2	176°C
8	Bonding	NA	NA	2	176°C

3.3.1 Test Matrix and Panel Fabrication

The following test panels were fabricated and tested for the characterizations of the different barrier films. Table 3.7 gives the test panel types and their features.

TABLE 3.7

TEST PANEL TYPES AND THEIR FEATURES.

Test Panel ID [2]	**Material Type**	**Style**	**Ply Number**	**Barrier Film**
AA-1C	Carbon	PW-193-3K	see note 1	none
AA-1K	Kevlar	285 K	see note 1	none
AA-1G	Glass	1581	see note 1	none
AA-2C	Carbon	PW-193-3K	see note 1	Tedlar, 0.025 mm
AA-2K	Kevlar	285 K	see note 1	Tedlar, 0.025 mm
AA-2G	Glass	1581	see note 1	Tedlar, 0.025 mm
AA-3C	Carbon	PW-193-3K	see note 1	PEEK, 0.0125 mm
AA-3K	Kevlar	285 K	see note 1	PEEK, 0.0125 mm
AA-3G	Glass	1581	see note 1	PEEK, 0.0125 mm
AA-4C	Carbon	PW-193-3K	see note 1	PEEK, 0.025 mm
AA-4K	Kevlar	285 K	see note 1	PEEK, 0.025 mm
AA-4G	Glass	1581	see note 1	PEEK, 0.025 mm
BB-1C	Carbon	PW-193-3K	4	none
BB-1K	Kevlar	285 K	4	none
BB-1G	Glass	1581	4	none
BB-2C	Carbon	PW-193-3K	4	Tedlar, 0.025 mm
BB-2K	Kevlar	285 K	4	Tedlar, 0.025 mm
BB-2G	Glass	1581	4	Tedlar, 0.025 mm
BB-3C	Carbon	PW-193-3K	4	PEEK, 0.0125 mm
BB-3K	Kevlar	285 K	4	PEEK, 0.0125 mm

TABLE 3.7 (Con't.)

BB-3G	Glass	1581	4	PEEK, 0.0125 mm
BB-4C	Carbon	PW-193-3K	4	PEEK, 0.025 mm
BB-4K	Kevlar	285 K	4	PEEK, 0.025 mm
BB-4G	Glass	1581	4	PEEK, 0.025 mm
CC-1C	Carbon	PW-193-3K	14	none
CC-1K	Kevlar	285 K	11	none
CC-1G	Glass	1581	11	none
CC-2C	Carbon	PW-193-3K	14	Tedlar, 0.025 mm
CC-2K	Kevlar	285 K	11	Tedlar, 0.025 mm
CC-2G	Glass	1581	11	Tedlar, 0.025 mm
CC-3C	Carbon	PW-193-3K	14	PEEK, 0.0125 mm
CC-3K	Kevlar	285 K	11	PEEK, 0.0125 mm
CC-3G	Glass	1581	11	PEEK, 0.0125 mm
CC-4C	Carbon	PW-193-3K	14	PEEK, 0.025 mm
CC-4K	Kevlar	285 K	11	PEEK, 0.025 mm
CC-4G	Glass	1581	11	PEEK, 0.025 mm
DD1	Tedlar			Tedlar, 0.025 mm
DD2	PEEK-05			PEEK, 0.0125 mm
DD3	PEEK-1			PEEK, 0.025 mm

Notes:
1. See Figure 30 for panel configuration
2. AA: Sandwich laminate, BB: 4 ply laminate, CC: 11 or 14 ply laminate, DD: Barrier film

Test panels were fabricated using prepreg materials of different kinds. A typical composite prepreg is a 0.13 mm to 0.38 mm thick sheet consisting of reinforcement and resin together for curing. The prepreg material is in a partially cured stage (B-stage). Prepreg raw material comes from the manufacturer in rolls with a width range of 0.3 m to 1.5 m and is kept in freezer storage under 0°C until lay-up time. Test panel thickness was chosen based on

recommended test methods. Ply number and panel thickness are defined in Table 3.7. Prepreg material sheets were cut to the required panel size, 33x33 cm. Hand cut carbon, glass, and Kevlar prepreg plies were layed up on a tool without any vacuum compaction. Barrier films were layed-up as the last ply on the bag side. After the panel layup was completed, it was covered with release film, which prevents resin contacting and bleeding into the breather material. Typical release material is 0.05 mm thick nylon or FEP film. For this lay-up, panels were covered with Airtech PTFE release film, Wrighton 5400. Breather material was placed over the release film to provide an air path for the cure gasses to escape. Typical breather material can be dry glass fabrics or up to 0.5 cm polyester pads. For this lay-up, Airtech N10 polyester breather was used. The part was bagged with a nylon vacuum bag and sealed to the tool with tacky tape to prevent outside gasses going into the layup. Approximately 1 atm vacuum was applied to the bagged assembly to evacuate air from the bag, and then the part was ready for curing.

A minimum of 54 cm-Hg vacuum was applied to the bagged test panels, which were then placed into the autoclave for curing. A heating rate of 1-4°C / minute was applied until cure temperature of 176 °C. When pressure inside the autoclave reached 103 kPa, vacuum ports were vented to the atmosphere. Pressure increased to 586 kPa and test panels were cured at 176°C / 586 kPa for 2 hours for laminates and 2 hours at 176°C / 200 kPa in autoclave for sandwich structures.

For this study, 1.25 cm thick aluminum tooling plates were used as the layup tool. The layup tool must be resistant to the cure temperature and pressure. The tool surface is prepared with Zyvax mold release to prevent resin from sticking to the tool surface. Figure 3.6 shows laminate configuration and bagging of a prepreg laminate in composite manufacturing. Figure

3.7 shows sandwich structure lay-ups and their progress (Figures 3.8 and 3.9) before an autoclave cure (Figure 3.10).

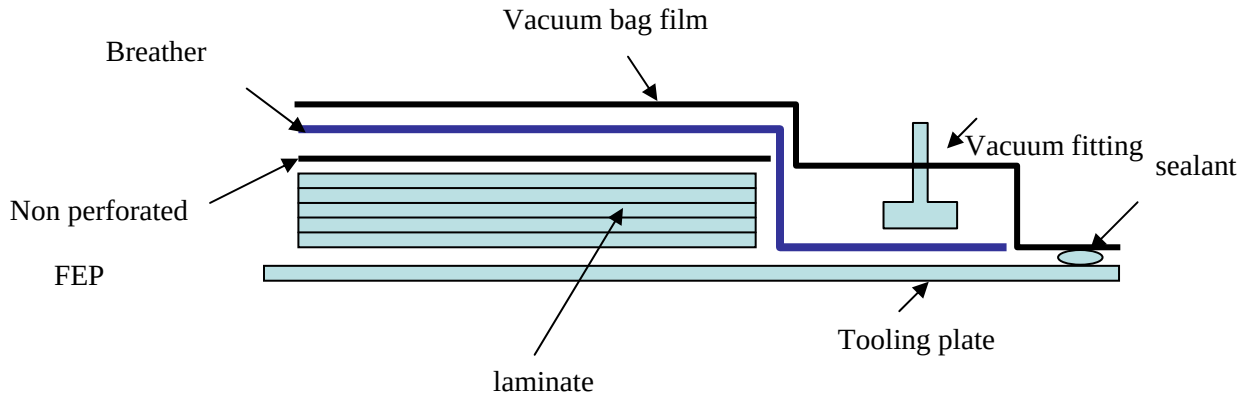

Figure 3.6 Laminate layup configuration and bagging for curing of laminate composites.

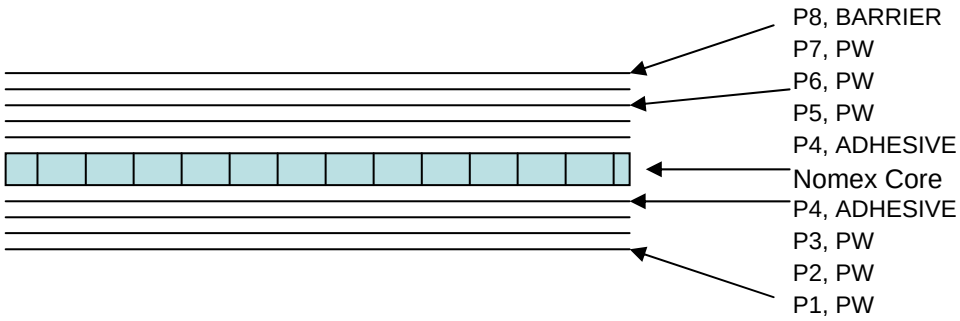

Figure 3.7 Sandwich panel layup configuration for the honeycomb composites

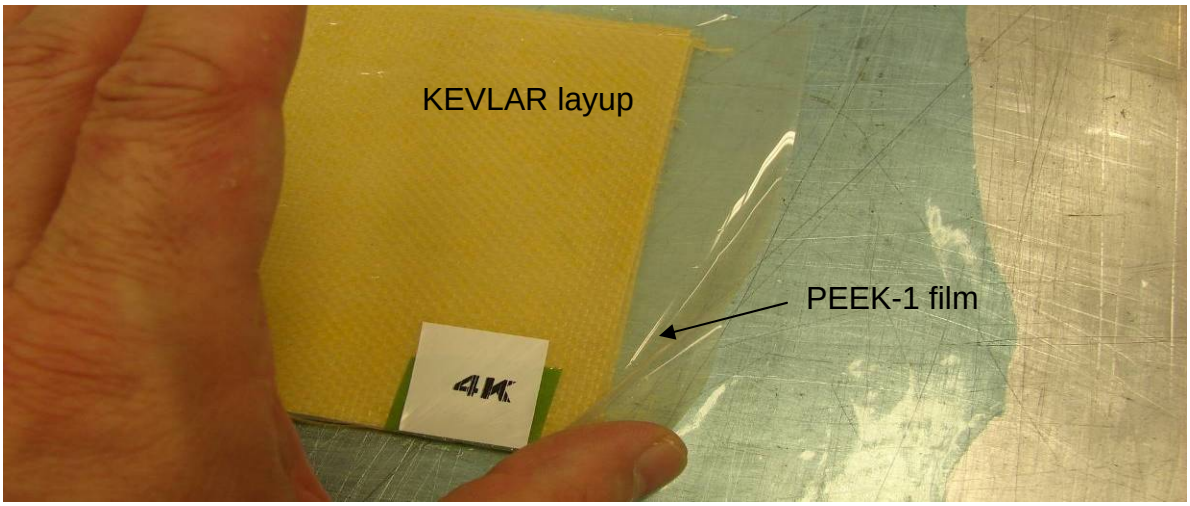

Figure 3.8 Laying-up barrier PEEK-1 film on Kevlar laminate as a last ply

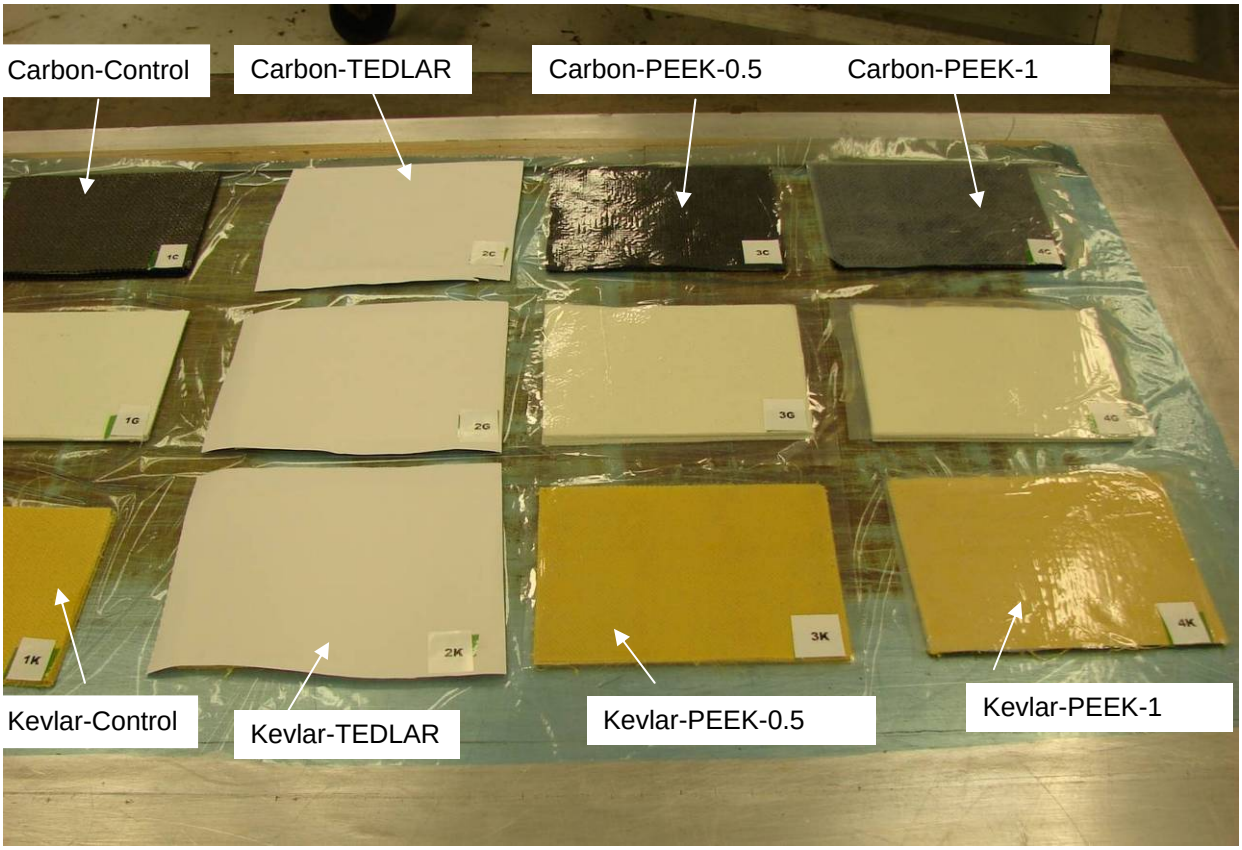

Figure 3.9 Panels layed up and covered with PTFE release films prior to the autoclaving

Figure 3.11 shows the autoclave cured composite test panels prior to debagging and further processing. These composite panels will be ready for future mechanical and other physical characterizations.

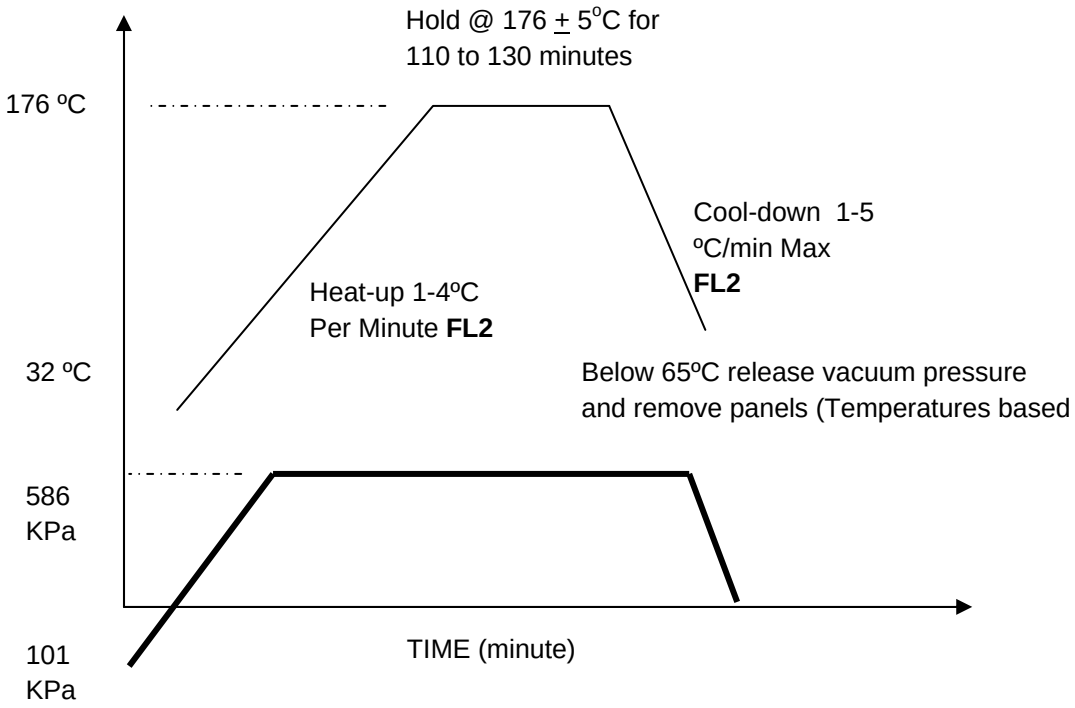

Figure 3.10 Autoclave cure program for the composite panel fabrications.

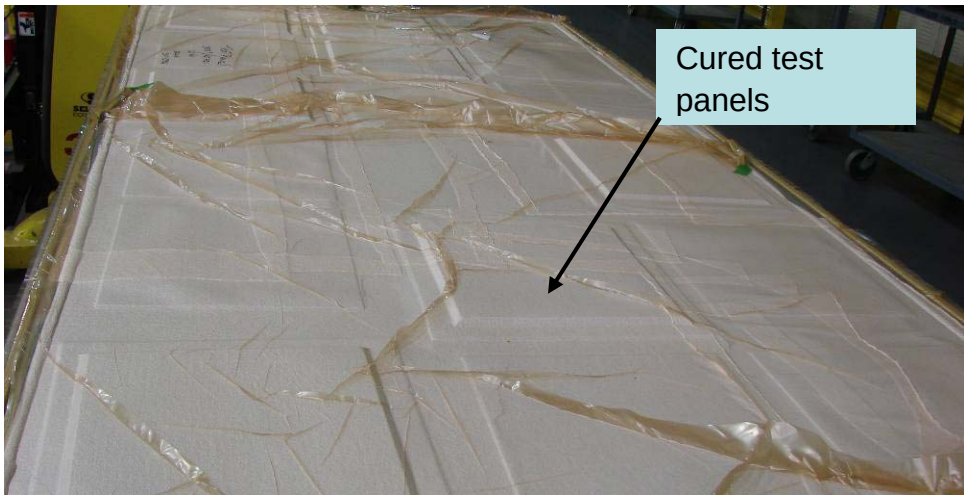

Figure 3.11 Autoclave cured composite test panels prior to debagging.

3.3.2 Test Methods

3.3.2.1 The 3-Point Bend (Short Beam Shear, SBS) or Interlaminar Shear Strength

The SBS test method provides shear strength properties of the composite materials. For the SBS test, ASTM D 2344 is referenced [28]. Specimens are machined from the laminate by cutting to 6.35 mm width x 25.4 mm length. The support span four times specimen thickness, and experimental setup occurs prior to the testing. Specimen length is defined as at least seven times the specimen thickness. The test coupon is located on the span support pins and center loaded during the testing. Calculation of the flexural shear stress, τ_f, for a rectangular cross section, equation (3.1) is used.

$$\tau_f = \frac{3P}{4bd} \tag{3.1}$$

where, τ_f is shear stress mid-plane of the beam, (MPa), P is load at a given point on the load deflection curve (N), L is support span(mm), b is width of beam (mm), d is the thickness of beam (mm). Coupon dimensions are 6.35 mm width by 25.4 mm length, and L = 4d. Figure 3.12 shows the 3-point bend test configuration for the laminate composite panels.

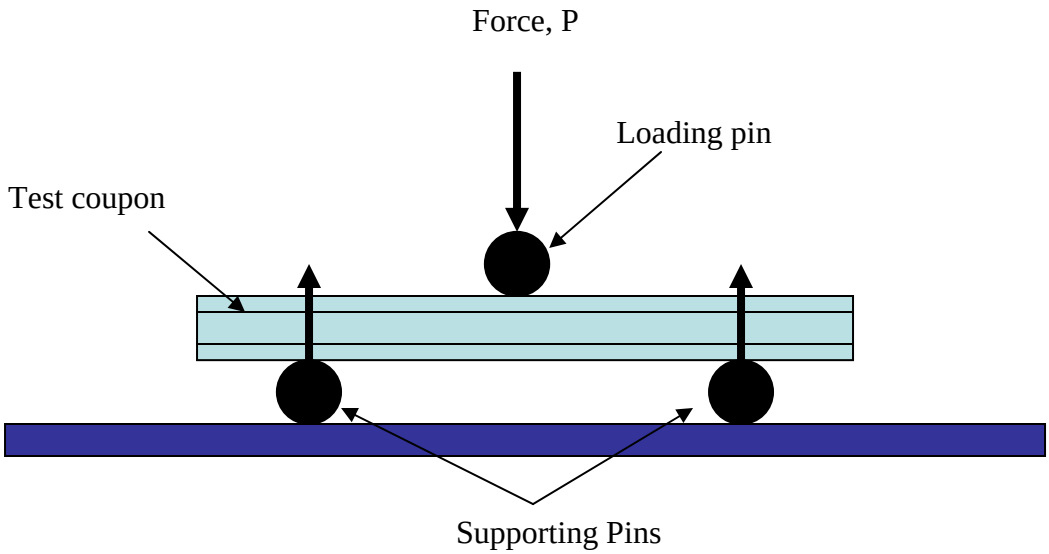

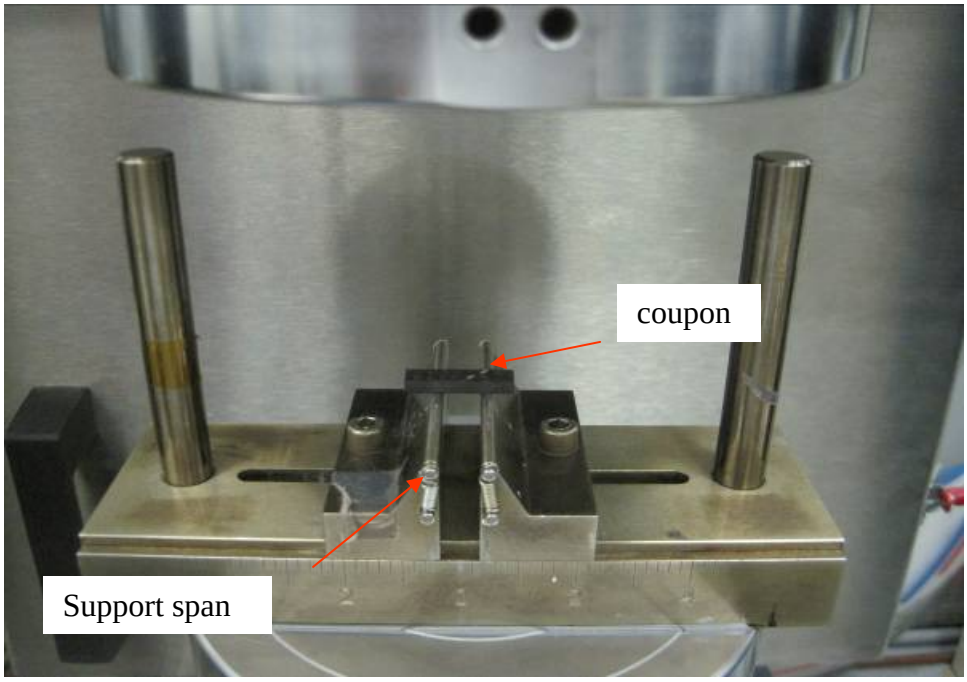

Figure 3.12 The schematic view of 3-point bend testing (above) and the laminate panel in the load frame.

3.3.2.2 The 4-Point Bend Tests

For this test, ASTM D 7249 test method is referenced [46]. The 4-point bend test provides information about facing properties of flat sandwich structures that are subjected to flexure. It is used to verify sandwich flexural stiffness, the core shear strength, and facing strength data for structural design allowables. A coupon is loaded with two heads. Face sheet failure is the only acceptable failure mode. Failure in core or between core and skin is not acceptable [26]. Flexural strength is calculated with equation 3.2,

$$\sigma = F(S-L)/(2(d+c)bt) \tag{3.2}$$

where σ is stress in outer fibers at midpoint (MPa), F is load at a given point on the load deflection curve (N), S is support span length between support pins (mm), L is loading span length (mm), t is nominal facing thickness (mm), b is width of beam (mm), and d is thickness of beam (mm). Setup dimensions include 10.16 cm loading span, 25.4 cm support span. Figure 3.13 shows the 4-point bend test configuration for the honeycomb composite samples.

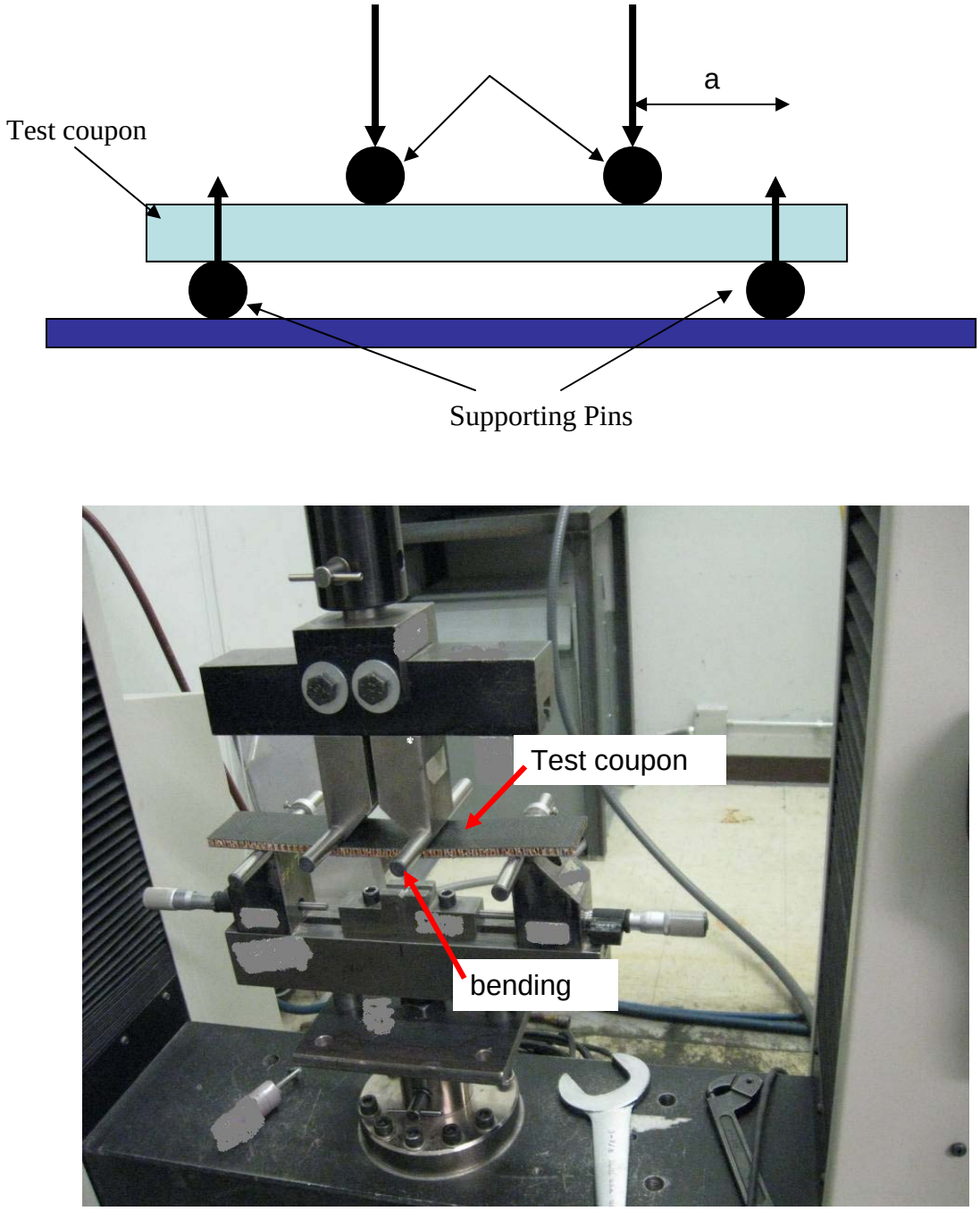

Figure 3.13 Schematic views of the 4-point flexure test (above) and the honeycomb sandwich composite in the load frame.

3.3.2.3 Compression Tests (Sandwich)

This test provides compressive properties of a coupon when subjected to compressive load [30]. Stress is calculated by using equation (3.3),

$$\sigma = F/(ab) \tag{3.3}$$

where, σ is stress (MPa), F is load at a given point on the load deflection curve (N), a is width of specimen (mm), and b is thickness of beam (mm). Coupon dimensions include 2.54 cm width, 13.97 cm length, and a 1.27 cm gage area. Figure 3.14 shows the compression setup for the sandwich structured panels.

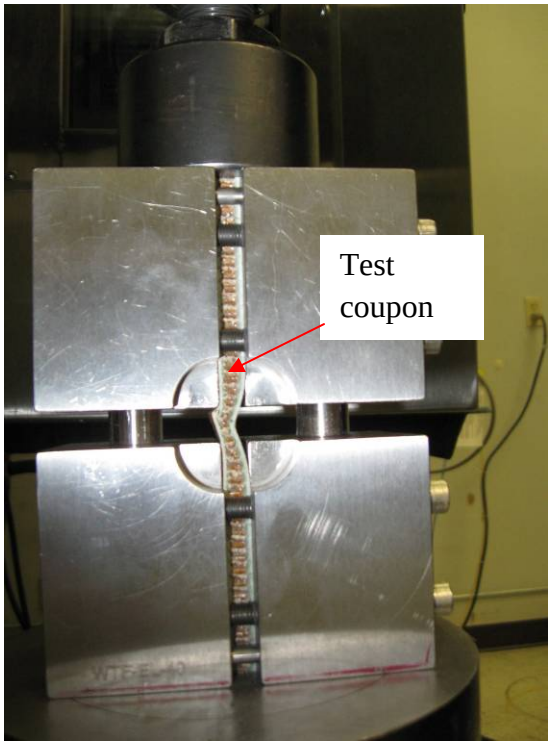

Figure 3.14 Compression testing of the sandwich structured Kevlar composite: it is buckling.

3.3.2.4 The Paint Tape Test

ASTM D3359 [31] is referenced to conduct tape test on the coatings and barrier films. This test provides paint adhesion properties of the composite samples. Cuts, v-shape and a minimum of 5 cm in length, are made with a sharp metal blade on the test samples and then the

samples are conditioned in a salt chamber for 128 hrs. A 2.54 cm width special tack tape was pressed firmly on the cut sections without any air gap. After 10 seconds, the tape was quickly pulled away from the composite surface. The sample is evaluated by quantifying the areas of paint removed. If there is no paint indication on the peeled tape surface, the paint bond is acceptable for adhesion of the films and coatings on the composite surface. If the paint on the composite (control) or barrier film comes off with tape, the coupon has failed on the tape test for the paint adhesion. Figure 3.15 shows the paint tape test and salt chamber [32].

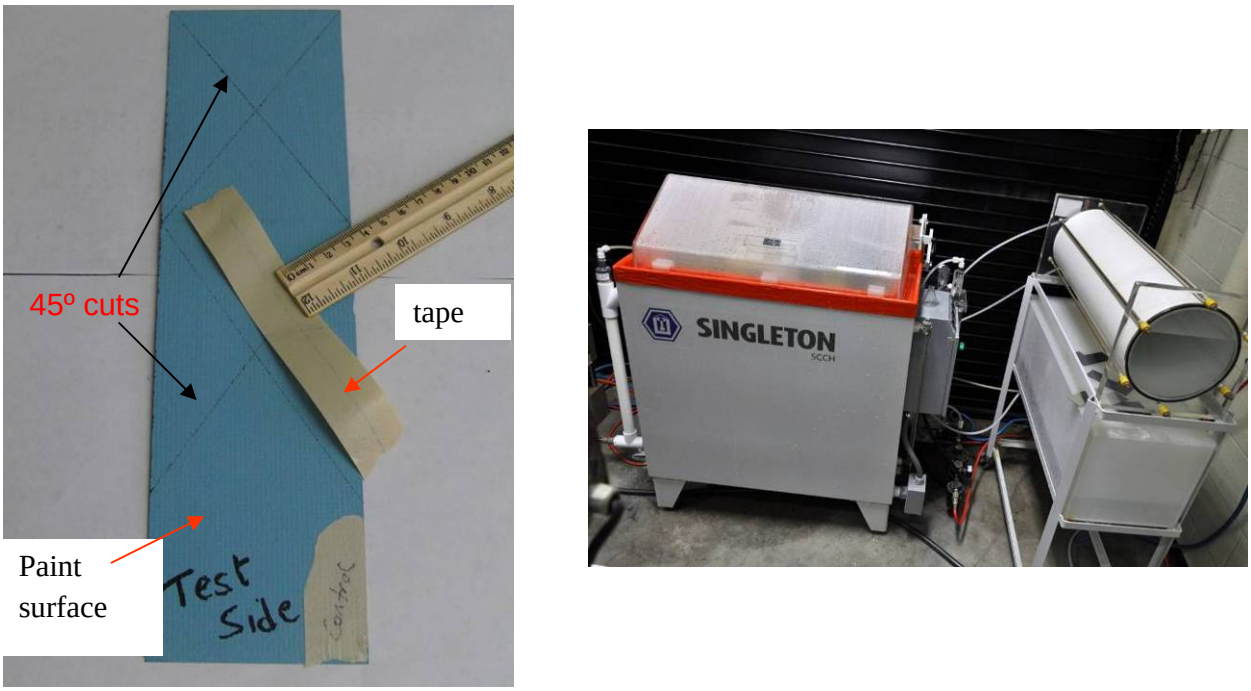

Figure 3.15 Paint tape (left) and Singleton salt chamber tests for the paint adhesion test (Wichita State University, WSU).

3.3.2.5 Moisture Ingression

ASTM D5229 is referenced for the moisture ingression tests [52]. Test coupons are cut from the composite panels and conditioned through the referenced method. Coupon weight is monitored for a maximum three day interval until the equilibrium weight is reached.

Equilibrium is reached when the average moisture content of the traveler specimen changes by less than 0.05% for two consecutive readings within a span of 3 ±0.5 days per equation 3.4.

$$(W_i - W_{i-1})/W_b < 0.0005 \quad (3.4)$$

where W_i is weight at current time, W_{i-1} is weight at previous time, and W_b is baseline weight prior to the conditioning.

3.3.2.6 Contact Angle

The wettability is a quantifiable characteristic that indicates a particular solid or substrate surface's capacity for adhesion or repellence. Repellency properties can be quantified through the contact angle measurement. Molecules that are not attracted to water are called hydrophobic. Hydrophobicity depends on the polarity of molecules. When electrical charges are separated in a molecule, multiple moments are established; this is called polarity. Water is a polar molecule due to sharing of its electrons unequally between atoms.

Contact angle (θ) is the angle formed by the liquid where the liquid and a solid intersect in a gas atmosphere at a triple point (solid-liquid-gas) [33], [34], [35]. It quantifies wetting characteristics of the solid by the liquid. Based on Young's definition, the shape of a liquid droplet on a solid is given in Figure 3.18 where the liquid droplet stays on the surface and orients to air with a contact angle. The equilibrium between the three interfacial energies can be expressed by Young's equation (3.5) which incorporates the contact angle. Schematic view of a water droplet on the surface of solid is shown at Figure 3.16

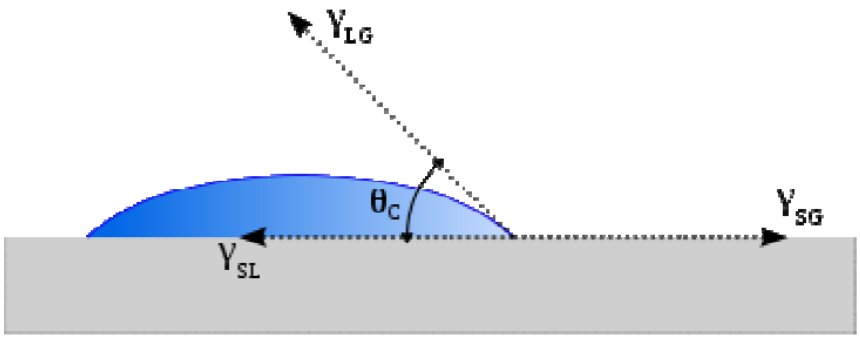

Figure 3.16 Schematic view of a water droplet on the surface of solid [33].

$$\gamma_{SG} = \gamma_{SL} + \gamma_{LG}\cos\theta \tag{3.5}$$

Equation (3.5) defines γ_{SG} at which γ_{SG} is the interfacial tension between the solid and gas, γ_{SL} is the interfacial tension between the solid and liquid, and γ_{LG} is the interfacial tension between the liquid and gas. Figure 3.17 shows the contact angle vs. wetting characteristics of water on three materials with different surface energies. Low contact angle indicates better wetting properties and stronger bonding. When the θ is higher than 90º, the solid is described as a non-wetting material, and 0º angle represents complete wetting.

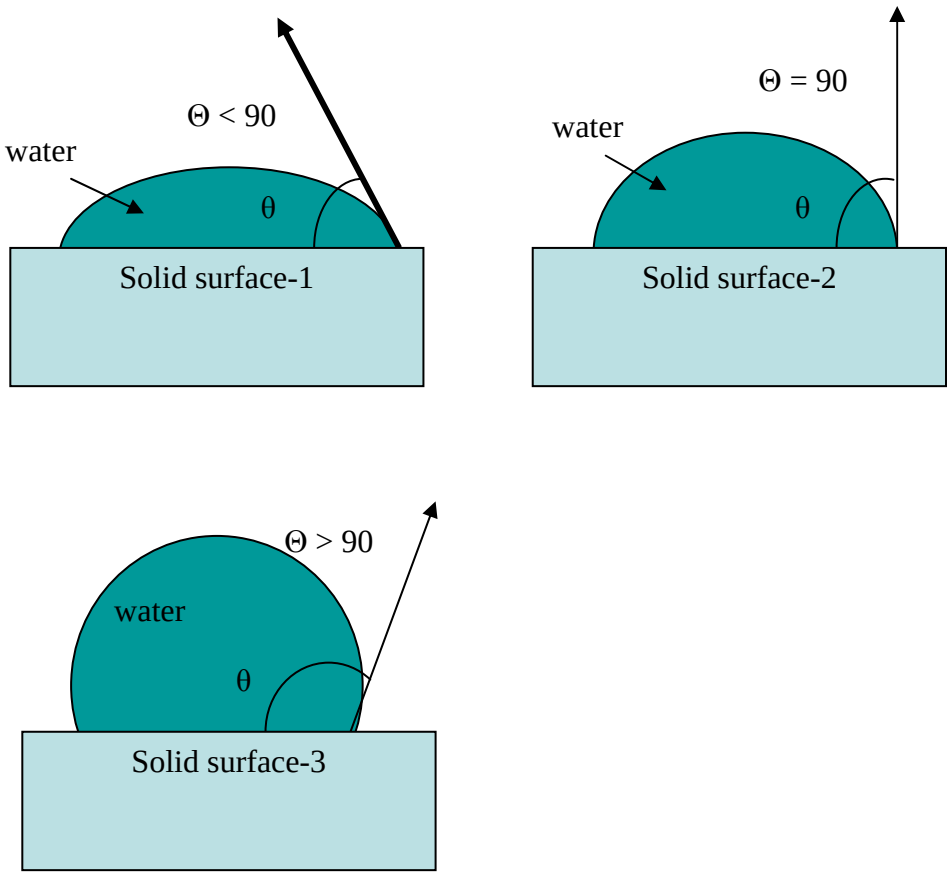

Figure 3.17 Wetting characteristics of water on different solid surfaces (hydrophilic: below 90º, hydrophobic: 90-150º, and superhydrophobic: 150-180º).

Hydrophobic surfaces where the contact angle is between 90 and 150º have low surface energies, such as PTFE (~115 º). Surface energy can be defined as the excess energy on the surface molecules which are not fully bonded compared to the bulk material. The less the surface energy, the fewer the interactions that happen with molecules. That is why PTFE has less potential to bond with other materials. Surface energy is quantified with contact angle [36].

For these tests, contact angles were measured by CAM 100 (KSV Instruments Ltd.). CAM 100 is a compact CCD camera-based instrument for measuring contact angles of liquids on solids and the free surface energy of solids. The samples were placed on the platform, and then a

drop of water was placed on the surface by a syringe needle. After the liquid droplet formed on the composite surfaces, a photograph was taken and imaged for the contact angle measurements. The software then used an applicable formula (Young-Dupre equation) to automatically determine the water contact angle. Drop shape analysis software provides user independent and robust error free measurements with reproducible results. Figure 3.18 shows a CAM 100 contact angle meter used for measuring contact angles on sample surfaces (WSU). Figure 3.19 shows the sample image of a contact angle measured on the glass fiber laminate coated with Tedlar barrier film before UV exposure.

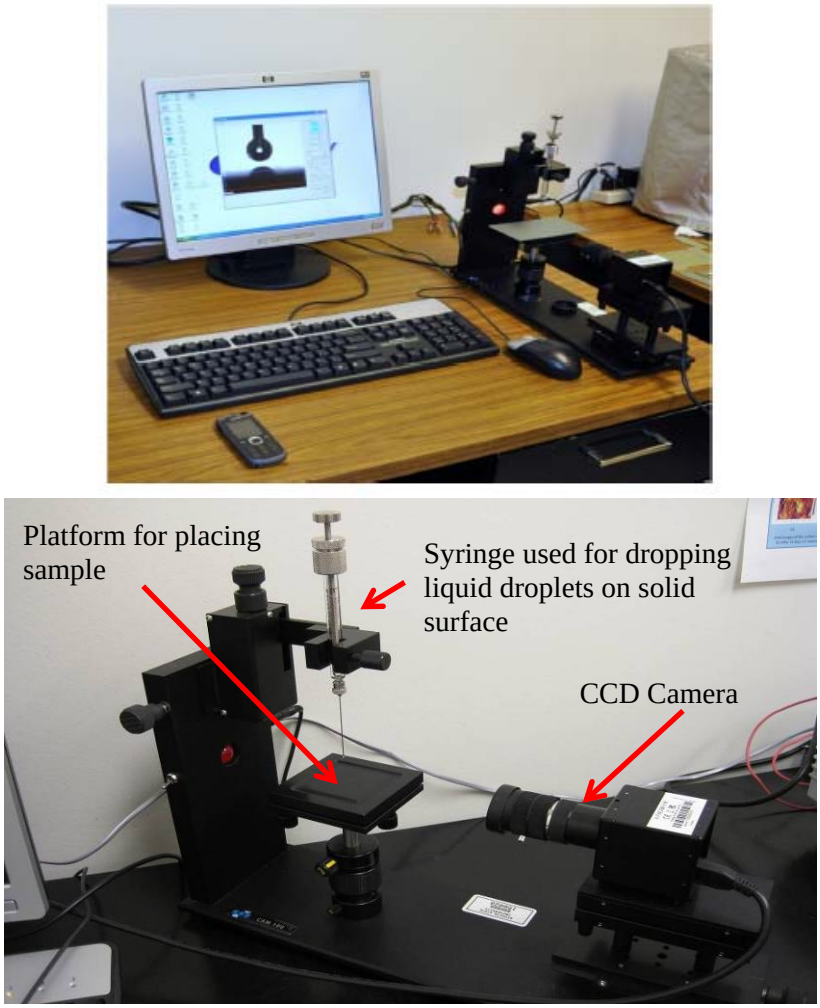

Figure 3.18 CAM 100 contact angle measurement device used to measure the contact angle values of the surfaces (Wichita State University).

a

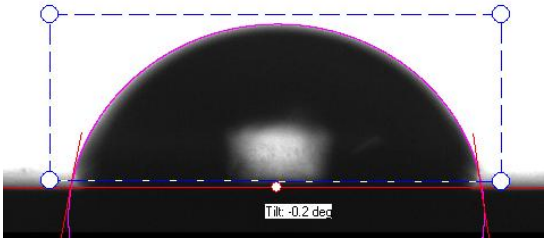

b

Measured values

Time [s]	CA [left]	CA [Right]	CA [Mean]
0.00	82.39	82.62	82.51
1.00	81.96	82.87	82.41
2.00	80.49	81.67	81.08
3.00	77.63	79.08	78.36
4.00	77.66	79.43	78.55
5.00	80.13	81.01	80.57
6.00	78.57	78.28	78.43
7.00	76.67	77.07	76.87
8.00	79.18	79.97	79.57
9.00	79.65	80.71	80.18
Average	79.43	80.27	79.85
Min	76.67	77.07	76.87
Max	82.39	82.87	82.51
Range	5.72	5.80	5.64
Stdev	1.87	1.87	1.85

Figure 3.19 Sample image of a contact angle measured on glass fiber laminate coated with Tedlar before the UV exposure (a), and the contact angle report generated by the software (b).

3.3.2.7 Shrinkage

Shrinkage properties of a film are characterized by exposing samples to heat. First, the barrier films are cut into the desired dimensions and then the specimens' lengths and widths are measured. Second, one end of each specimen is taped onto the tool surface and the samples are placed in the oven at 176ºC for 2 hours. After the conditioning at high temperature, length and width are re-measured to verify shrinkage characteristics.

3.3.2.8 Bonding

Bonding characteristics of the barrier films to the laminate are quantified during the laminate curing. In this test, the barrier films on the composite surfaces are removed by tape as is explained in the paint tape test.

3.3.3 Test Results

The 3-point bend, 4-point bend, and compression test specimens were conditioned by fully immersing them in water. The water conditioning duration was 29 days at 22± 2°C for the 3-point specimens and 14 days for the 4-point and compression test specimens. Water exposure duration was determined for the composite laminates based on the control coupons (no barrier

films applied) that were conditioned until the moisture equilibrium was reached. As the second fluid type, Skydrol was also used in these tests. The 4-point bend and compression coupons were fully exposed to Skydrol for 168 continuous hours (1 week). To ensure that the moisture diffused only through the barrier film side, the unprotected bottom sides of the laminate test panels were coated with polyurethane paint (5-10 mμ). The edges of the laminate coupons have no paint. Also, the honeycomb sandwich coupons' side edges were sealed with 3M aluminum foil tape # 25 in addition to the polyurethane coating on the bottom of these sandwich structures.

The samples were then placed in the conditioning environment. After the conditioning was done, water conditioned coupons were wrapped with a wet towel to keep moisture ingression on the surface. Oil conditioned coupons were placed into nylon zip bags and tested within one week. Figure 3.20 shows the aluminum tape edge sealed sandwich test coupon. Table 3.8 gives the composite test coupons and their conditions.

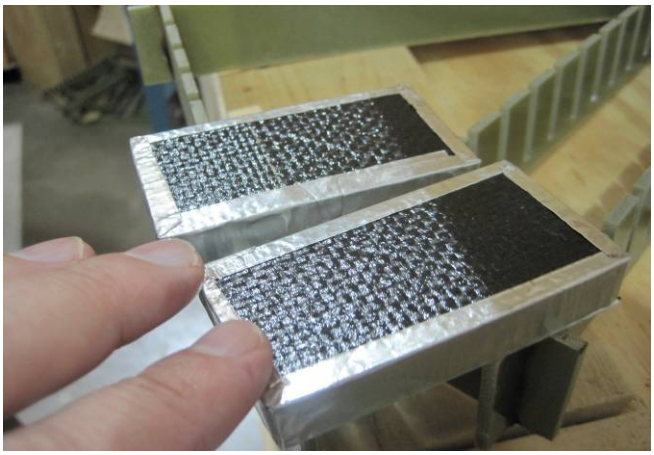

Figure 3.20 Aluminum tape (3M aluminum foil tape # 25) edge sealed sandwich test articles in water.

TABLE 3.8

TEST COUPON NOMENCLATURE FOR THE 3-POINT BEND TESTS

Coupon type	Barrier film	Condition
control	no	no, as fabricated
control-w	no	yes, in liquid
Tedlar	yes, Tedlar 0.0250 mm	yes, in liquid
Peek-1	yes, Peek 0.0225 mm	yes, in liquid
Peek-0.5	yes, Peek 0.0125 mm	yes, in liquid

3.3.2.1 The 3-Point Bend Test

The 3-point bend test strips (6.35 mm width and 25.4 mm length) were cut from the test panels with 0° fiber angle along the length. Cutting was done with a wet table saw which had 30.48 cm diameter 160-180 grit diamond blade. An RPM of 3000 is used to have an 812 µm or smoother surface (or roughness). Specimen width and thickness were measured, and then specimens were placed in a water bath for 29 days. Tests were conducted on a MTS test machine with a crosshead speed of 1.0 mm/min. Loading span was set to four times the specimen thickness. Figure 3.21 shows the short beam shear test coupons with the dimensioning stage and testing. Figures 3.22 through 3.24 show the 3-point bend results of the water immersion conditioned Kevlar, carbon and glass specimens.

Figure 3.21 Short beam shear test coupon in testing.

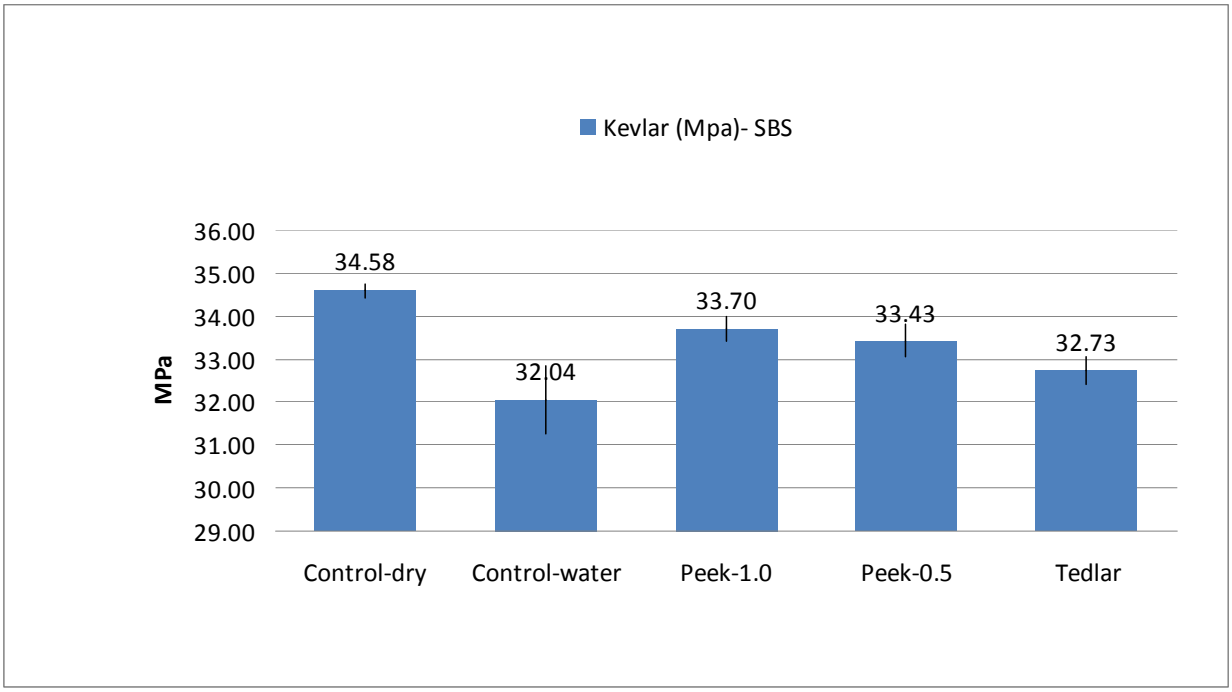

Kevlar (Mpa)					
Coupon	Control-dry	Control-water	Peek-1.0	Peek-0.5	Tedlar
1	34.36	32.66	33.69	34.01	33.09
2	34.58	32.69	33.87	33.57	32.42
3	34.63	32.41	33.42	33.11	32.86
4	34.76	31.02	34.09	33.31	32.5
5		31.44	33.43	33.16	32.78
Avg	34.58	32.04	33.70	33.43	32.73
Std dev	0.17	0.79	0.28	0.39	0.31

Figure 3.22 The 3-point bend results of the water immersion conditioned Kevlar fiber reinforced composites associated with the raw and statistical data.

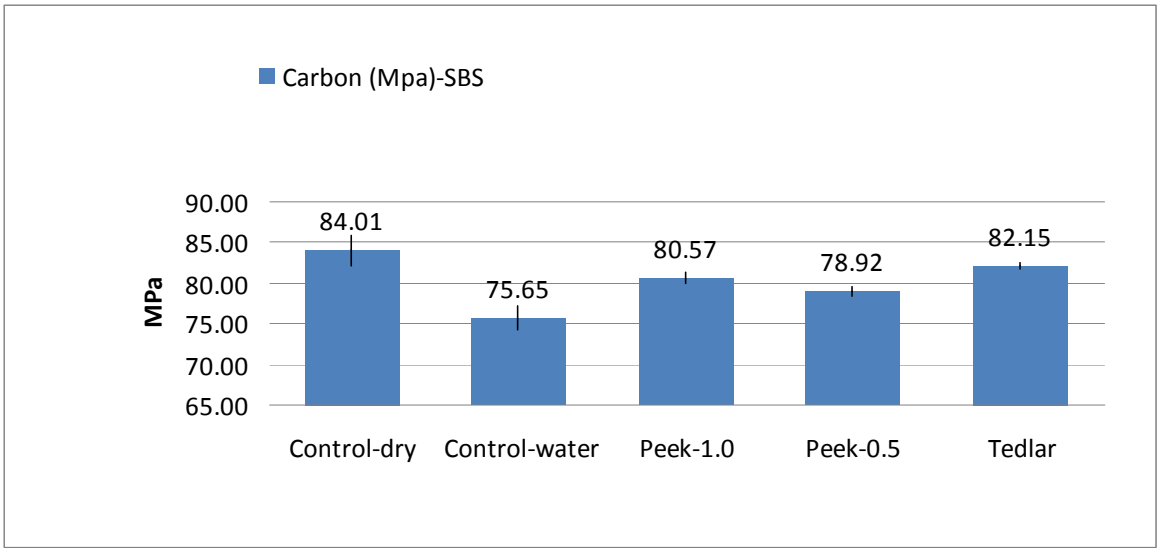

Carbon (Mpa)-SBS					
Coupon	Control-dry	Control-water	Peek-1.0	Peek-0.5	Tedlar
1	86.93	75.82	79.72	79.51	82.7
2	83.07	77.50	81.39	78.37	82.2
3	83.16	75.39	80.58	79.42	81.76
4	82.87	73.90	80.58	78.66	81.95
5				78.65	
Avg	84.01	75.65	80.57	78.92	82.15
Std dev	1.95	1.48	0.68	0.56	0.41

Figure 3.23 The 3-point bend results of the water immersion conditioned carbon fiber reinforced composites associated with the raw and statistical data.

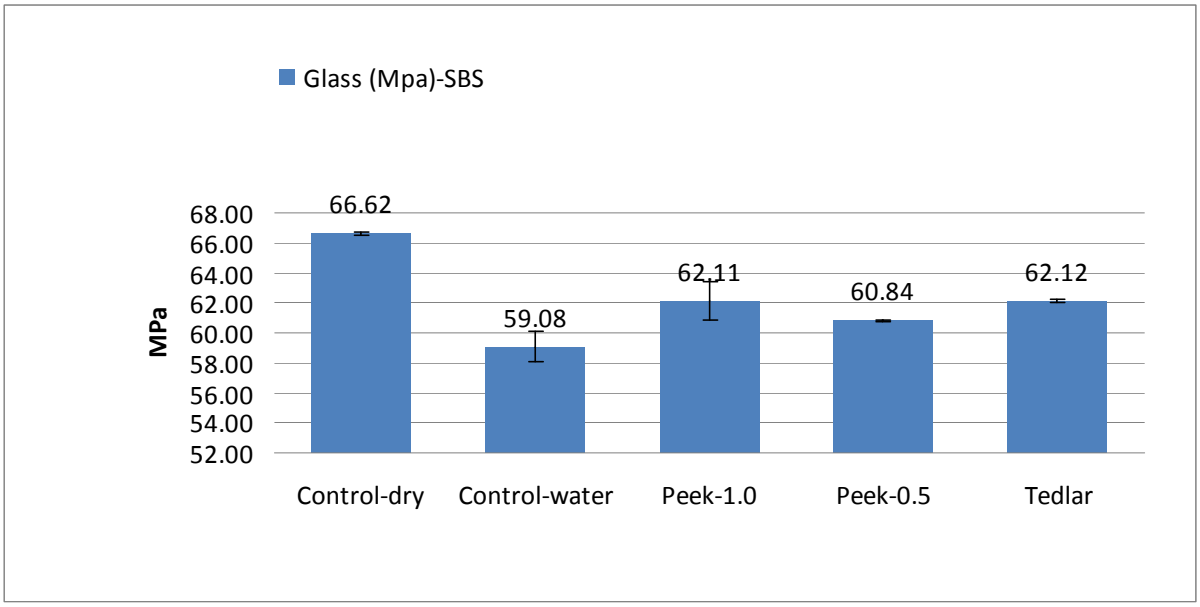

Glass (Mpa)-SBS					
Coupon	Control-dry	Control-water	Peek-1.0	Peek-0.5	Tedlar
1	66.45	57.75	63.95	60.88	62.02
2	66.58	59.84	61.69	60.80	62.23
3	66.75	59.88	61.74	60.78	62.2
4	66.70	58.85	61.07	60.88	62.02
5					
Avg	66.62	59.08	62.11	60.84	62.12
Std dev	0.13	1.01	1.26	0.05	0.11

Figure 3.24 The 3-point bend results of the water immersion conditioned glass fiber reinforced composites associated with the raw and statistical data.

For the Kevlar composite panels, water conditioned coupons with no barrier film showed about 10% lower shear strength compared to the unconditioned control ones. When the barrier films were applied on the composite panels, mechanical properties increased approximately 5%. Since the Kevlar is not a brittle material, the failure mode is observed as bending.

For the carbon composite panels, the water conditioned coupons without any barrier film displayed 12-15% lower shear strength compared to the unconditioned ones (or control coupons). When barrier films were applied on the surfaces of the panels, mechanical strength

increased up to 10% compared to the coupons immersed in water in the absence of the barrier films. In the last test, it was found that the glass coupons associated with the Tedlar and PEEK-1 barrier films had about 5% higher strength than the one without the barrier film.

Specimens were examined based on microscopic images to find out the failure modes. Carbon and glass specimens indicated a clear shear failure mode. However, Kevlar test coupons showed buckling or bending rather than shearing. Based on the theory [37], the area under the plot of stress vs. strain provides the energy amount, or toughness, so this sample can absorb energy during the stressed conditions. Deflection is an indication of the energy absorption capacity which allows energy dissipation. If the substrate cannot deform, energy is released through the coupon breaking. When the glass, carbon, and Kevlar plots are closely reviewed (see FEA model), the Kevlar composite has the largest area under the line of the plot. Test data indicates that for the same load, deflection is more for the Kevlar coupons compared to the carbon and glass coupons. This clearly proves that the Kevlar dissipated the energy by bending, so the Kevlar coupons did not indicate any shear failure but rather bending as is seen in Figure 3.14. This phenomenon was also observed in the Kevlar compression test results. Figure 3.25 shows the carbon composite short beam shear failure mode.

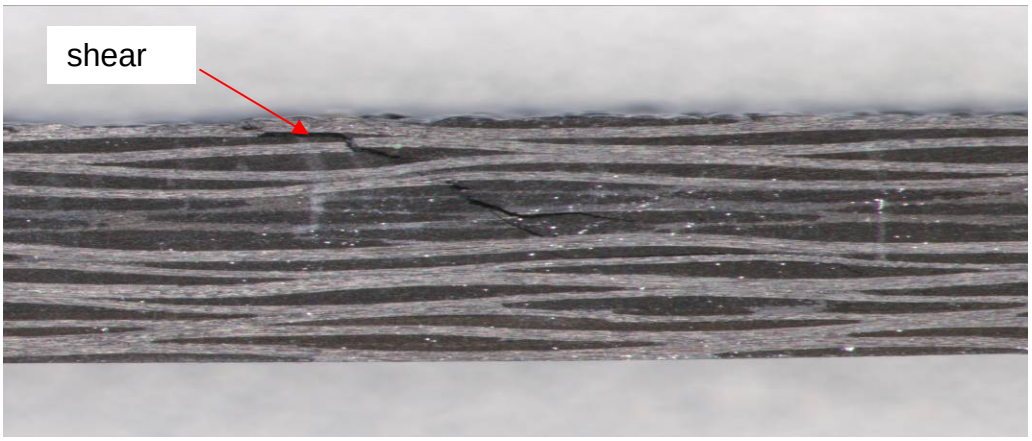

Figure 3.25 The short beam shear tests conducted on the carbon composite coupon and their failure mode (crack formations on the side of the laminates).

3.3.2.2 The 4-Point Bend Test

Test coupons of 30.48 cm length, 5.08 cm width and 0.95 cm thickness were cut from the standard test panels with 0° fiber angle and Nomex core ribbon along the length direction. Coupons were cut by a band saw. After the coupon labeling, specimen thickness and width dimensions were recorded. Exposed sides of coupons were sealed with aluminum tape to prevent fluid from going into Nomex core area. The tests were conducted using a MTS test machine with a crosshead speed of 1.0 mm/min. The loading span is set to 10.16 cm with a support span set of 25.4 cm.

The 4-Point Bend Water Conditioned Specimens: The honeycomb structured composite specimens (30.48 cm length, 5.08 cm width and 0.95 cm thick) were immersed and conditioned in a water bath for 14 days. When the conditioning was done, coupons were wrapped with a wet towel and placed in the zip bag until test day. Tests were conducted within one week after removing them from the conditioning step. Figures 3.26 through 3.28 show the 4-point bend results of the water immersion conditioned Kevlar, carbon and glass composites with honeycomb core structures.

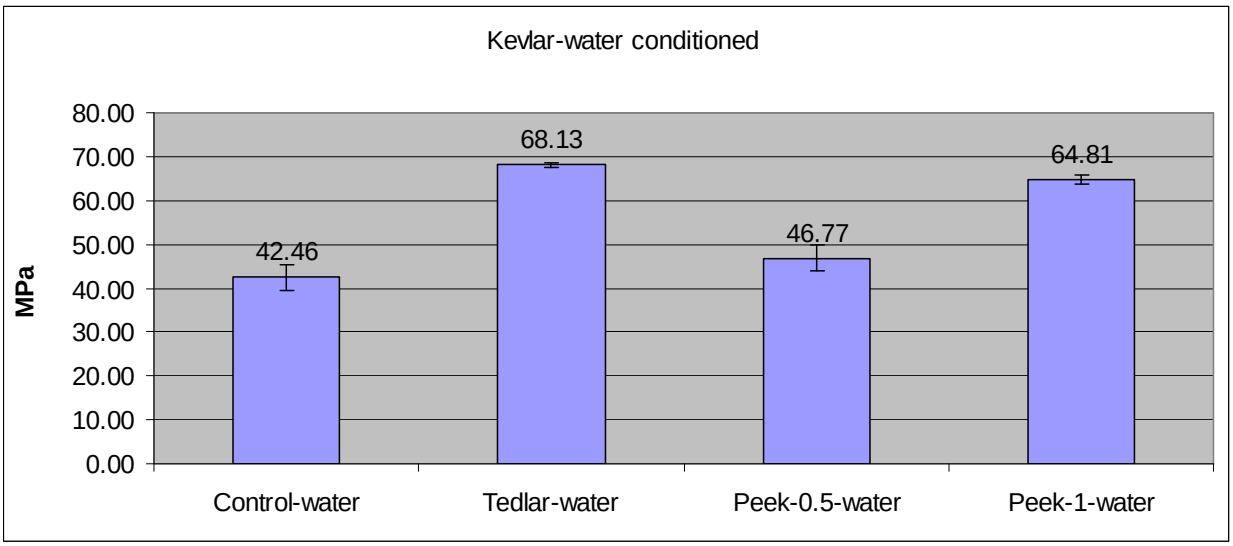

Kevlar-water conditioned				
Coupon	Control-water	Tedlar-water	Peek-0.5-water	Peek-1-water
1	39.25	67.65	43.59	65.31
2	45.10	67.97	49.38	63.65
3	43.03	68.77	47.35	65.46
4				
Avg	42.46	68.13	46.77	64.81
Std dev	2.97	0.58	2.93	1.01

Figure 3.26 The 4-point bend results of the water immersion conditioned Kevlar fiber reinforced sandwich composites associated with the raw and statistical data.

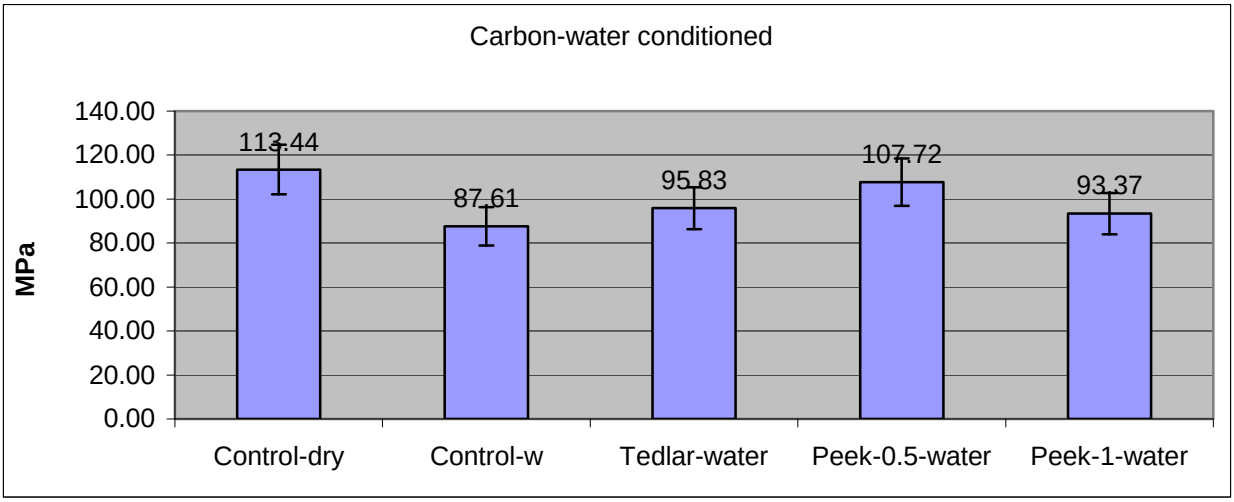

Carbon-water conditioned					
Coupon	Control-dry	Control-w	Tedlar-water	Peek-0.5-water	Peek-1-water
1	115.33	87.23	100.10	91.21	93.01
2	115.07	87.07	90.65	123.31	92.80
3	109.92	88.53	96.75	108.64	94.29
Avg	113.44	87.61	95.83	107.72	93.37
Std dev	3.05	0.80	4.79	16.07	0.80

Figure 3.27 The 4-point bend results of the water immersion conditioned carbon fiber reinforced sandwich composites associated with the raw and statistical data.

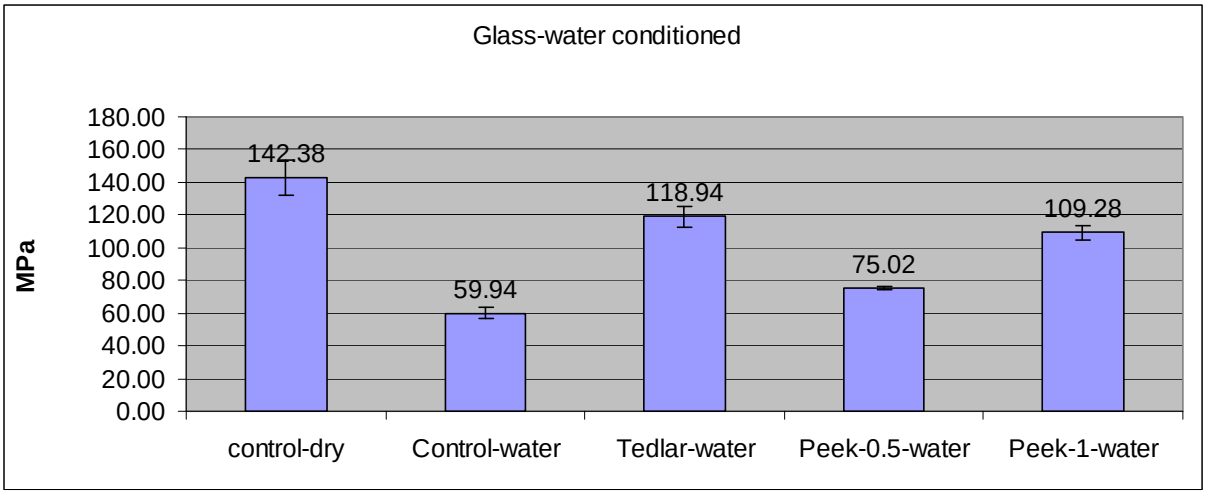

Glass-water conditioned					
Coupon	control-dry	Control-water	Tedlar-water	Peek-0.5-water	Peek-1-water
1	152.56	56.42	112.04	75.37	104.52
2	131.15	62.86	125.30	73.99	113.36
3	143.42	60.53	119.49	75.71	109.95
Avg	142.38	59.94	118.94	75.02	109.28
Std dev	10.74	3.26	6.65	0.91	4.46

Figure 3.28 The 4-point bend results of the water immersion conditioned glass fiber reinforced sandwich composites associated with the raw and statistical data (Control-dry coupons were taken from Skydrol test panels before immersing into liquid).

The Kevlar honeycomb core composites with the PEEK-1 barrier film provided about 52.64% higher mechanical strength than the control sample that has no barrier film. The carbon fiber reinforced honeycomb composite with the PEEK-0.5 barrier film showed up to 22.95% higher strength. The same test conducted on the glass fiber reinforced honeycomb composites associated with Tedlar barrier films had 98.43% higher mechanical properties. Based on the experimental results, it can be concluded that it is very critical to use a barrier film for the glass sandwich structures. Failure mode was usually the skin failure for all the coupons.

The 4-Point Bend Skydrol Conditioned Specimens: The honeycomb structured composite specimens (30.48 cm length, 5.08 cm width and 0.95 cm thick) were immersed in Skydrol bath for 7 days. When the conditioning was completed, the coupons were wrapped with wet Skydrol towels and placed in the zip bag until test is performed. The tests were conducted within one week time. Figures 3.29 through 3.31 show the 4-point bend results of the Skydrol conditioned Kevlar, carbon, and glass composites.

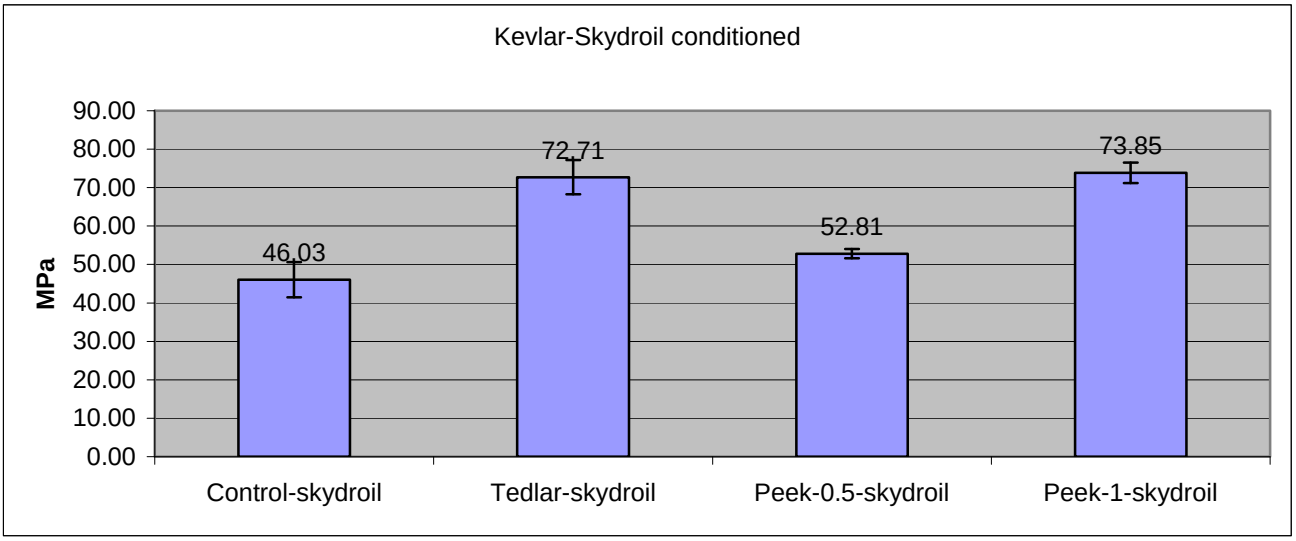

Kevlar-Skydrol conditioned				
Coupon	Control-Skydrol	Tedlar-Skydrol	Peek-0.5-Skydrol	Peek-1-Skydrol
1	41.30	67.99	51.39	70.89
2	50.46	76.81	53.60	76.17
3	46.34	73.34	53.43	74.47
Avg	46.03	72.71	52.81	73.85
Std dev	4.59	4.45	1.23	2.70

Figure 3.29 The 4-point bend results of the Skydrol immersion conditioned Kevlar fiber reinforced sandwich composites associated with the raw and statistical data.

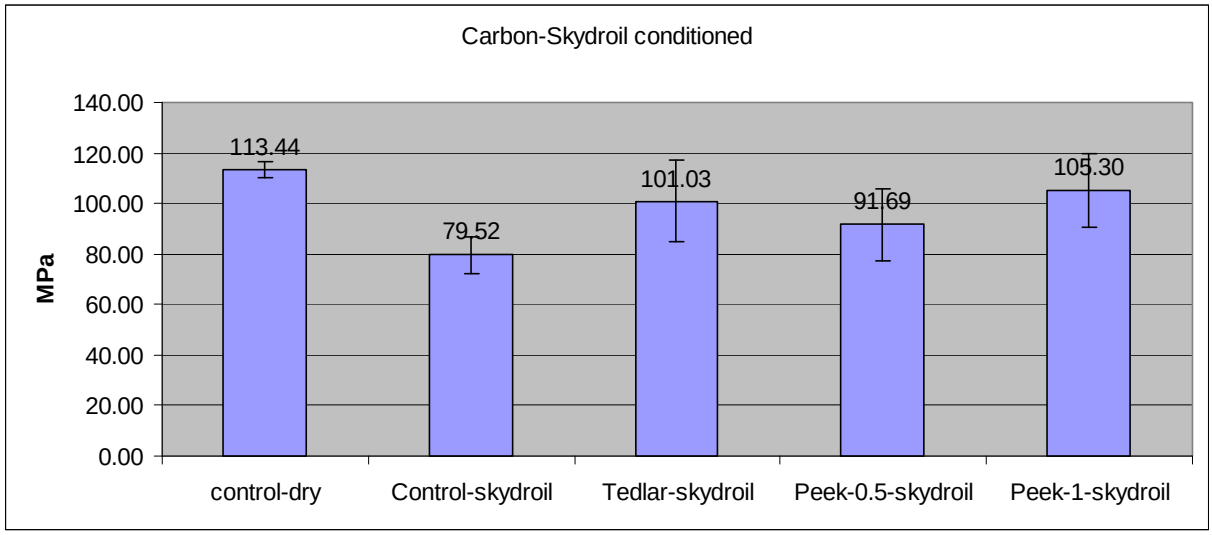

Carbon-Skydrol conditioned					
Coupon	control-dry	Control-Skydrol	Tedlar-Skydrol	Peek-0.5-Skydrol	Peek-1-Skydrol
1	115.33	71.73	116.93	76.78	119.29
2	115.07	86.51	84.30	105.48	90.47
3	109.92	80.32	101.85	92.81	106.14
Avg	113.44	79.52	101.03	91.69	105.30
Std dev	3.05	7.42	16.33	14.38	14.43

Figure 3.30 The 4-point bend results of the Skydrol immersion conditioned carbon fiber reinforced sandwich composites associated with the raw and statistical data.

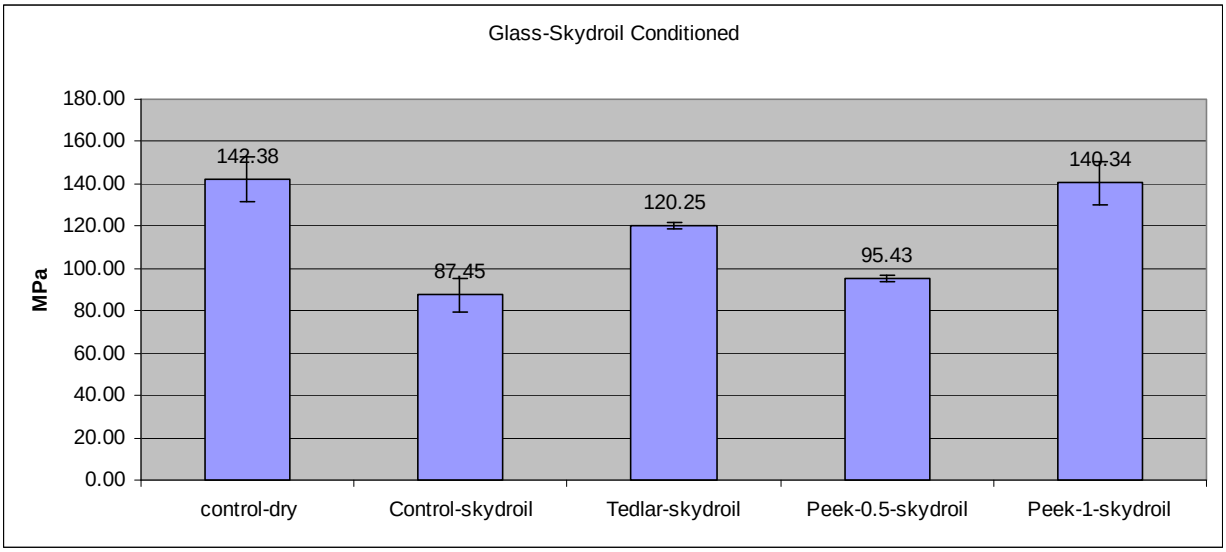

Glass-Skydrol conditioned					
Coupon	control-dry	Control-Skydrol	Tedlar-Skydrol	Peek-0.5-Skydrol	Peek-1-Skydrol
1	152.56	79.48	121.34	93.83	129.77
2	131.15	95.13	118.53	96.22	150.58
3	143.42	87.76	120.89	96.22	140.66
Avg	142.38	87.45	120.25	95.43	140.34
Std dev	10.74	7.83	1.51	1.38	10.41

Figure 3.31 The 4-point bend results of the Skydrol immersion conditioned glass fiber reinforced sandwich composites associated with the raw and statistical data.

The Kevlar fiber reinforced honeycomb composite coupons covered with barrier films of Tedlar and PEEK-1 indicated 40% higher strength than the coupons without any barrier films after conditioning of 7 days in the Skydrol solvent. The carbon fiber reinforced coupons with the PEEK 0.5 barrier film made the strength 20% higher. The same test conducted on the glass fiber reinforced coupons improved the strength about 50% when compared to the bare coupons. The test results of the Skydrol conditioned coupons showed a similar percentage increase with the water conditioned ones (see Figures 3.26 – 3.28). This result also showed that it is very important to use the barrier films for the sandwich structured composites.

3.3.2.3 Sandwich Compression Tests

The sandwich structured test coupons (13.97 cm length, 2.54 cm width and 1 cm thick) were extracted from the larger test panels with 0° fiber angle and Nomex core ribbon direction along the length. The test coupon sides were sealed with the aluminum tape to prevent fluid penetration into the core areas of the honeycomb structures. Figures 3.32 – 3.34 show the compression test results of the water immersion conditioned Kevlar, carbon and glass fiber reinforced sandwich composites.

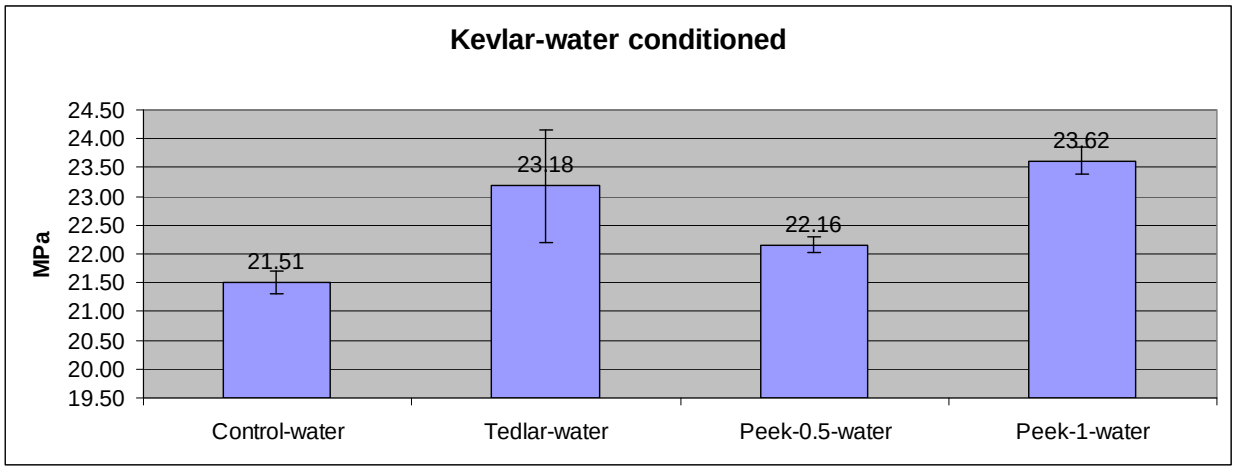

Kevlar-Water conditioned				
Coupon	Control-water	Tedlar-water	Peek-0.5-water	Peek-1-water
1	21.35	24.11	22.00	23.81
2	21.45	22.17	22.23	23.34
3	21.73	23.25	22.24	23.71
Avg	21.51	23.18	22.16	23.62
Std dev	0.20	0.98	0.14	0.25

Figure 3.32 The compression test results of the water immersion conditioned Kevlar fiber reinforced sandwich composites associated with the raw and statistical data.

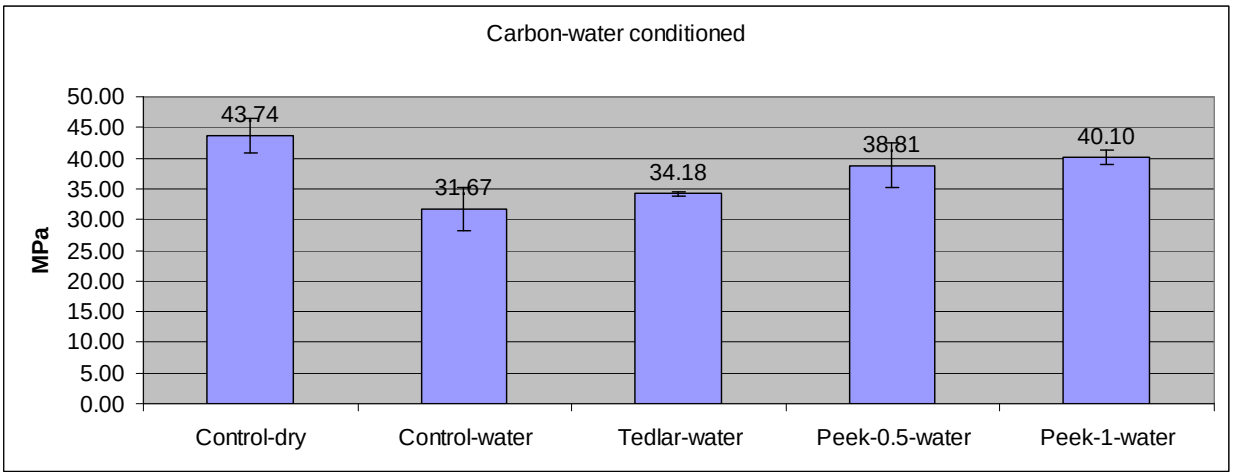

Carbon-Water conditioned					
Coupon	Control-dry	Control-water	Tedlar-water	Peek-0.5-water	Peek-1-water
1	46.49	35.07	33.80	42.43	38.87
2	40.88	28.19	34.48	35.13	41.27
3	43.85	31.74	34.25	38.87	40.17
Avg	43.74	31.67	34.18	38.81	40.10
Std dev	2.81	3.44	0.35	3.65	1.20

Figure 3.33 The compression test results of the water immersion conditioned carbon fiber reinforced sandwich composites associated with the raw and statistical data.

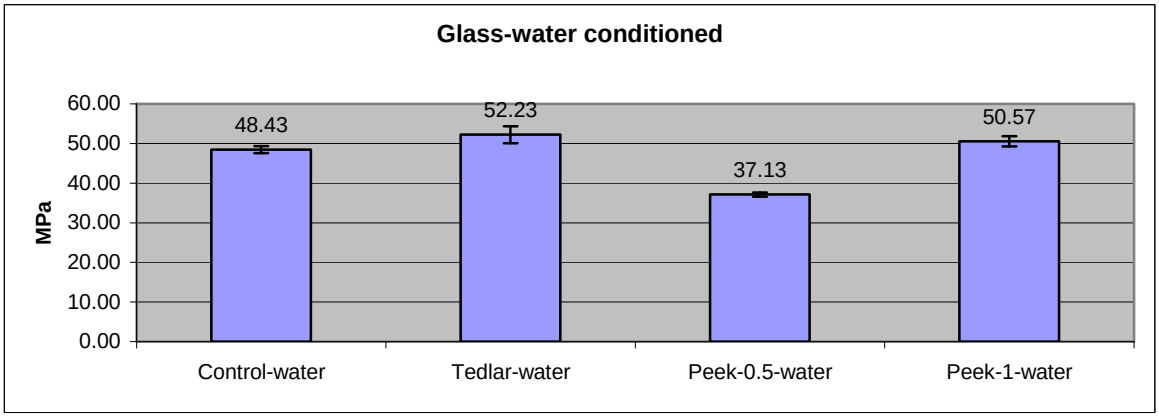

Glass-Water conditioned				
Coupon	Control-water	Tedlar-water	Peek-0.5-water	Peek-1-water
1	47.52	54.38	36.56	51.81
2	49.26	50.09	37.59	49.26
3	48.51	52.24	37.23	50.65
Avg	48.43	52.23	37.13	50.57
Std dev	0.87	2.15	0.52	1.28

Figure 3.34 The compression test results of the water immersion conditioned glass fiber reinforced sandwich composites associated with the raw and statistical data.

The sandwich structured Kevlar composites covered with the PEEK-1 thin film gave 9.81% higher compression strength improvement as compared to the control composite (or no barrier films) after the immersion in water. As is observed in the previous tests, the Kevlar coupons failure mode was found to be bending again for the compression test, as well. It was concluded that the Kevlar compression test results do not represent true the compression strength. For the carbon coupons, there was about 20-30 % strength increase when the PEEK barrier films were used. The similar results were also seen on the Tedlar barrier film covered glass coupons.

The same test coupons were also immersed in the Skydrol solvent for the compression tests. These tests provide the compression stress behavior of the sandwiched structures composite coupons under the harsh environmental conditions. Figures 3.35 – 3.37 shows the compression test results of the Skydrol solvent conditioned Kevlar, carbon and glass fiber reinforced sandwich composites.

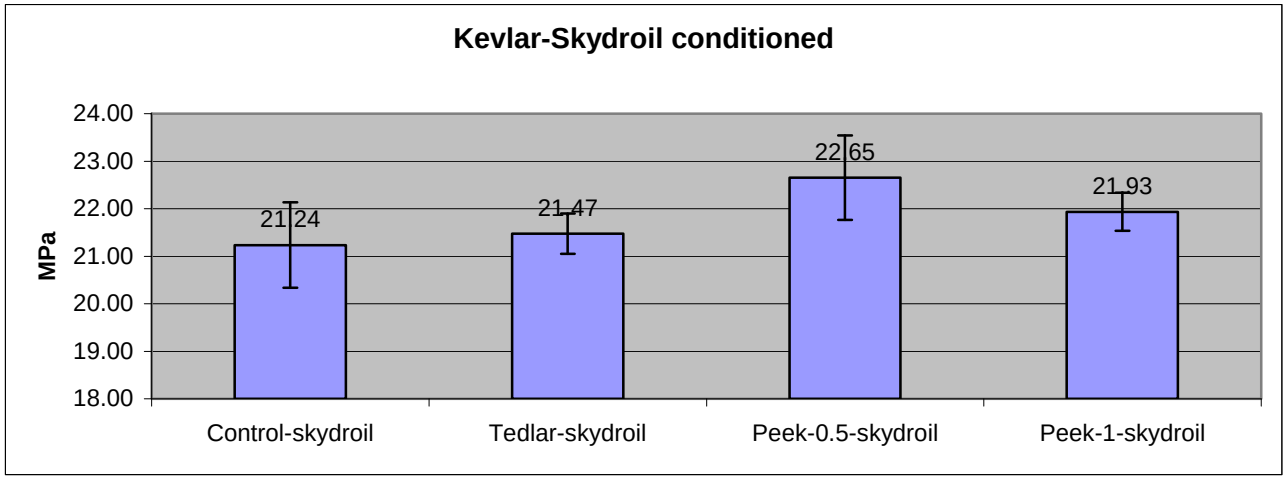

Kevlar-Skydrol conditioned (Mpa)				
Coupon	Control-Skydrol	Tedlar-Skydrol	Peek-0.5-Skydrol	Peek-1-Skydrol
1	20.39	21.91	21.80	22.29
2	22.18	21.07	23.57	21.50
3	21.14	21.44	22.60	22.01
Avg	21.24	21.47	22.65	21.93
Std dev	0.90	0.42	0.89	0.40

Figure 3.35 The compression test results of the Skydrol conditioned Kevlar fiber reinforced sandwich composites associated with the raw and statistical data.

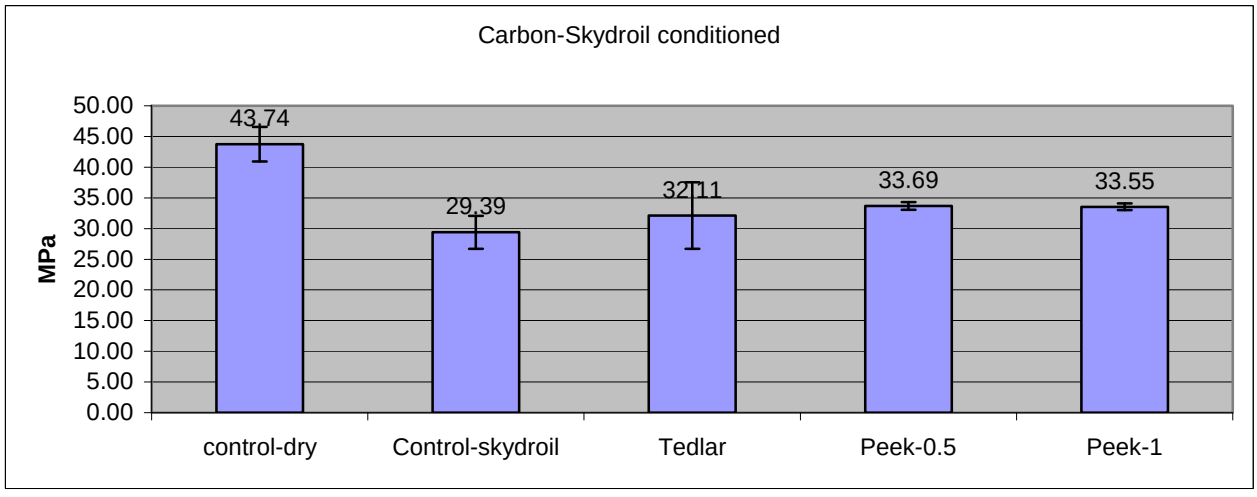

Carbon-Skydrol conditioned					
Coupon	control-dry	Control-Skydrol	Tedlar	Peek-0.5	Peek-1
1	46.49	29.66	37.81	34.39	32.94
2	40.88	31.94	27.06	33.16	33.70
3	43.85	26.58	31.46	33.50	34.00
Avg	43.74	29.39	32.11	33.69	33.55
Std dev	2.81	2.69	5.41	0.63	0.55

Figure 3.36 The compression test results of the Skydrol conditioned carbon fiber reinforced sandwich composites associated with the raw and statistical data.

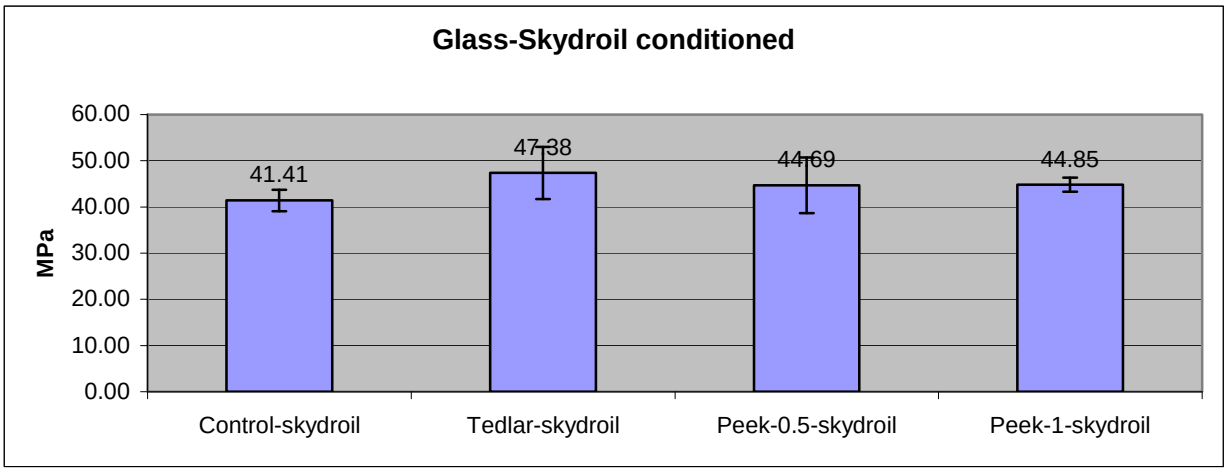

Glass-Skydrol conditioned				
Coupon	Control-Skydrol	Tedlar-Skydrol	Peek-0.5-Skydrol	Peek-1-Skydrol
1	43.68	41.73	38.67	43.32
2	39.03	53.00	50.71	46.38
3	41.51	47.40	44.69	44.86
Avg	41.41	47.38	44.69	44.85
Std dev	2.33	5.63	6.02	1.53

Figure 3.37 The compression test results of the Skydrol conditioned glass fiber reinforced sandwich composites associated with the raw and statistical data.

The compression tests conducted on the sandwiched Kevlar composites incorporated with the barrier films did not make significant change on the mechanical strength. The failure mode of

the Kevlar composites was bending because of the lack of the stiffness of the material and the tendency of buckling under compression. Therefore, the Kevlar compression results did not reflect true compression strength values. However, the carbon fiber reinforced honeycomb coupons indicated very clear respond to the barrier films. PEEK and Tedlar barrier film applied carbon sandwich coupons indicated up to 14.63 % strength increase. The glass fiber reinforced coupons consisting of the Tedlar film indicated 14.42 % compression strength increase. It is concluded that the Skydrol make more severe damage on the honeycomb structured composite panels than water at the same conditions.

3.3.2.4 Paint Tape Test

Different thickness glass laminate composites were prepared for the paint tape tests of the barrier films and coatings. First, the panels were washed with water and soup to clean the tool surface which may have residual silicon release agent from the layup mold. Then, the panels were dried for 30 minutes at room temperature (RT). The barrier film faces were lightly sanded with 180 sand grit paper, and wiped out with a cloth consisting of acetone. Sherwin Williams CM0482300 brand 2 coats of an epoxy primer applied on the surfaces of the barrier films. After the coatings (primer and polyurethane top coatings), the panels were cured in air circulating oven for 1 hr at 80 ºC. Then, the coupons were extracted by cutting 7.5 cm width by 30 cm length.

For the structural aircraft assemblies, in addition to the water and Skydrol exposure, environmental factors such as rain, humidity, and atmospheric pollutants can also cause a degradation of the protective film surface. To replicate those conditions, salt chamber conditioning was conducted and carried out in a Singleton salt spray chamber according to ASTM B117-09 standard. Salt chamber environmental conditions were pH 6.8-7.2 and average fog concentration of 1.2 ml/hour at 55 ºC. The samples were placed on a rack at a 15 degree angle for 128 hr. After the conditioning, paint tape test conducted by using 3M 250 tape.

The test results indicated that the control and barrier film applied coupons, Tedlar, PEEK-0.5, PEEK-1, did not have any paint on the peeled tape surfaces. With this, it is concluded that paint can be adhered or bonded on these barrier films. Figure 3.38 shows the paint tape test for the various coatings on the barrier films.

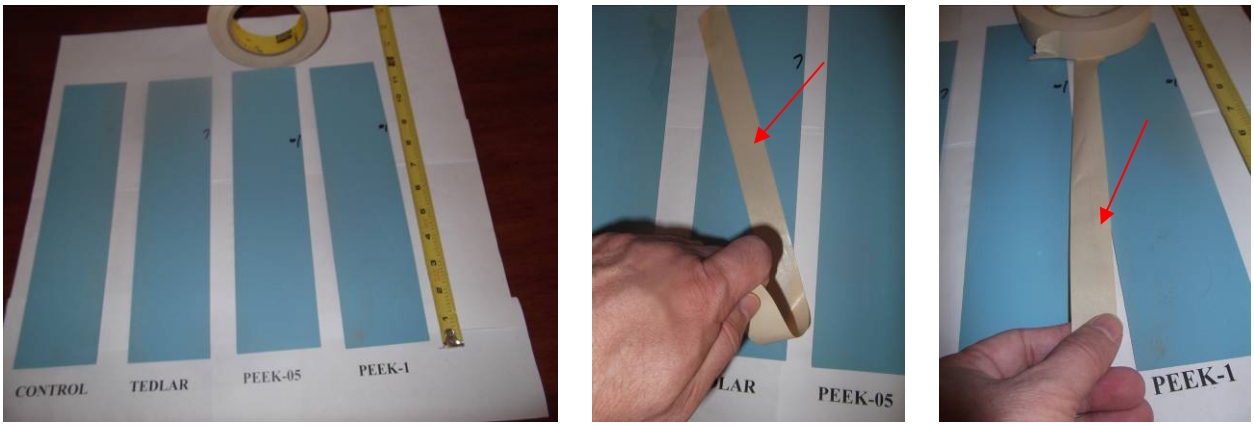

Specimens are ready for tape test | Placing 3M-Tape | No residue after pull test

Figure 3.38 The photographs showing the step-by-step paint tape tests for the various coatings on the barrier films.

3.3.2.5 Moisture Ingression Test

The laminate coupons were prepared with the dimensions of 7.62 cm x 5.08 cm in order to get the better moisture ingression test results. The edges of the coupons were polished by a finer polisher (32 RMS). Polished coupons were washed in distilled water to remove all traces of polishing rouge. Coupons were dried in an air circulating oven at 82 ± 5°C. The drying process is continued until a constant weight is achieved or weight difference within 2 consecutive measurements within 2 hr time elapse is less than 0.01%. The coupons were weighed to the nearest milligram on an analytical balance, 0.0001. Tool side of the specimens was coated with polyurethane paint to prevent water to ingress through the unprotected surface. The coupons were conditioned in full water immersion, 32 ± 5 °C. Figure 3.39 shows the moisture conditioning of different size of coupons.

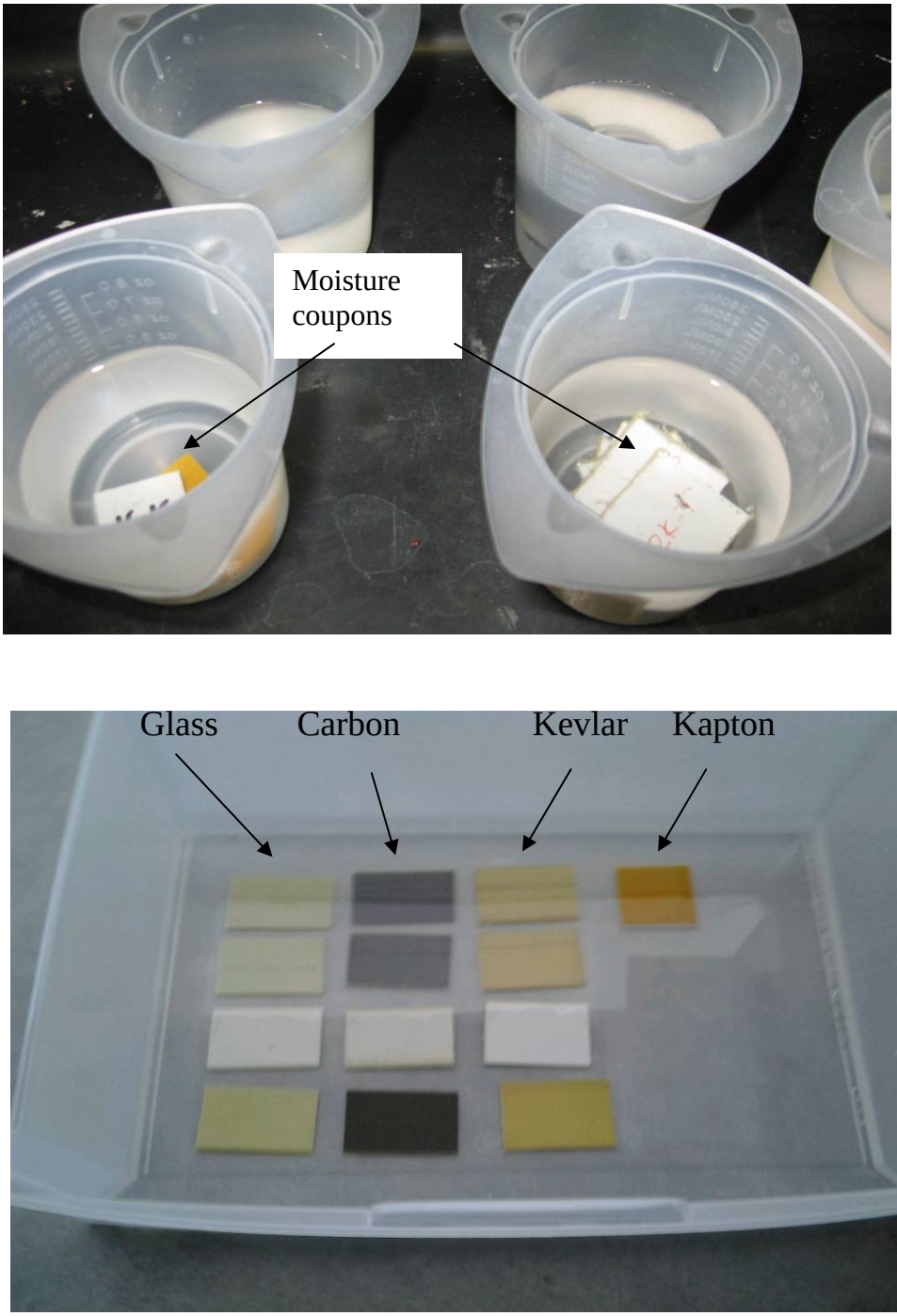

Figure 3.39 The composite test coupons (2.54 cm x 2.54 cm) top, (7.62 cm x 5.08 cm) conditioned in DI water for the moisture ingression tests, bottom.

Figures 3.40 and 3.41 show the moisture gains and moisture equilibrium of the glass laminate composite in DI water as a function of the immersion time. As is seen, the glass composite coupons without any barrier film reached moisture equilibrium in 27 days. The PEEK-1 applied

coupons gained lesser weight than the other alternatives. It is found that the PEEK-1 barrier film is able to prevent moisture ingression as good as the Tedlar barrier applied coupons for the glass laminates.

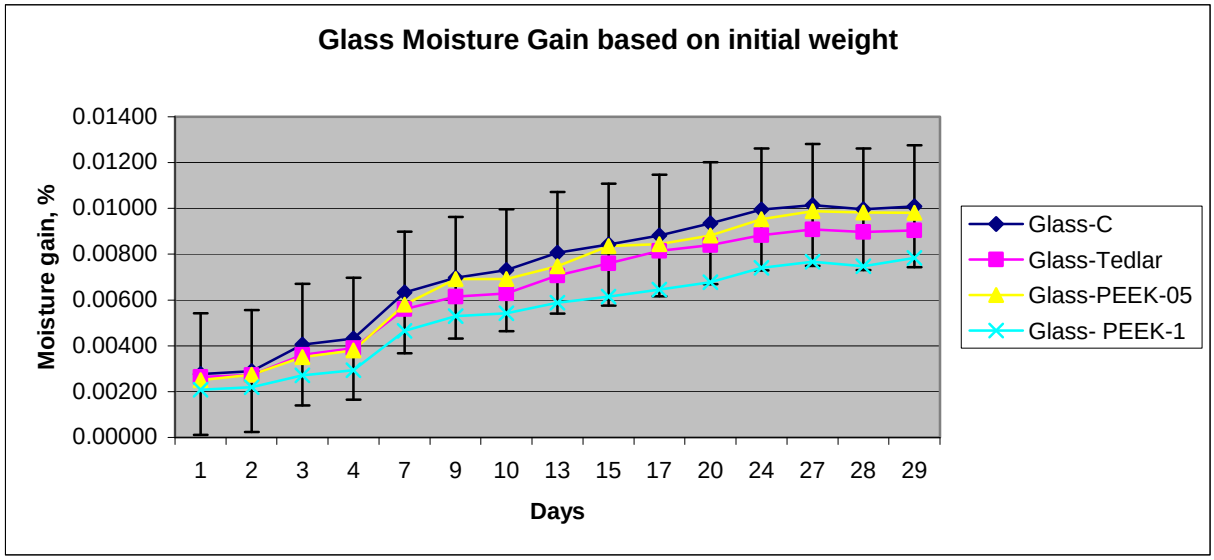

	Glass-C	Glass-Tedlar	Glass-PEEK-05	Glass-PEEK-1	Moisture % gain based on initial weight			
0	7.64983	7.87732	7.99510	7.66132	Glass-C	Glass-Tedlar	Glass-PEEK-05	Glass-PEEK-1
1	7.67099	7.89811	8.01513	7.67722	0.00277	0.00264	0.00251	0.00208
2	7.67199	7.89881	8.01699	7.67811	0.00290	0.00273	0.00274	0.00219
3	7.68080	7.90570	8.02310	7.68210	0.00405	0.00360	0.00350	0.00271
4	7.68281	7.90807	8.02548	7.68377	0.00431	0.00390	0.00380	0.00293
7	7.69825	7.92148	8.04150	7.69698	0.00633	0.00561	0.00580	0.00465
9	7.70314	7.92573	8.05037	7.70190	0.00697	0.00615	0.00691	0.00530
10	7.70570	7.92690	8.05040	7.70280	0.00730	0.00629	0.00692	0.00541
13	7.71150	7.93304	8.05487	7.70635	0.00806	0.00707	0.00748	0.00588
15	7.71425	7.93719	8.06188	7.70837	0.00842	0.00760	0.00835	0.00614
17	7.71730	7.94152	8.06256	7.71076	0.00882	0.00815	0.00844	0.00645
20	7.72137	7.94350	8.06560	7.71323	0.00935	0.00840	0.00882	0.00678
24	7.72597	7.94683	8.07123	7.71802	0.00995	0.00882	0.00952	0.00740
27	7.72746	7.94886	8.07404	7.72007	0.01015	0.00908	0.00987	0.00767
28	7.72605	7.94799	8.07365	7.71860	0.00996	0.00897	0.00982	0.00748
29	7.72703	7.94855	8.07350	7.72132	0.01009	0.00904	0.00981	0.00783

Figure 3.40 The moisture gains of the glass composites in DI water as a function of the immersion duration.

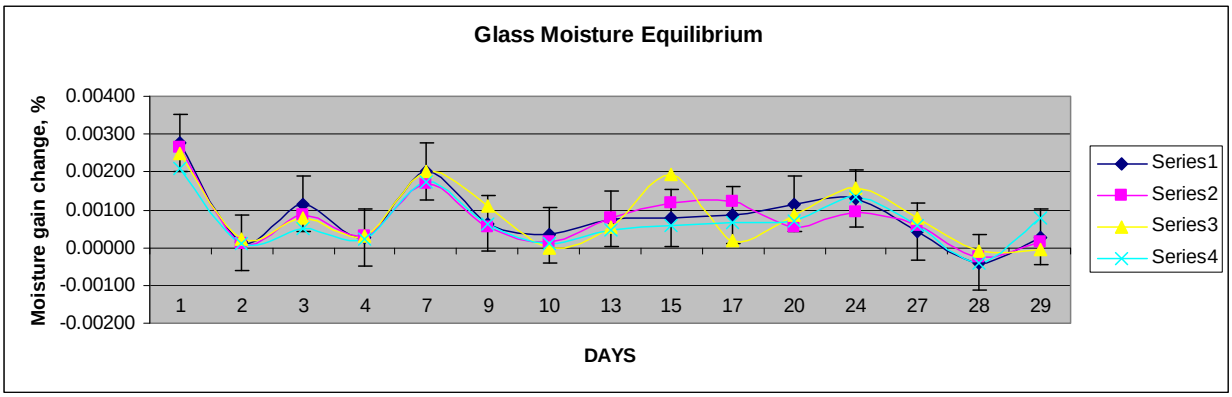

					< 0.0005			
	Glass-C	Glass-Tedlar	Glass-PEEK-05	Glass-PEEK-1	Moisture Equilibrium			
0	7.64983	7.87732	7.99510	7.66132	Glass-C	Glass-Tedlar	Glass-PEEK-05	Glass-PEEK-1
1	7.67099	7.89811	8.01513	7.67722	0.00277	0.00264	0.00251	0.00208
2	7.67199	7.89881	8.01699	7.67811	0.00013	0.00009	0.00023	0.00012
3	7.68080	7.90570	8.02310	7.68210	0.00115	0.00087	0.00076	0.00052
4	7.68281	7.90807	8.02548	7.68377	0.00026	0.00030	0.00030	0.00022
7	7.69825	7.92148	8.04150	7.69698	0.00202	0.00170	0.00200	0.00172
9	7.70314	7.92573	8.05037	7.70190	0.00064	0.00054	0.00111	0.00064
10	7.70570	7.92690	8.05040	7.70280	0.00033	0.00015	0.00000	0.00012
13	7.71150	7.93304	8.05487	7.70635	0.00076	0.00078	0.00056	0.00046
15	7.71425	7.93719	8.06188	7.70837	0.00078	0.00116	0.00194	0.00057
17	7.71730	7.94152	8.06256	7.71076	0.00086	0.00121	0.00019	0.00067
20	7.72137	7.94350	8.06560	7.71323	0.00115	#REF!	0.00084	0.00069
24	7.72597	7.94683	8.07123	7.71802	0.00130	0.00093	0.00156	0.00135
27	7.72746	7.94886	8.07404	7.72007	0.00042	0.00057	0.00078	0.00058
28	7.72605	7.94799	8.07365	7.71860	-0.00040	-0.00024	-0.00011	-0.00041
29	7.72703	7.94855	8.07350	7.72132	0.00028	0.00016	-0.00004	0.00076

Figure 3.41 The moisture equilibrium of the glass composites in DI water as a function of the immersion duration.

Figures 3.42 and 3.43 show the moisture gains and moisture equilibriums of the carbon laminate composite in DI water as a function of the immersion time. The carbon fiber reinforced composite coupons without any barrier film reached the moisture equilibrium in 20 days of the immersion. After the 20 days of the immersion, the weight gain was considerably low or negligible. However, all the barrier films on the composite laminates significantly reduced the

moisture gains. Based on the experimental results, it is concluded that the resin and reinforcement material significantly affect the moisture absorption.

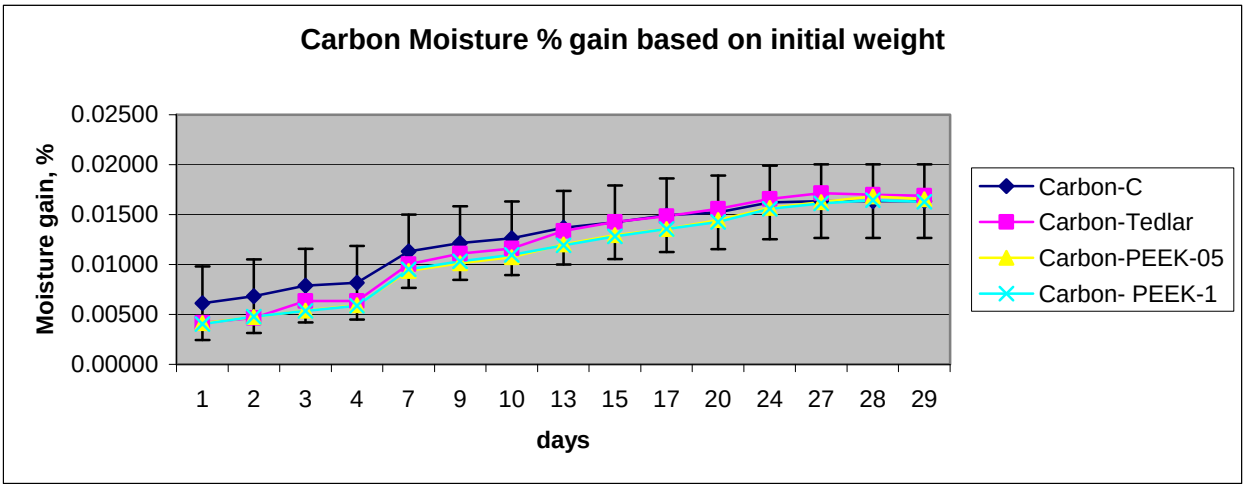

Day	Carbon-C	Carbon-Tedlar	Carbon-PEEK-05	Carbon-PEEK-1	Moisture % gain based on initial weight			
0	4.85437	4.79305	4.87510	4.98677	Carbon-C	Carbon-Tedlar	Carbon-PEEK-05	Carbon-PEEK-1
1	4.88414	4.81298	4.89525	5.00696	0.00613	0.00416	0.00413	0.00405
2	4.88754	4.81539	4.89823	5.01052	0.00683	0.00466	0.00474	0.00476
3	4.89260	4.82340	4.90130	5.01350	0.00788	0.00633	0.00537	0.00536
4	4.89398	4.82350	4.90400	5.01602	0.00816	0.00635	0.00593	0.00587
7	4.90937	4.84110	4.92080	5.03425	0.01133	0.01002	0.00937	0.00952
9	4.91332	4.84625	4.92440	5.03820	0.01214	0.01110	0.01011	0.01031
10	4.91570	4.84870	4.92740	5.04150	0.01263	0.01161	0.01073	0.01098
13	4.92076	4.85708	4.93374	5.04619	0.01368	0.01336	0.01203	0.01192
15	4.92340	4.86140	4.93820	5.05070	0.01422	0.01426	0.01294	0.01282
17	4.92684	4.86424	4.94122	5.05443	0.01493	0.01485	0.01356	0.01357
20	4.92820	4.86768	4.94550	5.05796	0.01521	0.01557	0.01444	0.01428
24	4.93313	4.87241	4.95158	5.06450	0.01622	0.01656	0.01569	0.01559
27	4.93378	4.87528	4.95437	5.06718	0.01636	0.01716	0.01626	0.01612
28	4.93366	4.87448	4.95711	5.06879	0.01633	0.01699	0.01682	0.01645
29	4.93370	4.87404	4.95574	5.06796	0.01634	0.01690	0.01654	0.01628

Figure 3.42 The moisture gains of the carbon composites in DI water as a function of the immersion duration.

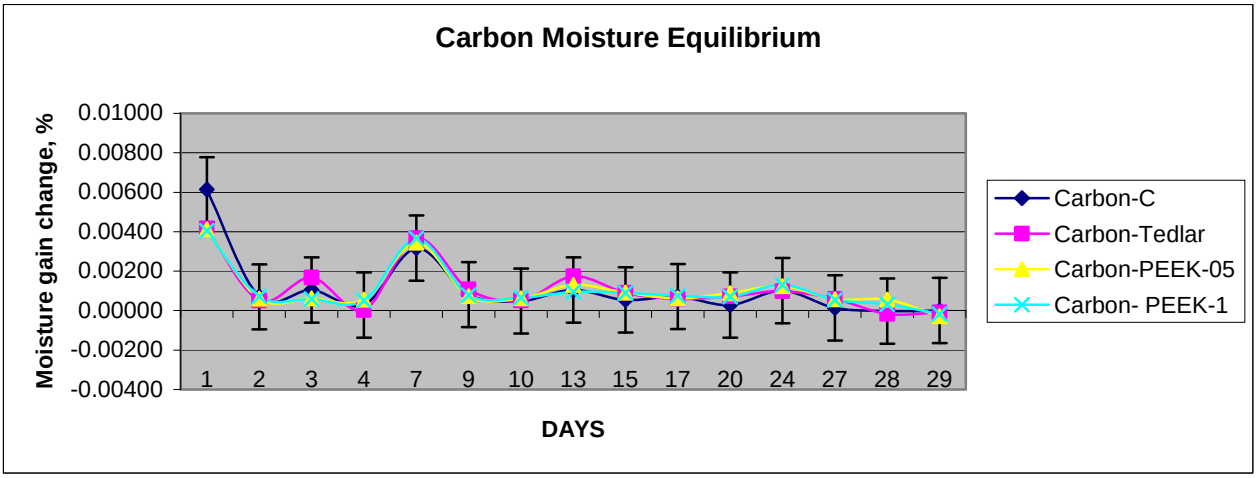

					< 0.0005			
Day	Carbon-C	Carbon-Tedlar	Carbon-PEEK-05	Carbon-PEEK-1	Moisture Equilibrium			
					Carbon-C	Carbon-Tedlar	Carbon-PEEK-05	Carbon-PEEK-1
0	4.85437	4.79305	4.87510	4.98677				
1	4.88414	4.81298	4.89525	5.00696	0.00613	0.00416	0.00413	0.00405
2	4.88754	4.81539	4.89823	5.01052	0.00070	0.00050	0.00061	0.00071
3	4.89260	4.82340	4.90130	5.01350	0.00104	0.00167	0.00063	0.00060
4	4.89398	4.82350	4.90400	5.01602	0.00028	0.00002	0.00055	0.00051
7	4.90937	4.84110	4.92080	5.03425	0.00317	0.00367	0.00345	0.00366
9	4.91332	4.84625	4.92440	5.03820	0.00081	0.00107	0.00074	0.00079
10	4.91570	4.84870	4.92740	5.04150	0.00049	0.00051	0.00062	0.00066
13	4.92076	4.85708	4.93374	5.04619	0.00104	0.00175	0.00130	0.00094
15	4.92340	4.86140	4.93820	5.05070	0.00054	0.00090	0.00091	0.00090
17	4.92684	4.86424	4.94122	5.05443	0.00071	0.00059	0.00062	0.00075
20	4.92820	4.86768	4.94550	5.05796	0.00028	0.00072	0.00088	0.00071
24	4.93313	4.87241	4.95158	5.06450	0.00102	0.00099	0.00125	0.00131
27	4.93378	4.87528	4.95437	5.06718	0.00013	0.00060	0.00057	0.00054
28	4.93366	4.87448	4.95711	5.06879	-0.00002	-0.00017	0.00056	0.00032
29	4.93370	4.87404	4.95574	5.06796	0.00001	-0.00009	-0.00028	-0.00017

Figure 3.43 The moisture equilibrium of the carbon composites in DI water as a function of the immersion duration.

Figures 3.44 and 3.45 show the moisture gains and moisture equilibriums of the Kevlar laminate composite in DI water as a function of the immersion times. The Kevlar moisture equilibrium time for the control coupons were about the half of the equilibrium time of the glass and carbon fiber laminates. The Kevlar specimens reached to the equilibrium within 13 days. Although

there was a peek after 7th days, the weight gain went back to less than 0.05 %. The moisture gain was about 10 % less for the coupon with the PEEK-05 barrier film compared to the control one.

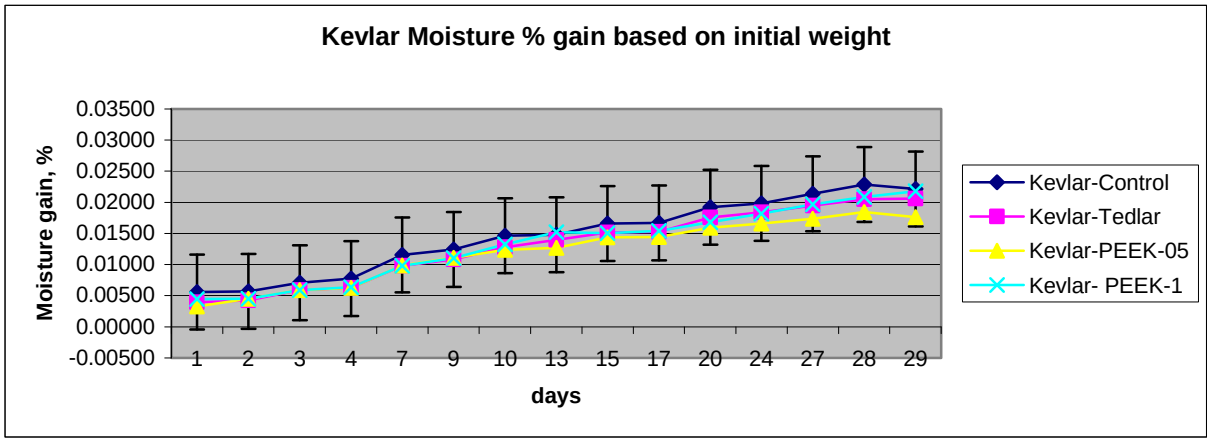

Day	Kevlar-Control	Kevlar-Tedlar	Kevlar-PEEK-05	Kevlar-PEEK-1	Moisture % gain based on initial weight			
0	5.50992	5.66429	5.65290	5.59657	Kevlar-Control	Kevlar-Tedlar	Kevlar-PEEK-05	Kevlar-PEEK-1
1	5.54069	5.68672	5.67152	5.62151	0.00558	0.00396	0.00329	0.00446
2	5.54137	5.68827	5.67841	5.62184	0.00571	0.00423	0.00451	0.00452
3	5.54900	5.69760	5.68620	5.62970	0.00709	0.00588	0.00589	0.00592
4	5.55250	5.69963	5.68832	5.63232	0.00773	0.00624	0.00627	0.00639
7	5.57349	5.71976	5.70874	5.65155	0.01154	0.00979	0.00988	0.00982
9	5.57839	5.72565	5.71564	5.65844	0.01243	0.01083	0.01110	0.01105
10	5.59060	5.73660	5.72300	5.67080	0.01464	0.01277	0.01240	0.01326
13	5.59134	5.74336	5.72453	5.68171	0.01478	0.01396	0.01267	0.01521
15	5.60140	5.75010	5.73410	5.68070	0.01660	0.01515	0.01436	0.01503
17	5.60182	5.75057	5.73462	5.68276	0.01668	0.01523	0.01446	0.01540
20	5.61573	5.76381	5.74302	5.69049	0.01920	0.01757	0.01594	0.01678
24	5.61916	5.76834	5.74667	5.69848	0.01983	0.01837	0.01659	0.01821
27	5.62781	5.77473	5.75100	5.70659	0.02140	0.01950	0.01735	0.01966
28	5.63597	5.78047	5.75711	5.71341	0.02288	0.02051	0.01843	0.02088
29	5.63206	5.78110	5.75241	5.71844	0.02217	0.02062	0.01760	0.02178

Figure 3.44 The moisture gains of the Kevlar composites in DI water as a function of the immersion duration.

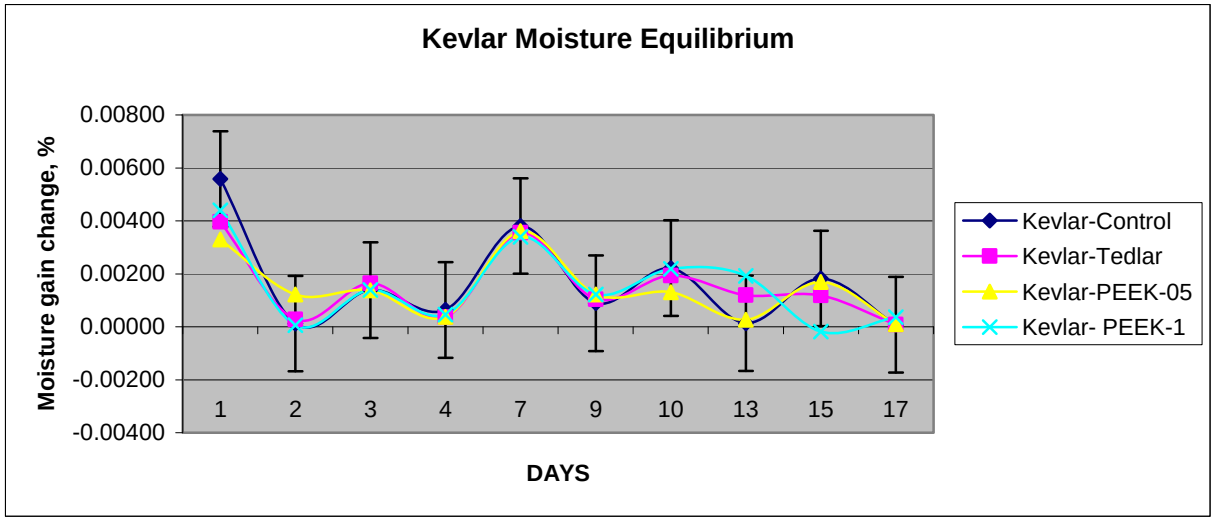

					< 0.0005			
Day	Kevlar-Control	Kevlar-Tedlar	Kevlar-PEEK-05	Kevlar-PEEK-1	Moisture Equilibrium			
0	5.50992	5.66429	5.65290	5.59657	Kevlar-Control	Kevlar-Tedlar	Kevlar-PEEK-05	Kevlar-PEEK-1
1	5.54069	5.68672	5.67152	5.62151	0.00558	0.00396	0.00329	0.00440
2	5.54137	5.68827	5.67841	5.62184	0.00012	0.00027	0.00122	0.00006
3	5.54900	5.69760	5.68620	5.62970	0.00138	0.00165	0.00138	0.00139
4	5.55250	5.69963	5.68832	5.63232	0.00064	0.00036	0.00038	0.00046
7	5.57349	5.71976	5.70874	5.65155	0.00381	0.00355	0.00361	0.00339
9	5.57839	5.72565	5.71564	5.65844	0.00089	0.00104	0.00122	0.00122
10	5.59060	5.73660	5.72300	5.67080	0.00222	0.00193	0.00130	0.00218
13	5.59134	5.74336	5.72453	5.68171	0.00013	0.00119	0.00027	0.00193
15	5.60140	5.75010	5.73410	5.68070	0.00183	0.00119	0.00169	-0.00018
17	5.60182	5.75057	5.73462	5.68276	0.00008	0.00008	0.00009	0.00036

Figure 3.45 The moisture equilibrium of the Kevlar composites in DI water as a function of the immersion duration.

Figures 3.46 and 3.47 show the moisture gains and moisture equilibriums of the glass laminate composite covered with the Kapton barrier films in DI water as a function of the immersion duration. In the absence of the Kapton barrier film, the glass composite laminates gained about %400 moisture; however, in the presence of the Kapton film on the glass composites, the moisture gain was significantly low (less than 50%). The test results clearly revealed that the

Kapton barrier film is more effective for moisture prevention than both PEEK and Tedlar barrier films.

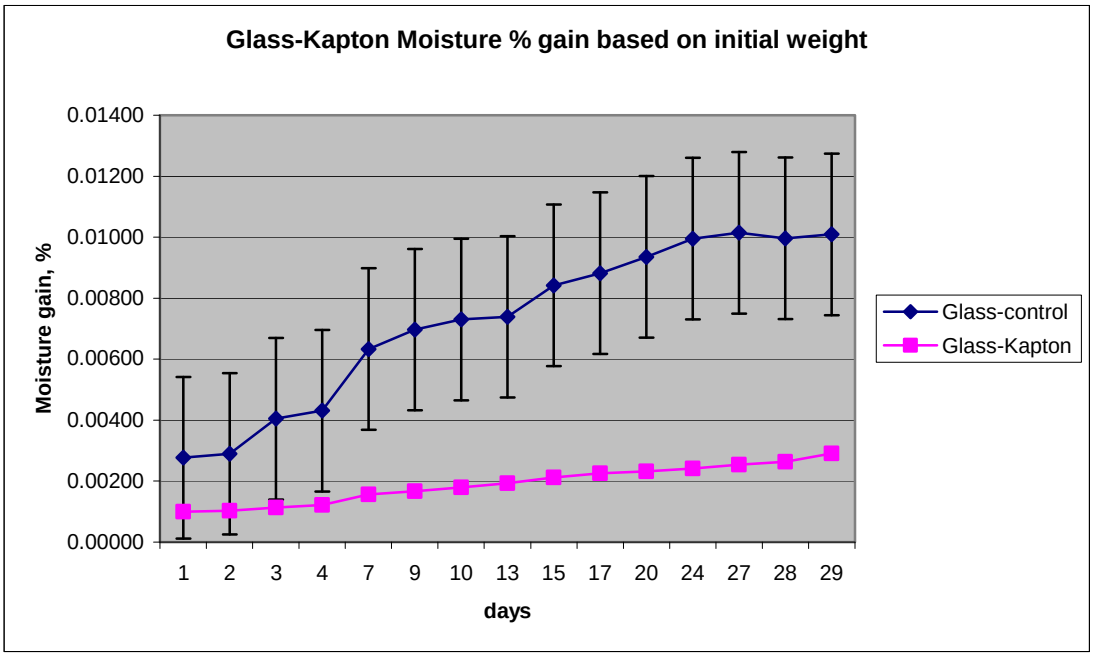

Day	Glass-control	Glass-Kapton	Moisture % gain based on initial weight	
0	7.64983	18.91852	Glass-control	Glass-Kapton
1	7.67099	18.93742	0.00277	0.00100
2	7.67199	18.93803	0.00290	0.00103
3	7.68080	18.94000	0.00405	0.00114
4	7.68281	18.94156	0.00431	0.00122
7	7.69825	18.94805	0.00633	0.00156
9	7.70314	18.95017	0.00697	0.00167
10	7.70570	18.95240	0.00730	0.00179
13	7.70635	18.95510	0.00739	0.00193
15	7.71425	18.95858	0.00842	0.00212
17	7.71730	18.96117	0.00882	0.00225
20	7.72137	18.96243	0.00935	0.00232
24	7.72597	18.96416	0.00995	0.00241
27	7.72746	18.96661	0.01015	0.00254
28	7.72605	18.96838	0.00996	0.00264
29	7.72703	18.97344	0.01009	0.00290

Figure 3.46 The moisture gains of the glass composites covered with the Kapton film in DI water as a function of the immersion duration.

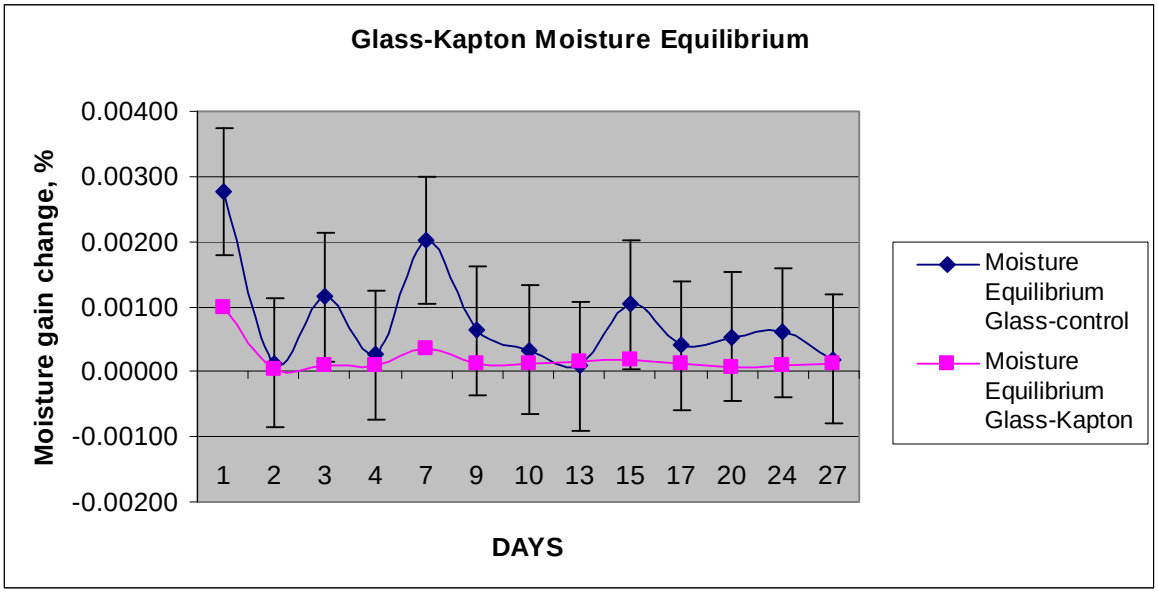

			< 0.0005	
Day	Glass-control	Glass-Kapton	Moisture Equilibrium	
0	7.64983	18.91852	Glass-control	Glass-Kapton
1	7.67099	18.93742	0.00277	0.00100
2	7.67199	18.93803	0.00013	0.00003
3	7.68080	18.94000	0.00115	0.00010
4	7.68281	18.94156	0.00026	0.00008
7	7.69825	18.94805	0.00202	0.00034
9	7.70314	18.95017	0.00064	0.00011
10	7.70570	18.95240	0.00033	0.00012
13	7.70635	18.95510	0.00008	0.00014
15	7.71425	18.95858	0.00103	0.00018
17	7.71730	18.96117	0.00040	0.00014
20	7.72137	18.96243	0.00053	0.00007
24	7.72597	18.96416	0.00060	0.00009
27	7.72746	18.96661	0.00019	0.00013

Figure 3.47 The moisture equilibrium of the glass composites covered with the Kapton film in DI water as a function of the immersion duration.

Figure 3.48 shows the percentage moisture gains for the glass, carbon, and Kevlar fiber reinforced composite laminates. The experimental data clearly revealed that the moisture gains were approximately 1%, 1.5% and 2% for the glass, carbon and Kevlar fiber reinforced laminate composites, respectively.

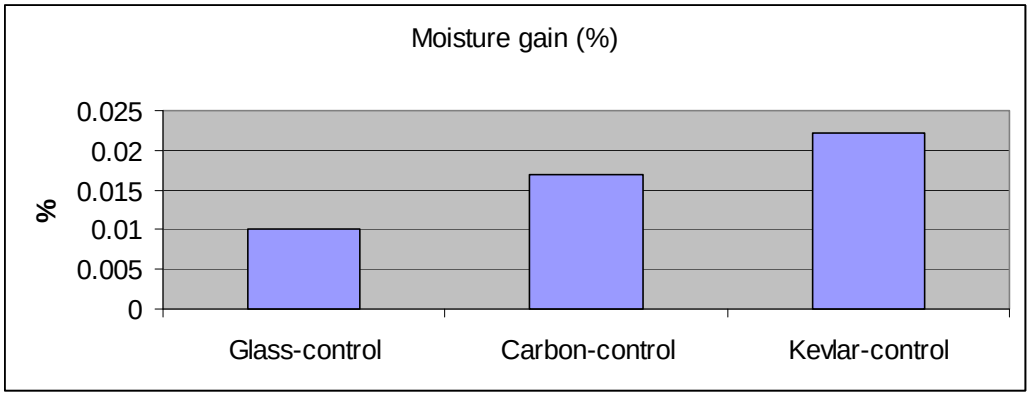

Figure 3.48 The percentage moisture gains for the glass, carbon, and Kevlar fiber reinforced composite laminates.

3.3.2.6 Water Contact Angle Measurements

Surface hydrophobic properties of barrier films were characterized with water contact angle. An optical water contact angle goniometer, KSV Instruments, Model CAM 100 was used to conduct the test. Prior to the contact angle measurements, the barrier film surfaces were degraded with short wavelength UV (Ultraviolet) light to simulate the environmental degradation conditions using a UV chamber [19], [48]. The UV chamber has UVA-340 lamps which can produce the UV spectrum. The UV chamber used in our testing was called QUV Accelerated Weathering Tester (Figure 3.49). The UV exposed samples were placed in the UV chamber for 15 days, and then every 5 days of the exposure the samples were taken out for the contact angle measurement.

Figure 3.49 The UV chamber used for the accelerated weathering test (WSU).

Figure 3.50 shows the contact angle measurements on the UV exposed barrier films bonded to the surfaces of the Kevlar laminates. In general, water contact angle values of the barrier film surfaces are higher than the control ones, and these values are gradually reduced. The Tedlar and PEEK-0.5 barrier film applied coupons resulted in 20% higher contact angle compared to the control coupons. As is mentioned in the previous section, lower contact angle indicates better wetting properties and higher moisture absorption into the composite structures.

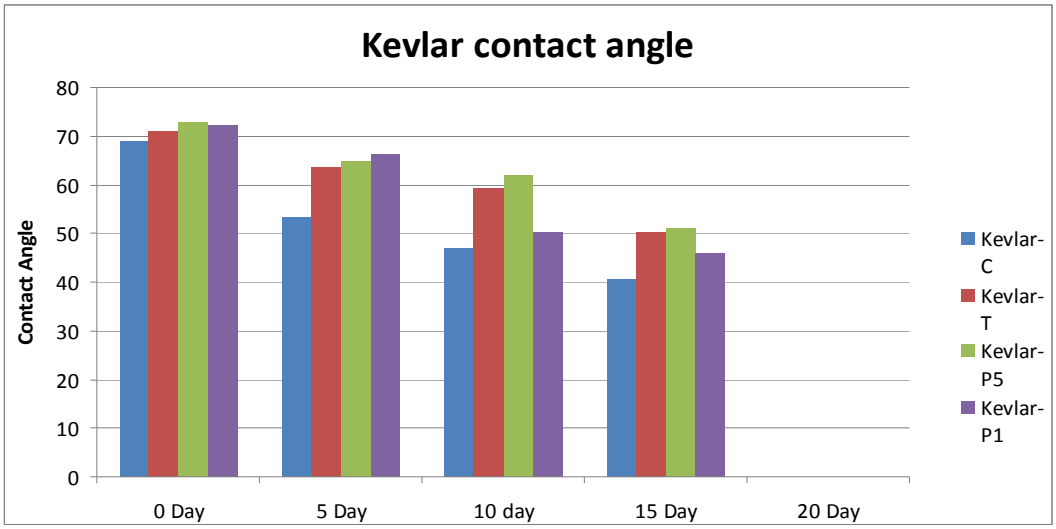

	Time	Kevlar-C	Kevlar-T	Kevlar-P05	Kevlar-P1
Contact θ (º)	0 Day	68.92	70.97	72.81	72.28
	5 Day	53.33	63.65	64.79	66.28
	10 day	46.79	59.38	62.07	50.2
	15 Day	40.48	50.31	51.15	45.72

Figure 3.50 Contact angle measurements on the UV exposed barrier films bonded to the surfaces of the Kevlar laminates.

Figure 3.51 shows the contact angle measurements on the UV exposed barrier films bonded to the surfaces of the carbon composite laminates. The test results indicated that all the UV exposed surfaces lost the surface properties as a function of the UV exposure times. However, the PEEK barrier film applied coupons could give up to 20 % higher contact angle values than the control specimens.

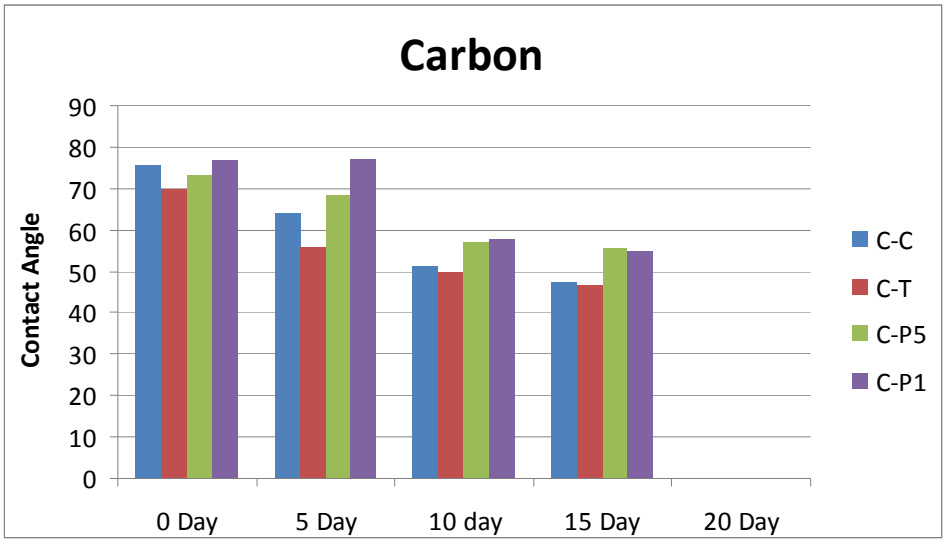

		Carbon-C	Carbon-T	Carbon-P05	Carbon-P1
Contact θ	0 Day	75.62	69.9	73.46	76.87
	5 Day	64.05	55.92	68.54	77.21
	10 day	51.28	49.94	57.06	57.92
	15 Day	47.38	46.87	55.6	54.83

Figure 3.51 Contact angle measurements on the UV exposed barrier films bonded to the surfaces of the carbon laminates.

Figure 3.52 shows the contact angle measurements on the UV exposed barrier films bonded to the surfaces of the glass composite laminates. With the UV conditioning, the control specimens' surface degraded quickly, and after 15 days, the control coupons had the lowest contact angle values. The contact angle values of PEEK barrier film coated glass coupons are approximately 30% higher than the uncoated composite coupons.

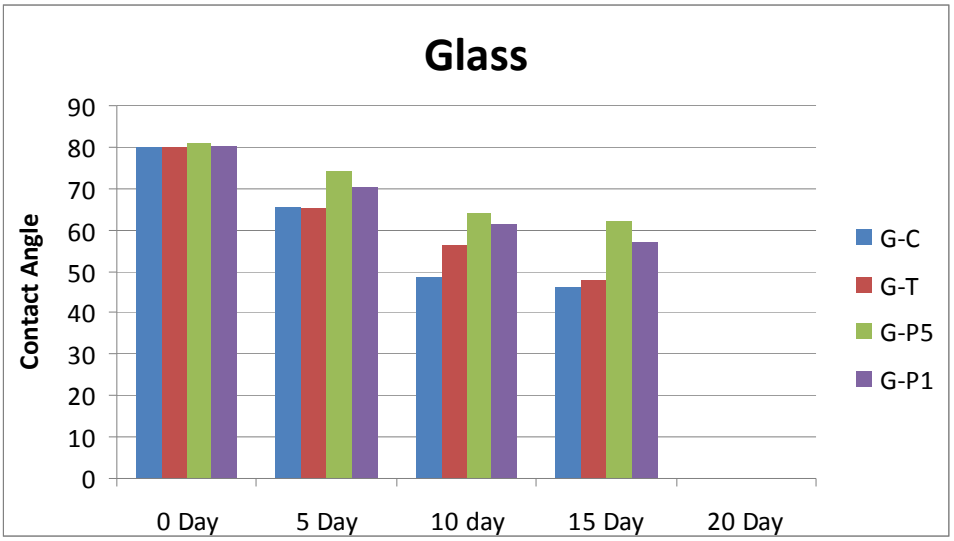

		Glass-C	Glass-T	Glass-P0.5	Glass-P1
Contact θ	0 Day	79.98	79.85	80.97	80.41
	5 Day	65.59	65.26	74.16	70.36
	10 day	48.49	56.36	64.3	61.54
	15 Day	46.16	47.98	62.03	57.3

Figure 3.52 Contact angle measurements on the UV exposed barrier films bonded to the surfaces of the glass composite laminates.

UV light has rays and photons, so the rays most likely break the polymeric chains of the barrier films while the high energy level photons degrade their structures through oxidation and cross-linking. It is know that resin in the composites have higher UV degradation level than the barrier films. The experimental data revealed that using barrier film increased the contact angle values of all the composites. Contact angle measurement supports the experimental moisture absorption data. For example, the Kevlar contact angle is the lowest among the other samples. As is revealed in the section 3.3.2.5, the Kevlar gained most weight percentage than the others during water conditioning.

Another conclusion is that although barrier films (such as PEEK-1) are the same for different base materials (Kevlar, carbon, glass), contact angle results are different after 15 days

UV light conditioning. This concludes that a chemical reaction happened between barrier film and prepreg during polymerization that affects surface characteristics of the barrier films. Table 3.9 shows the contact angle values of the glass fiber reinforced laminates after 15 days of UV exposure.

TABLE 3.9

CONTACT ANGLE VALUES OF DIFFERENT BARRIER FILMS ON THE GLASS FIBER REINFORCED COMPOSITES AFTER 15 DAYS OF THE UV LIGHT CONDITIONING

Material	**Contact angle-control (°)**	**Contact angle - P1 (°)**
Kevlar	40	45
Carbon	47	55
Glass	46	57

3.3.2.7 Shrinkage Test on Barrier Films

17.5 cm length x 7.5 cm width barrier films were cut using a sharp blade, and placed on a 1.25 cm thick epoxy primed aluminum mold. One side of the films was taped on the Al mold, while the other side was free to move. The specimens were placed in an air circulating oven, heated up to 176 °C at 5 °C/min, and dwelled for 2 hours. The test results indicated that the Tedlar film shrunk about 4 cm or 40 % on the length dimension. In contrast, there was no sign of a shrinkage on the PEEK and Kapton specimens. It is conclude that Tedlar barrier films might introduce the internal stresses during the laminate curing cycle. Figure 3.53 shows the barrier films after the heat exposure.

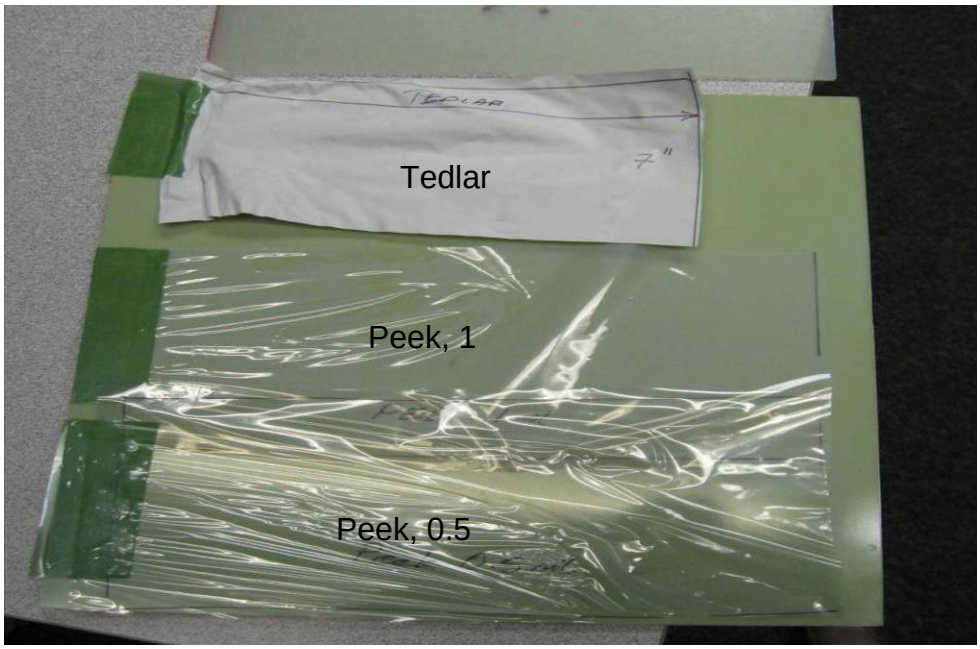

Figure 3.53 The shrinkage tests conducted on the barrier films at elevated temperature.

3.3.2.8 Bonding Test on Barrier Films

The different barrier films were evaluated for the bonding properties on the composite laminates and sandwich structures. The bonding tests were conducted based on the visual inspection of bonding process for the barrier films, as well as during the paint tape tests. The PEEK, Tedlar and Kapton barrier films were bonded well to the composite surfaces during theduring of the prepregs; however, the Teflon films were peeled off quickly and easily from the composite surfaces. This is because the Teflon film has a very low surface energy and is very hard to do plasma and other treatment. Therefore, Teflon is not tested further for moisture evaluations and other mechanical testing. Figure 3.54 shows the de-bonding of the Teflon films from the composite surface.

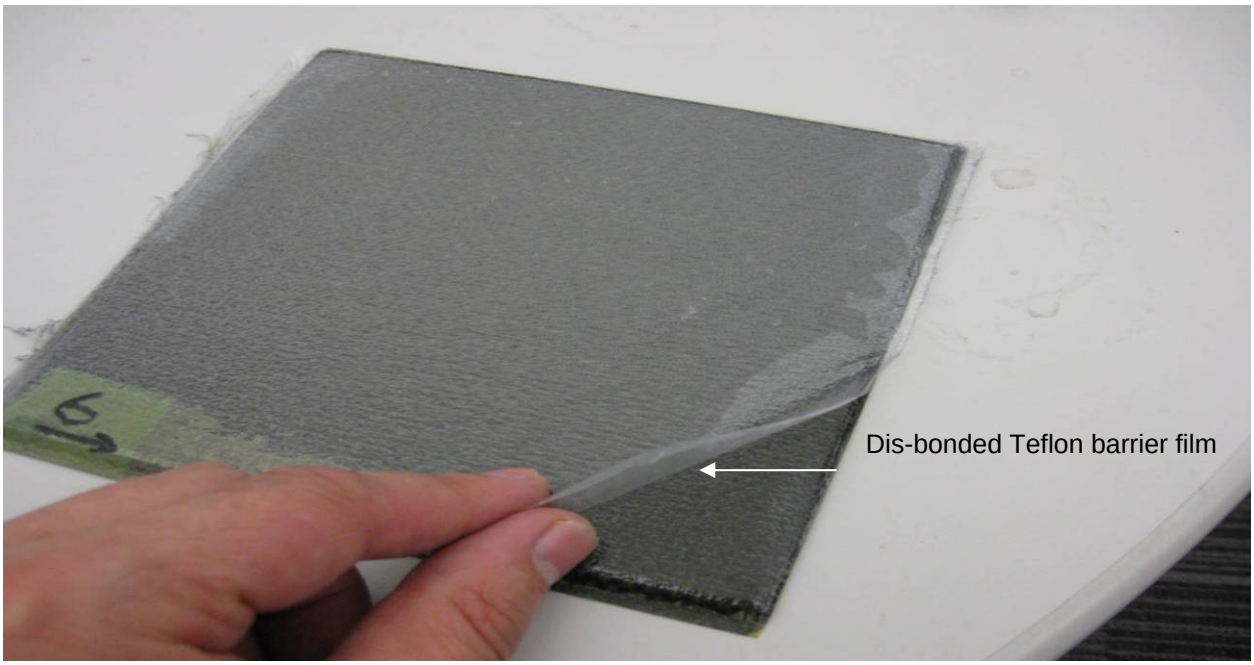

Figure 3.54 The de-bonding of the Teflon barrier film on the carbon laminate.

CHAPTER 4

MODELING

4.1 Modeling

In this chapter, effect of moisture ingression on the stiffness of the materials is studied. To analyze the experimental data, modeling was simulated on 3-Point bend test coupons. FEA is used to estimate the changes in the modulus of elasticity. For each experiment, the slope of force-displacement curve, stiffness, is determined. Then, finite element simulations are run to obtain the same stiffness by adjusting the modulus in FEA.

4.1.1 Theory of Elasticity

For a regular tension or compression, modulus can be calculated by using the Equation (4.1),

$$\sigma = E.\ \varepsilon \quad \text{then } E = \sigma / \varepsilon = (P/A)/(\delta/L) = PL/\delta A \qquad (4.1)$$

where ε is strain, E is modulus, σ is stress, P is load, L is length of span, δ is displacement, A is cross sectional area. Figure 4.1 shows the compression and tension loading on the materials.

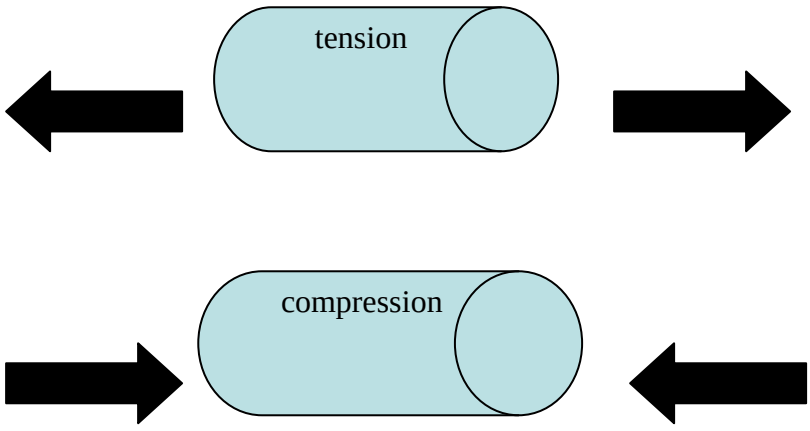

Figure 4.1 Tension and compression loadings on the materials.

For the 3-point bend (Figure 4.2.), Equation (4.1) might not be directly applicable since the load is not applied on the length direction. The closest equation for estimating the modulus of elasticity from the 3-point bend test is Eq. 4.4, where the beam is supported at both ends, as shown in Figure 4.2.

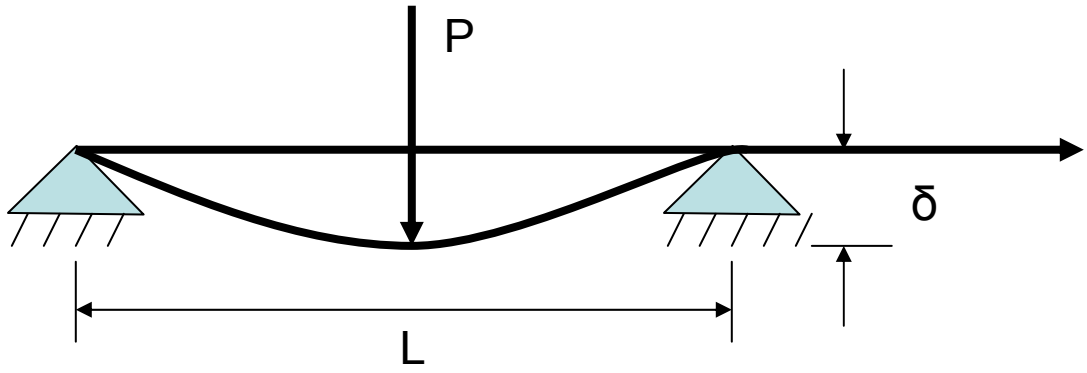

Figure 4.2 Beam supported at the end with a point load in the center, maximum and center deflection.

For the simple model is Figure 4.2, deflection can be calculated using equation (4.2),

$$\delta_{max} = \frac{PL^3}{48E} \tag{4.2}$$

where I is moment of inertia calculated using equation (4.3),

$$I = \frac{wt^3}{12} \tag{4.3}$$

E can be calculated from experimental data using Eq. 4.4.

$$E = (PL^3)/(48\,\delta_{max}I) \tag{4.4}$$

where w is width, t is thickness, L is Length of span, δ is displacement, P is Load

4.1.2 Finite Element Analysis (FEA)

FEA is used to estimate the changes in modulus of elasticity at the 3-Point bend specimens before and after water ingression. For each experiment, using the slope of force-displacement curve, stiffness is determined. Then, finite element simulations are run to obtain

the same stiffness by adjusting the modulus in FEA. As is shown in the flow chart (Figure 4.3), stiffness from experiments is compared with the stiffness from FEA and the modulus that was used for the FEA was adjusted to try to replicate the behavior of the specimen in the experiments. After finding the modulus that result in the same stiffness as the experimental data, it can be concluded that the modulus of the specimen is obtained.

For FEA, model created by using dimensions, w = 0.253", t = 0.125", meshed by 4 node bilinear plane strain quadrilateral (4 sided) and it was solved by an implicit (not time based) simulation using abaqus standard, 910 elements. Material is defined perfectly elastic with Poisson's ratio of 0.3 then adjusted young modulus to match the elastic behavior of the experimental test. Forces vs. displacement curves were compared to match experimental data. Simulation is done by applying displacement to top pin. Upper and lower pins are modeled per analytical rigid bodies. Contacts between the pin and part are considered frictionless (0 value). Boundary conditions, lower pins are fixed and upper pin loaded to create displacement (0.001"). Boundary conditions are divided into two simulation 2-D plane strain. Slope of load/displacement curve is stiffness of the beam. Figure 4.3 is showing FEA flow chart. Figure 4.4 is showing FEA input simulation theory.

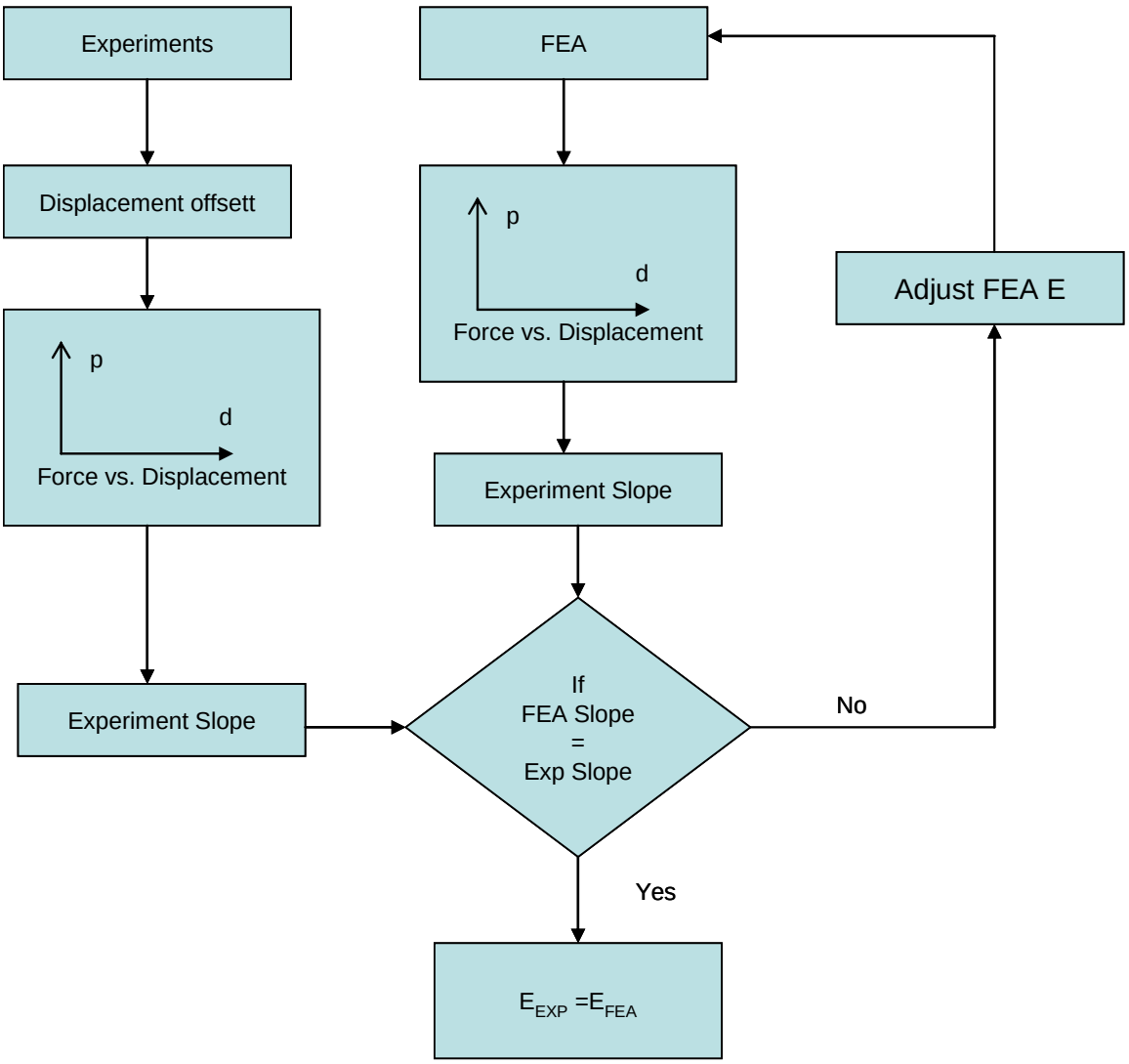

Figure 4.3 FEA Flow chart for the simulation.

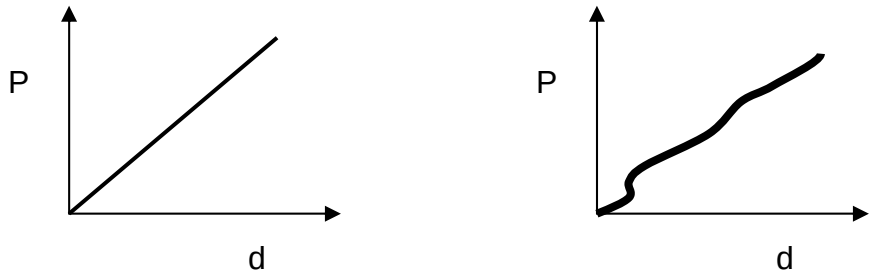

Input: E1, v1

FEA Model - 1

Experimental

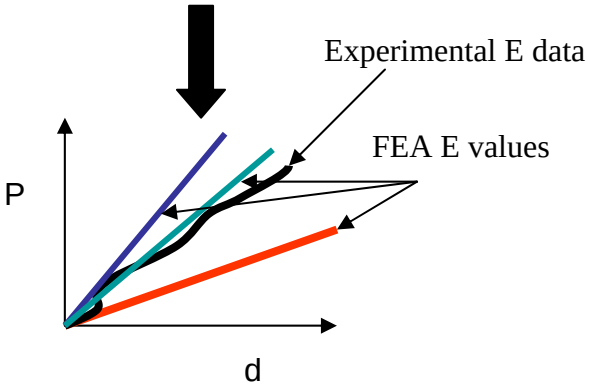

Adjusted Input: E2, v2

FEA Model -2

Figure 4.4 FEA input simulation for the materials.

4.1.2.1 Glass Fiber Composites

Based on the experimental data (load vs. displacement), slopes are calculated and shown in Table 4.1. Since C1 and CW are the extreme conditions based on Figure 4.5., instead of using three different slope values for P05, T1, P1, an average slope calculated using P05, T1, P1 called as “coated”. Then, FEA model is created to obtain the slope values similar to experimental slope data as described earlier. Figures 4.5 and 4.6 show the glass experimental deflection plot and slope.

TABLE 4.1

GLASS SLOPE VALUES

Glass	Slope (lbf/in)
C1	20913
P05	14986
T1	13488
CW	8563
P1	15397

Glass	Slope (lbf/in)
C1	20913
Coated	14624
CW	8563

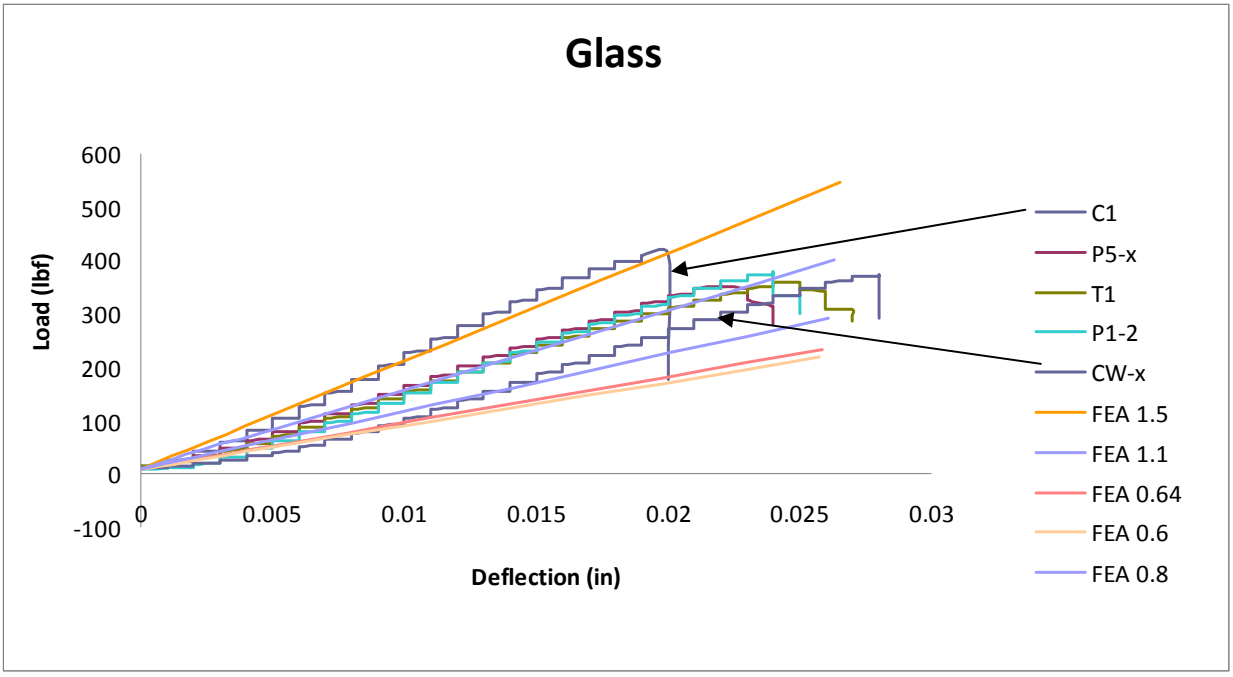

Figure 4.5 Load vs. deflection for experiment and FEA data.

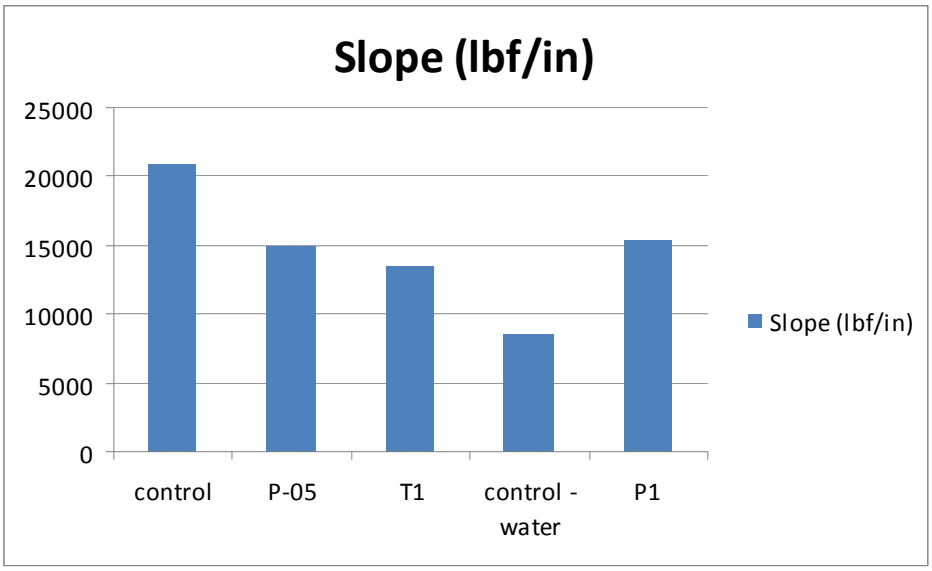

Figure 4.6 Slope values from the experimental data.

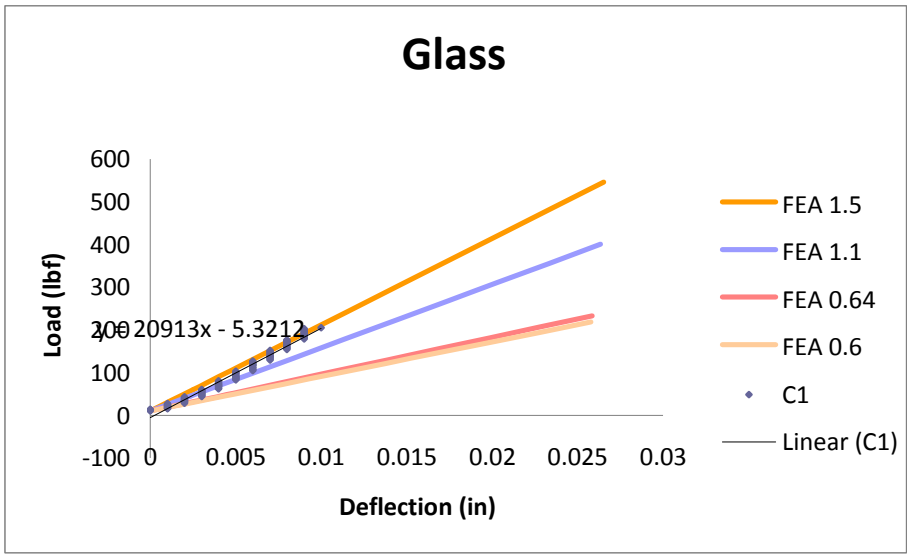

Figure 4.7 FEA estimation for modulus of the materials.

Figure 4.7 shows a sample set of data from FEA simulation. The experimental data from C1 is plotted along with FEA data for E = 1.5, 1.1, 0.64, and 0.6. Each FEA line fitted to the experimental data shows a slope at 20913 lb/in. It can be seen that FEA results for E=1.5 is the closest to the experimental data. By going thru the same process for other cases, the modulus for

C1, CW and coated average are obtained and given below. Table 4.2 gives the extreme modulus values for experimental data calculated thru FEA.

TABLE 4.2

MODULUS VALUES FOR EXTREME CONDITIONS AND AVERAGE BARRIER FILM APPLIED COUPON

Experimental data		FEA	
ID	E (msi)	E(msi)	Slope
		0.8	10783
		0.6	8087
CW	8563	**0.64**	**8626**
Coated avg	14624	**1.1**	**14825**
0		1.5	20216
C1	20913	**1.54**	**20755**

As a conclusion, the modulus for each case is estimated as 1.54, 1.1 and 0.64 Msi for the curves of C1, coated, CW respectively. As it can be seen from Table 4.2., the control sample (C1), has the highest modulus, 1.54, but when exposed into water (CW), the modulus degrades significantly to 0.64. However, with application of the barrier film, moduli increase to 1.1 under same conditions, which confirms the validation of the experimental results. Inputs for FEA Modeling, E gives the estimated values such as 1.5, 1.1, 08, 0.64, 0.6. Dimensions and deflections are L is 0.5", A is 0.253" x 0.250", and δ is 0.001". Figures 4.8 shows SBS model, Figure 4.9 and 4.10 showing the FEA simulations of various conditions.

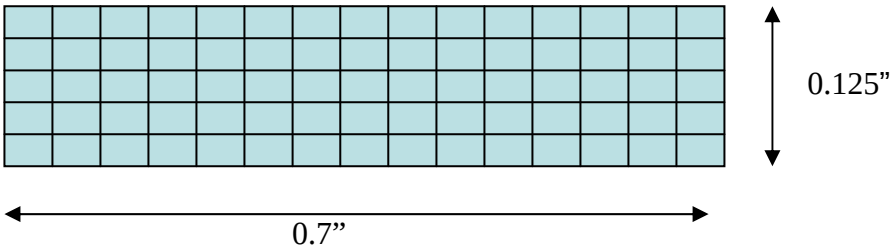

Figure 4.8 SBS model for FEA analysis

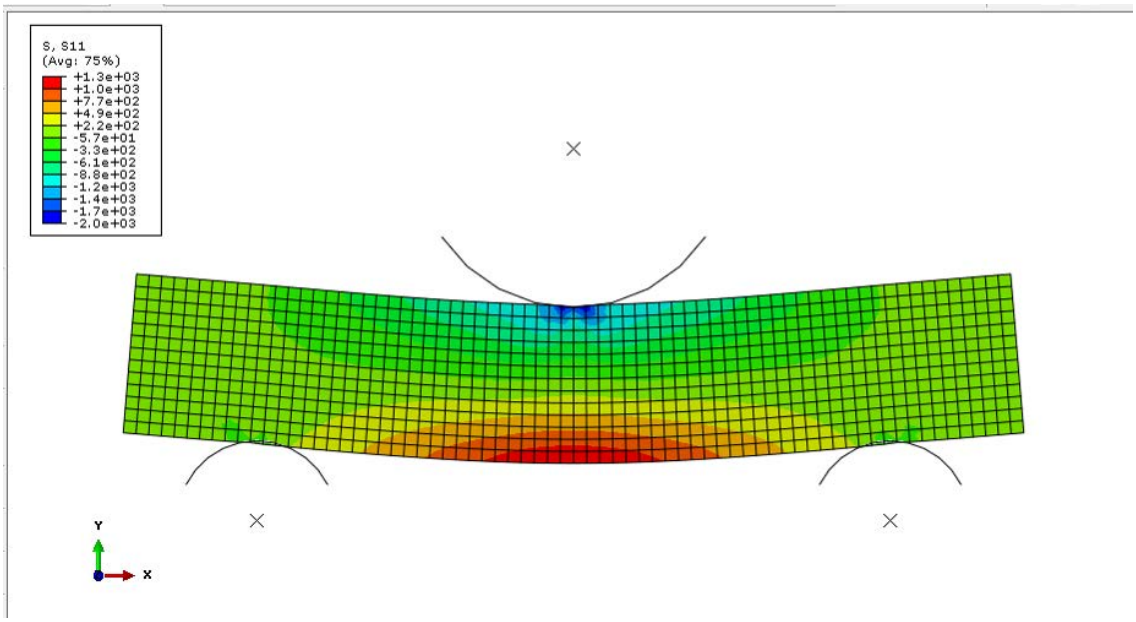

Figure 4.9 Stress in X-direction (psi) for E=0.64 Msi.

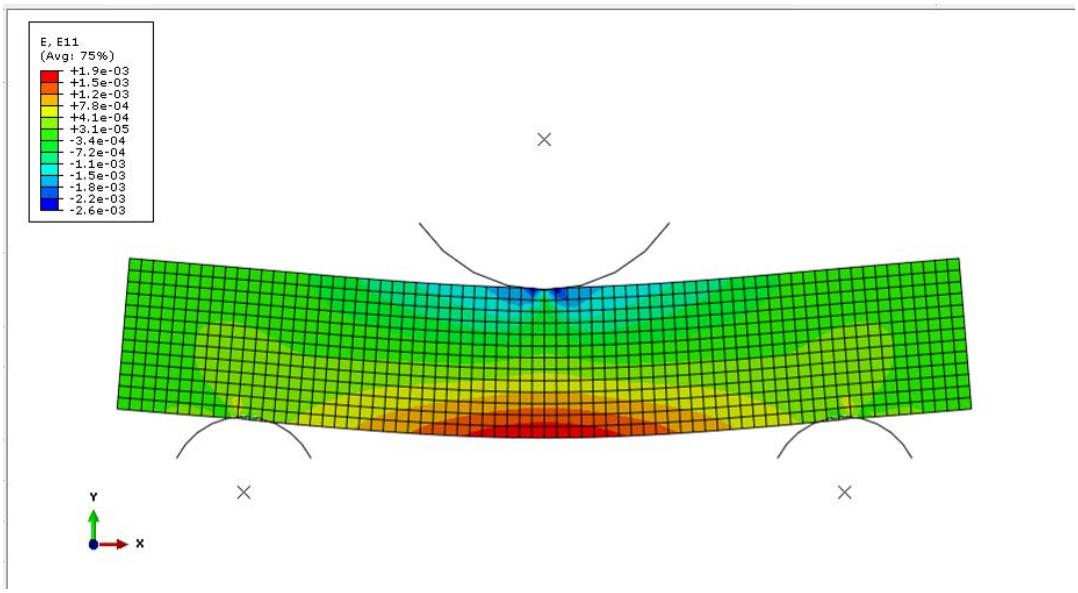

Figure 4.10 Strain in X-direction (in/in) for E=0.64 Msi.

4.1.2.2 Carbon and Kevlar Fiber Composites

For the carbon fiber composites, there was no significant change in modulus values within control vs. control with water and control with water vs. barrier film covered laminates

(Figure 4.11). This might be attributed to the carbon coupons' stiffer and breaking (releasing energy) without deflection and not as sensitive to moisture effects due to the loads causing shear rather than the compression or tension. For the Kevlar fiber composites, as explained in Section 3.3.2.1, material has a more energy absorbent mode (tough) compared to the glass or carbon fiber composites. During the testing, energy is dissipated by deforming, and slope within sample types are not significant enough to detect modulus as is shown in Figure 4.12 (experimental data). Failure mode is in bending rather than shear. That's why it is also not a common practice for industry to conduct 3-point test for the Kevlar fiber composites. Figure 4.11 and 4.12 show the experimental deflection plots for carbon and Kevlar fiber composite coupons.

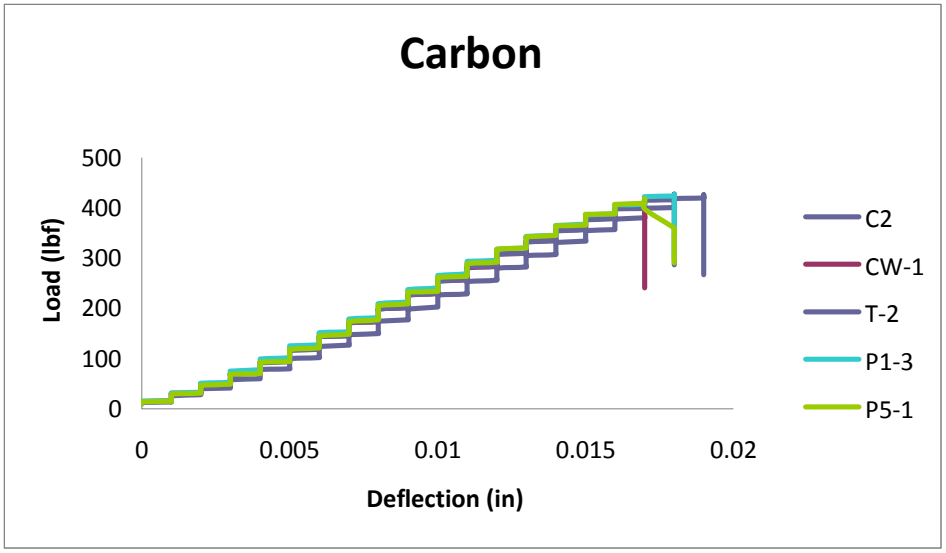

Figure 4.11 Load vs. deflection plot for carbon fiber composite along with the experimental data.

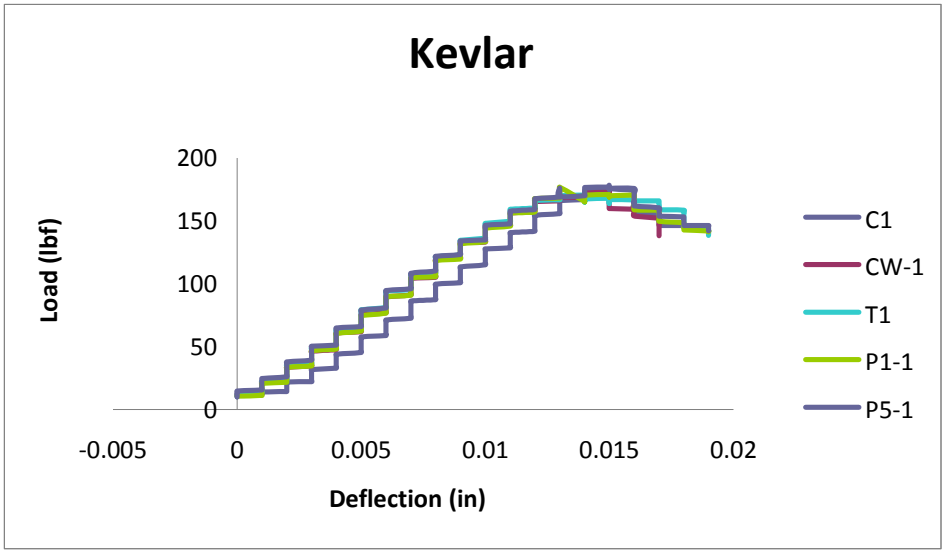

Figure 4.12 Load vs. deflection plot for Kevlar fiber composite along with the experimental data.

For a more detail of the experimental data used during the FEA modeling and simulation, see the Appendixes D for FEA estimation data and E for offset raw data.

CHAPTER 5

CONCLUSION

In this dissertation, moisture prevention and absorption characteristics of a variety of hydrophobic barrier films were investigated by evaluating mechanical and other physical properties. Hydrophobic films were co-bonded to the polymeric composite laminates and sandwich articles, and a variety of tests were conducted to verify their moisture prevention characteristics. Eight types of different tests were conducted for comparison and evaluation: laminate short beam shear (SBS), sandwich flexure, compression, paint tape test, moisture absorption, contact angle, shrinkage, and bonding following the ASTM standards. In addition to testing, finite element analysis (FEA) was used to analyze the stiffness of the conditioned composite laminates.

For moisture absorption, water was chosen as the primary fluid. Compression and 4-point bend sandwich specimens were conditioned by fully immersing them in water at 22 ±2°C for 14 days prior to the mechanical testing. Moisture equilibrium and 3-point bend testing coupons were conditioned in water for 29 days. The duration of water exposure was determined based on the equilibrium time of coupons which had no moisture barrier films. For the second fluid type, Skydrol hydraulic fluid was chosen. Conditioning was conducted for the 4-point bend and compression test coupons by exposing them to a Skydrol bath for 168 hr at 22 ±2°C.

Experimental results indicated that using barrier films significantly improved mechanical properties by reducing water ingression, and improving contact angles. For the 3-Point bend short beam shear (SBS) test on carbon laminates, water conditioned coupons with no barrier films gave up to 15% lower shear strength compared to the unconditioned samples. For the 4-point bend tests, water conditioned glass coupons associated with the barrier film gave between

40 and 100% strength improvement. Skydrol conditioned carbon test coupons incorporated the Tedlar and PEEK-1 barrier films demonstrated about a 20% increase in mechanical strength. The glass coupons with Tedlar and PEEK-1 barrier films showed about 50% higher strength compared to the coupons without any barrier film.

In the water conditioned compression tests for carbon, there was an approximately 20-30% strength increase when the PEEK barrier film was used on the test coupons. The same tests performed on the glass composite coupons associated with the Tedlar barrier film had about 10% better results. There was no significant compression strength difference between the barrier film and control coupons in the Skydrol and water-conditioned Kevlar coupons. This may be attributed to the fact that Kevlar is a tough, but not a stiff, and dissipates the energy by deforming. For the glass and carbon coupons, PEEK and Tedlar barrier film coupons indicated about 15% strength enhancement when compared to the control coupons.

In the moisture ingression tests, glass-PEEK-1 barrier coupons gained 25 % less weight than the control specimens (no barrier films applied). Using a barrier film reduced moisture gain about 400% for the glass-Kapton laminates. After 27 days of the conditioning tests, there was still 50% more weight gain observed on the control specimen than the glass-Kapton coupons. The experimental results also revealed that the glass laminates gained the lowest weight among the test coupons.

Other tests have also been conducted on the barrier and non-barrier composite coupons using paint adhesion tests, shrinking tests, UV light and water contact angle tests. Experimental results confirmed that the barrier films significantly increased the physical properties of the composite coupons, which is a significant improvement for aerospace applications. Finally, the FEA model was developed to predict the mechanical behavior of the composites associated with

barrier films. It is determined that the test results of the FEA are closely related to the experimental results found for the composite coupons.

In addition to what test results revealed about the effect of barrier films on moisture absorption characteristics, the following are the reasons why moisture was detrimental for the composite laminates and sandwich structures. In the 3-point bend test, the experimental data revealed that the barrier film-applied coupons had 5-15% higher shear strength. However, the strength difference between barrier vs. uncoated coupons is not significant as indicated in the 4-point bend tests. This is attributed to the SBS coupons absorbing less moisture due to the laminate's processing conditions and the test method's insufficient sensitivity to detect the moisture effect. Relevant to the processing, the composite laminates were cured at three times higher cure pressure (546 KPa) compared to sandwich structures (200 KPa). During the material curing process, micro-voids can be created due to the out gassing and flow dynamics. Those voids are minimized with the higher cure pressure, so the structure is packed more densely and results in less porosity [6,38]. Moisture effects are more significant at the matrix and resin-fiber interface. Matrix absorption on a composite can be quantified through changes of fracture toughness of the resin or fiber-resin interface. Under loading conditions, cracks grow through the resin matrix or interfacial surface rather than the fiber since fiber is stronger [40,41, 51] and the resin has high moisture absorption characteristics compared to the fiber.

Kevlar coupons indicated buckling/bending failure mode during the 3-point bend and compression testing. The loaded samples absorb energy during a stressed condition. Deflection is an indication of energy absorbent capacity, which allows energy to dissipate during the failure. If the substrate cannot deform or cannot release the energy, it will break (known as a brittle failure). Therefore, Kevlar coupons dissipated the energy by buckling.

The 4-point bend tests of the water conditioned glass sandwich revealed that barrier-applied coupons showed up to a 100% flex strength increase. The 4-point bend tests of the Skydrol conditioned Kevlar sandwich composite showed that the barrier applied coupons had a 40% flex strength increase. It is concluded that the use of barrier films is critically important for the glass and Kevlar sandwich assemblies.

The failure mode was skin failure for all the 4-point bend coupons except Kevlar, which showed buckling. This indicates that the laminate skin surface is more affected than the adhesive bond, or that moisture was not able to ingress fully into the bond area to have delamination.

Moisture equilibrium is reached when the average moisture content of the traveler specimen changes by less than 0.05% for two consecutive readings within a span of 3 ±0.5 days. When the experimental data is examined, each material shows different absorption rate, and using the recommended procedure might lead to an incorrect moisture equilibrium duration and absorption rate. The laminate absorption rate depends on material characteristics, such as how densely the laminate is packed. It is concluded that there is no standard span time for the consecutive measurements.

In the paint tape test, barrier film-applied coupons did not have any paint on the peeled tape surface. Although barrier films are plasma treated to have low surface energies, test results indicated that the barrier films, except Teflon, which has very low surface energy, have enough bond properties to bond to resin during polymerization.

Moisture absorption tests showed that the weight gain was 1% for glass, 1.5% for carbon, and 2% for Kevlar when moisture equilibrium point is at the maximum. It is determined that based on resin and reinforcement material characteristics, the weight gain can significantly change all the properties even though samples for the same type of barrier films are processed with the same temperature and pressure.

Experimental data for contact angle measurements showed that at the beginning of testing, control specimens' contact angle values were similar to the barrier films due to high gloss resin surfaces. After the UV exposure, control specimen surfaces degraded quickly, in 15 days, and measurements indicated that the control specimens had the lowest contact angle values. On the other hand, barrier films' contact angles did not decrease as dramatically as the controls. It has been found that contact angle measurements correlate with moisture ingression test results by showing that using barrier films increases contact angle; as a result, moisture ingression rates decrease significantly.

The experimental data showed that the contact angle values of the Kevlar composites are the lowest. This supports the moisture absorption results obtained throughout the experimental data where the Kevlar composites gained more weight than the others during conditioning. Although the same barrier film was used for Kevlar, carbon, and glass, the contact angles are still different after 15 days of conditioning. This gives an indication that polymerization during resin curing might be affecting the surface characteristics of the barrier films.

The contact angle measurements revealed that the glass reinforced laminates provided higher contact angle values. It is recommended that using glass as a most outer prepreg ply on composite assemblies can increase repellency properties and reduce moisture ingression, which may drastically change the mechanical properties of the composites. The experimental results also indicated that the barrier films (Tedlar) can shrink significantly. It is concluded that depending on barrier film thickness and characteristics, the barrier films might introduce internal stresses during the laminate curing cycle.

CHAPTER 6

FUTURE RESEARCH

Based on the experimental results, there are significant scientific findings in the field. For future studies it is recommended that research studies are conducted to:

- Investigate the disadvantages of the barrier film relative to the porosity level, as the barrier films may entrap the gasses created during the curing process.
- Make uncured barrier films which can co-cure together with resin, allowing the cure gasses to escape during polymerization.
- Use moisture absorption tests for variable traveler dimensions by changing the width, length, and thickness to verify the effect of dimensions on the moisture absorption gain and rate.
- Verify the effect of conditioning methods based on the moisture absorption gain. For example, conditioning in a chamber (85-95 % RH at 70-80 °C) vs. direct water immersion may determine short conditioning durations.
- Model NDI (non destructive inspection) properties related to the moisture absorption rates. This might provide verification of moisture absorption amounts in the structures without extensive destructive testing.
- Investigate the effect of moisture relative to aircraft icing.
- Verify the effect of weight measurement span time for moisture equilibrium. The current industry standard span time of seven days is restricted to stop conditioning when consecutive measurement weight change reaches less than 0.05% [47].
- Investigate the effect of temperature and pressure fatigue tests for the moisture exposed aircraft structural composite assemblies.

REFERENCES

REFERENCES

[1] Higgins, R.A., "Properties of Engineering Materials", 2nd addition, 1994, ISBN 0-8311-3055-5.

[2] Menail, Y., El Mahi, A., Assarar, M., Redjel, B., Kondratas, A., "The effects of water aging on the mechanical properties of glass-fiber and Kevlar-fiber epoxy composite materials", ISSN 1392-1207, MECHANIKA, 2009, Nr. 2(76).

[3] Garton, A., Daly, J. H., "The Crosslinking of Epoxy Resins at Interfaces. II. At an Aromatic Polyamide Surface", Journal of Polymer Science: Polymer Chemistry Edition Vol. 23, 1031-1041 (1985).

[4] Lee, B.L., Yang, T.W., "Moisture Effects on Isobutylene-Isoprene Copolymer-Based Composite Barrier. I: Moisture Diffusion and Detection" Polymer Engineering and Science, Mid-May 1996, Vol. 36, No. 9.

[5] Pilli, S. P., Simmons, K.L., Holbery, J.D., Shutthanandan, V., Stickler, P.B., Smith, L.V., "A novel accelerated moisture absorption test and characterization" ScienceDirect, Composites Part A 40 (2009) 1501-1505.

[6] Abot, J.L., Yasmin, A., Daniel, M. I., " Hygroscopic Behaviour of Woven Fabric Carbon-Epoxy Composites ", Journal of Reinforced Plastics and Composites, Vol, 24, No. 2/2005.

[7] Browning, C.E, Husman, C.E., Whitney, J.M., "Moisture Effects in Epoxy Matrix Composite" Technical Report AFML-TR-77-17, 1978, Air force Materials Laboratory, Wright-Patterson Airforce Base, OH.

[8] Earl, J.S., Shendi, R.A., "Determination of the Moisture Uptake Mechanism in Closed Cell Polymeric Structural Foam During Hygrothermal Exposure" Journal of Composite Materials, Vol. 38, No. 15/2004.

[9] Katzman, H.A., Castaneda, R.M., Lee, H.S., "Moisture diffusion in composite sandwich structures". ScienceDirect, Composites Part A 39 (2008) 887-892. ScienceDirect, Composites Part A 37 (2006) 636-645.

[10] Shi, B., Hinderliter, B.R., Croll, S.G "Environmental and time dependence of moisture transportation in an epoxy coating and its significance for accelerated weathering" 2009 CoatingTech Conference, April 28-29, 2009, IN.

[11] Wang, C.H., Tsai, C., "Theoretical Study for Moisture Diffusion in a Carbon/Epoxy Composite Laminate Accompanied by Thermal Conduction" Journal of Composite Materials, Vol. 44, No. 18/2010.

[12] BASF Corporation , “Effects of Moisture Conditioning Methods on Mechanical Properties of Injection Molded Nylon 6”, New Jersey, 2003.

[13] Czel, G., Czigany, T., “A study of water absorption and mechanical properties of glass fiber/polyester composite pipes-effects of specimen geometry and preparation” Journal of Composite Materials, Vol. 42, No 26, 2008.

[14] Carfagna, C., Amendola, M., Giamberini, M., Menstier, G., Del Nobile, M.A., “ Water Sorption in a Novel Liquid Crystalline Epoxy Resin ”, Polymer Engineering and Science, January 1995, Vol. 35, No. 2.

[15] Krumweide, G.C., Derby, E.A., Chamberlin, D.N., “The Performance of Effective Moisture Barriers for Graphite/Epoxy Instruments Structures” 21st International SAMPE Technical Conference September 25-28, 1989.

[16] Jedidi, J. Jacquemin, F. , Vautrin, A., “ Accelerated hygrothermal cyclical tests for carbon/epoxy Laminates” ScienceDirect, Composites Part A 37 (2006) 636-645.

[17] Thellen, C., Rattlo, A., “Influence of Moisture on the Mechanical and Barrier Properties of Multilayer Aromatic Polyamide Nanocomposite Films”, US Army NSRDEC, Natick, MA.

[18] Sun, Q., Schork, J. F., Deng, Y., “Water-based polymer/clay nanocomposite suspension for improving water and moisture barrier in coating” Composite Science and Technology, Vol. 67, Issue 9, July 2007, 1823-1829.

[19] Asmatulu, R., Khan, S.I., Misak, H., Nuraje, N. “Graphene Based Nanocomposite Coating on Fiber Reinforced Composites Subjected to UV Degredation” MS Thesis, Wichita State University, 12/2010.

[20] Burack, J.J., Legrance, J.D., Lin, W., “Enhanced Moisture Protection of Eloctronic Devices by Ultra-Thin Polyimide Films” IEEE Transactions on Components, Hybrids, and Manufacturing Technology, Vol. 13. No. 1. March 1990.

[21] Stone, C.J. “Additive Regression and Other Nonparametric Models“ Analaysis of Statistics, 13, 689-705, 1985.

[22] Mensitieri, G., Lavorgna, M. Musto, P., Ragosta, G., “Water transport in densely crosslinked networks: A comparison between epoxy systems having different interactive characters” ScienceDirect, Polymer 47 (2006) 8326-8336.

[23] Czabaj, M.W., Zehnder, A.T., Chuang, K.C., “Blistering of Moisture Saturated Graphite/Polyimide Composites Due to Rapid Heating” Journal of Composite Materials, Vol. 43, No. 02/2009.

[24] Chang, TW, Wang, C.H., Tsai, C., “Advancing Boundary Model for Moisture Diffusion in A Composite Laminate” Journal of Composite Materials, Vol. 42, No. 10/2008.

[25] Tedlar product and performance guide, “dupont.com/Tedlar_PVF_Film.pdf”

[26] Fogarty, J.H., “Honeycomb Core and Myth of Moisture Ingression” Appl Composite Materials (2010) 17:293-307.

[27] Miller, F.P., Vandome, A.F. McBrewster, J., Chemical Polarity, Alphascript Publishing, 2011, ISBN: 6130248091.

[28] American Society for Testing and Materials, “Standard Test Methods for Short Beam strength of Polymer matrix composite materials and their laminates”, in ASTM Standard: ASTM D 2344.

[29] Mensitieri, G., Lavorgna, M., Musto, P., Ragosta, G., “ Water transport in densely crosslinked networks: A comparison between epoxy systems having different interactive characters” Science Direct, Polymer 47 (2006) 8326-8336.

[30] American Society for Testing and Materials, “ Standard Test Methods for Compressive Properties of combine loading compression”, in ASTM Standard: D 3410.

[31] American Society for Testing and Materials, “Standard Test Methods for Measuring Adhesion by Tape Test”, ASTM Standard: D 3359-09.

[32] ASTM B117-09: Standard practice for operating Salt Spray (Fog) Apparatus, American Society for Testing and Materials, 2009.

[33] Hameed, N., Thomas, S.P., Abraham, R., Thomas, S. “Morphology and contact angle studies of poly modified epoxy resin blends and their glass fibre reinforced composites” eXPRESS Polymer letters, Vol. 1, No. 6 2007.49

[34] Wenzel, R.N., “Surface Roughness and Contact Angle”, The Journal of Physical Chemistry, 1949, 53 (9), pp 1466-1467.

[35] American Society for Testing and Materials, “Standard Test Methods for Measurement of the Surface Tension of Solid Coatings Substrates and Pigments Using Cntact Angle Measurement”, ASTM D 7490-08.

[36] Vandencasteele, N., Merche, D., Reniers, F. “XPS and contact angle study of N_2 and O_2 plasma-modified PTFE, PVDF, and PVF surfaces” Surface and Interface Analysis, 2006: 38: 526-530.

[37] Odian, G., “Principles of Polymerization”, 3rd ed., J. Willey, New York, 1991.

[38] Olivero, K.A., Barraza, H.J., O’Rear, E.A., Altan, M.C., “Effect of injection rate and post -fill cure pressure on properties of resin transfer molded Disks” Journal of Composite Materials, Vol. 36, No 16, 2002.

[39] Kapton product and performance guide, DuPont "dupont.com/Kapton/en_US Assets/downloads/pdf.

[40] Bradley, W.L., Cohen, R.N., "Matrix deformation and Fracture in graphite-reinforced Epoxies", Delamination and Debonding of materials, ASTM STP 876 W.S. Johnson Ed., ASTM, Philadelphia 1985 pp 389-410.

[41] Lekatou, A., Qian, Y., Faide, S.E., Lyon, S.B., Islam, N., Newman, R.C., "Interfacial Water Transport and Embrittlement in Polymer-Matrix Composites" Mat. Res. Soc. Symp. Proc. Vol. 304, 1993.

[42] ASM International, Engineering Plastics, ISBN: 0-87170-280-0, Vol. 2, Engineered Materials Handbook, 1988.

[43] Owen, W. J., "An Exponential Damage Model for Strength of Fibrous Composite Materials" IEEE Transactions on Reliabilty, Vol. 56, No 3, September 2007.

[44] Li, G Helms, J. E., Pang, S "Analytical Modeling of Tensile Strength of Particulate-Filled Composites" Polymer Composites, October 2001, Vol. 22, No. 5.

[45] Askeland, D. R., The Science and Engineering of Materials, PWS Publishing Company, 1994. 2nd ed. ISBN: 0534916570.

[46] American Society for Testing and Materials, "Facing Properties of Sandwich Construction by Long Beam Flexure", ASTM Standard: D 7249/ D 7249M-06.

[47] Advanced General Aviation Technology Experiments (AGATE) "Material Qualification and Equivalency for Polymer Matrix Composite Material" DOT/FAA/AR-09-47.

[48] Lee, B.S., Lee, D.C., "Surface Degredation Properties of Ultraviolet Treated Epoxy/Glass Fiber" IEEE Transactions on Dielectrics and Electrical Insulation, Vol. 6, December 1999.

[49] Morgan, B., Madhukar, M., Walsh, J., Hooker, M., Grandlienard, S. "Moisture Degradation of Cyanate Ester/S2 Glass Composite Insulation Systems" Journal of Composite Materials, Vol. 44, No. 7/2010.

[50] Iqbal, M.M., Liang, W., "Modeling the moisture effects of solid ingredients on composite propellant properties" Science Direct, Aerospace Science and Technology 10 (2006) 695-699.

[51] J.P. Lucas, J. Zhou, " Moisture Absorption Effects on Delamination Fracture Mechanism of Carbon Fiber Polymeric Matrix Composites' ICCM/9 proceedings of the ninth international Volume1, 3, 5. Society for the Advancement of Material and Process Engineering, 1993 pp-633-640.

[52] American Society for Testing and Materials, “ Standard Test Methods for Moisture Absorption Properties and Equilibrium Conditioning of Polymer Matrix Composite Materials”, in ASTM Standard: D 5229/ D 5229M-92.

[53] Ghosh, K.M., Mittal, K.L., “Polylmides: Fundamentals and Applications”, Marcel Dekker, Inc. July 1996 ISBN : 0-8247-9466-4.

APPENDIXES

APPENDIX A.

KEVLAR 3-POINT BEND RESULTS FROM MTS TEST MACHINE

Sample ID: KEVLAR Test Date:
Method: ASTM 2344 Short Beam Shear with specimen ID.msm Operator: Erkan

Sample Information:

Name	Value
1- Material Description	KEVLAR
2- Material Specification	N/A
3-	
4-Test Machine	ALLIANCE RF/ XXX
5-Load Cell	1000 LB S/N XXXX
6-Test Condition	RTA
7-Data File	K1
8-Calculation explanation	(load x .75)/(with x thick)
9-Sample Comments	0.250 load point/0.125 reaction points (tested 4 x thickness) label side up
Load limit	1000
span	.426

Sample Results:
Specimen Results:

Specimen #	Specimen ID	Width in	Thickness in	Peak Load lbf	Shear Strength ksi		Condition
1	C-1	0.253	0.1060	178.3	5.0	Control	No water
2	C-2	0.256	0.1080	185.0	5.0		No water
3	C-3	0.256	0.1080	185.3	5.0		No water
4	C-4	0.253	0.1060	180.4	5.0		No water
5	CW-1	0.256	0.1070	173.1	4.7	Control water	Water 14 days
6	CW-2	0.256	0.1070	173.3	4.7		Water 14 days
7	CW-3	0.256	0.1080	173.4	4.7		Water 14 days
8	CW-4	0.256	0.1040	159.8	4.5		Water 14 days
9	CW-5	0.256	0.1040	162.0	4.6		Water 14 days
10	P1-1	0.256	0.1060	176.9	4.9	PEEK 1 MIL	Water 14 days
11	P1-2	0.253	0.1060	175.8	4.9		Water 14 days
12	P1-3	0.253	0.1070	175.1	4.9		Water 14 days
13	P1-4	0.255	0.1070	180.0	4.9		Water 14 days
14	P1-5	0.253	0.1060	173.5	4.9		Water 14 days
15	P05-1	0.256	0.1050	176.9	4.9	PEEK 0.5 MIL	Water 14 days
16	P05-2	0.256	0.1080	179.6	4.9		Water 14 days
17	P05-3	0.255	0.1060	173.2	4.8		Water 14 days
18	P05-4	0.256	0.1080	178.2	4.8		Water 14 days
19	P05-5	0.255	0.1070	175.1	4.8		Water 14 days
20	T1	0.256	0.1050	172.1	4.8	TEDLAR	Water 14 days
21	T2	0.255	0.1060	169.6	4.7		Water 14 days
22	T3	0.256	0.1040	169.3	4.8		Water 14 days
23	T4	0.255	0.1060	170.0	4.7		Water 14 days
24	T5	0.256	0.1080	175.4	4.8		Water 14 days
Mean		0.255	0.106	173.5	4.80		
Std. Dev.		0.0012	0.0013	5.3784	0.1234		
% COV		0.46	1.19	3.10	2.57		

Calculation Inputs:
Test Inputs:

Name	Value	Units
Data Acquisition Rate	10.0	Hz
Test Speed	0.05	in/min

APPENDIX B.

GLASS 3-POINT BEND RESULTS FROM MTS TEST MACHINE

Sample ID: GLASS Test Date:
Method: ASTM 2344 Short Beam Shear with specimen ID.msm Operator: Erkan

Sample Information:

Name	Value
1- Material Description	GLASS
2- Material Specification	N/A
3-	
4-Test Machine	ALLIANCE RF/ XXX
5-Load Cell	1000 LB S/N
6-Test Condition	RTA
7-Data File	GLASS
8-Calculation explanation	(load x .75)/(with x thick)
9-Sample Comments	0.250 load point/0.125 reaction points (tested 4 x thickness) label side up
Load limit	1000
span	.500

Sample Results:
Specimen Results:

Specimen #	Specimen ID	Width in	Thickness in	Peak Load lbf	Shear Strength ksi	CONDITION	
1	Control/No water	0.252	0.1260	408.3	9.6	No water	
2	Control/No water	0.251	0.1260	402.0	9.5	No water	
3	Control/No water	0.251	0.1260	408.5	9.7	No water	
4	Control/No water	0.251	0.1260	408.2	9.7	No water	
5	Control/water	0.253	0.1250	353.4	8.4	14 days in water	
6	Control/water	0.253	0.1250	366.2	8.7	14 days in water	
7	Control/water	0.255	0.1240	366.4	8.7	14 days in water	
8	Control/water	0.255	0.1240	360.1	8.5	14 days in water	
9	Tedlar/water	0.252	0.1230	373.5	9.0	14 days in water	
10	Tedlar/water	0.253	0.1230	373.3	9.0	14 days in water	
11	Tedlar/water	0.252	0.1230	373.1	9.0	14 days in water	
12	Tedlar/water	0.252	0.1230	373.5	9.0	14 days in water	
13	Peek-05/water	0.253	0.1250	372.6	8.8	14 days in water	
14	Peek-05/water	0.253	0.1250	372.1	8.8	14 days in water	
16	Peek-05/water	0.255	0.1240	371.9	8.8	14 days in water	
17	Peek-05/water	0.255	0.1240	372.5	8.8	14 days in water	
18	Peek-1/water	0.255	0.1240	391.3	9.3	14 days in water	
19	Peek-1/water	0.255	0.1240	377.5	9.0	14 days in water	
20	Peek-1/water	0.255	0.1240	377.8	9.0	14 days in water	
21	Peek-1/water	0.255	0.1240	373.7	8.9	14 days in water	
Mean		0.253	0.124	378.8	9.01		
Std. Dev.		0.0016	0.0010	16.1193	0.3726		
% COV		0.62	0.84	4.26	4.14		

Calculation Inputs:
Test Inputs:

Name	Value	Units
Data Acquisition Rate	10.0	Hz
Test Speed	0.05	in/min

APPENDIX C.

CARBON 3-POINT BEND RESULTS FROM MTS TEST MACHINE

Sample ID: Carbon Test Date:
Method: ASTM 2344 Short Beam Shear with specimen ID.msm Operator: Erkan

Sample Information:

Name	Value
1- Material Description	CARBON
2- Material Specification	N/A
3-Melr #	
4-Test Machine	ALLIANCE RF/ 100
5-Load Cell	1000 LB
6-Test Condition	RTA
7-Data File	C1
8-Calculation explanation	(load x .75)/(with x thick)
9-Sample Comments	0.250 load point/0.125 reaction points (tested 4 x thickness) label side up
Load limit	1000
span	.426

Sample Results:
Specimen Results:

Specimen #	Specimen ID	Width in	Thickness in	Peak Load lbf	Shear Strength ksi	Condition	Notes
1	C1	0.250	0.1060	445.8	12.6	No water	Control
2	C2	0.250	0.1060	426.0	12.1	No water	
3	C3	0.251	0.1070	432.2	12.1	No water	
4	C4	0.251	0.1070	430.7	12.0	No water	
5	Cw1	0.254	0.1080	402.5	11.0	Water, 14 days	Control water
6	Cw2	0.254	0.1080	411.4	11.2	Water, 14 days	
7	Cw3	0.251	0.1070	391.8	10.9	Water, 14 days	
8	Cw4	0.258	0.1050	387.4	10.7	Water, 14 days	
9	P05-1	0.254	0.1070	418.2	11.5	Water, 14 days	PEEK 0.5 MIL
10	P05-2	0.254	0.1070	412.2	11.4	Water, 14 days	
11	P05-3	0.258	0.1040	412.4	11.5	Water, 14 days	
12	P05-4	0.257	0.1070	418.6	11.4	Water, 14 days	
13	P05-5	0.256	0.1080	420.8	11.4	Water, 14 days	
14	T-1	0.251	0.1060	425.8	12.0	Water, 14 days	TEDLAR 1 MIL
15	T-2	0.251	0.1070	427.2	11.9	Water, 14 days	
16	T-3	0.258	0.1011	412.3	11.9	Water, 14 days	
17	T-4	0.258	0.1060	433.7	11.9	Water, 14 days	
18	P-1	0.254	0.1080	423.2	11.6	Water, 14 days	PEEK 1 MIL
19	P-2	0.255	0.1090	437.8	11.8	Water, 14days	
20	P-3	0.253	0.1080	426.1	11.7	Water, 14 days	
21	P-4	0.257	0.1090	436.8	11.7	Water, 14 days	
Mean		0.254	0.107	420.6	11.63		
Std. Dev.		0.0029	0.0017	14.5523	0.4635		
% COV		1.13	1.63	3.46	3.98		

Calculation Inputs:
Test Inputs:

Name	Value	Units
Data Acquisition Rate	10.0	Hz
Test Speed	0.05	in/min

APPENDIX D.

ESTIMATED E VALUES FOR FEA ANALYSIS FOR SLOPE

For estimated E as 0.64 Msi, slope is 8626 lb/in

FEA 0.64

time	Deflection (in)	Load (lbf)
0	0	0
0.1	0.0001	0.006274
0.2	0.0002	0.861648
0.3	0.0003	1.72408
0.4	0.0004	2.58665
0.5	0.0005	3.44936
0.6	0.0006	4.3122
0.7	0.0007	5.17518
0.8	0.0008	6.0383
0.9	0.0009	6.90156
1	0.001	7.76497

Deflection (in)	offset	Load (lbf)	
0		0	
0.003		0.18821	Slope
0.004147	0	10	8626.36
0.006	0.001853	25.84944	
0.009	0.004853	51.7224	
0.012	0.007853	77.5995	
0.015	0.010853	103.4808	
0.018	0.013853	129.366	
0.021	0.016853	155.2554	
0.024	0.019853	181.149	
0.027	0.022853	207.0468	
0.03	0.025853	232.9491	

For estimated E as 0.60 Msi, slope is 8087 lb/in

E=.6msi

FEA 0.6

time	Deflection (in)	Load (lbf)
0	0	0
0.1	0.0001	0.005882
0.2	0.0002	0.807795
0.3	0.0003	1.61633
0.4	0.0004	2.42498

0.5	0.0005		3.23377
0.6	0.0006		4.04269
0.7	0.0007		4.85173
0.8	0.0008		5.66091
0.9	0.0009		6.47022
1	0.001		7.27966

Deflection (in)	offset	Load (lbf)	
0		0	
0.003		0.176447	Slope
0.004225	0	10	8087.32
0.006	0.001775	24.23385	
0.009	0.004775	48.4899	
0.012	0.007775	72.7494	
0.015	0.010775	97.0131	
0.018	0.013775	121.2807	
0.021	0.016775	145.5519	
0.024	0.019775	169.8273	
0.027	0.022775	194.1066	
0.03	0.025775	218.3898	

For estimated E as 0.80 Msi, slope is 10782 lb/in

E=.8msi
FEA 0.8

time	Deflection (in)	Load (lbf)
0	0	0
0.1	0.0001	0.007842
0.2	0.0002	1.07706
0.3	0.0003	2.1551
0.4	0.0004	3.23331
0.5	0.0005	4.31169
0.6	0.0006	5.39025
0.7	0.0007	6.46897
0.8	0.0008	7.54788
0.9	0.0009	8.62695
1	0.001	9.70621

Deflection (in)	offset	Load (lbf)	
0		0	
0.003		0.235263	Slope
0.003913	0	10	10782.53
0.006	0.002087	32.3118	
0.009	0.005087	64.653	
0.012	0.008087	96.9993	

0.015	0.011087	129.3507
0.018	0.014087	161.7075
0.021	0.017087	194.0691
0.024	0.020087	226.4364
0.027	0.023087	258.8085
0.03	0.026087	291.1863

For estimated E as 1.1 Msi, slope is 10782 lb/in

	FEA 1.1	
time	Deflection (in)	Load (lbf)
0	0	0
0.1	0.0001	0.010783
0.2	0.0002	1.48096
0.3	0.0003	2.96327
0.4	0.0004	4.44581
0.5	0.0005	5.92858
0.6	0.0006	7.41159
0.7	0.0007	8.89484
0.8	0.0008	10.3783
0.9	0.0009	11.8621
1	0.001	13.346

Deflection (in)	offset	Load (lbf)	
0		0	
0.003		0.323487	Slope
0.003658	0	10	14825.33
0.006	0.002342	44.4288	
0.009	0.005342	88.8981	
0.012	0.008342	133.3743	
0.015	0.011342	177.8574	
0.018	0.014342	222.3477	
0.021	0.017342	266.8452	
0.024	0.020342	311.349	
0.027	0.023342	355.863	
0.03	0.026342	400.38	

For estimated E as 1.5 Msi, slope is 10782 lb/in

	FEA 1.5	
time	Deflection (in)	Load (lbf)
0	0	0
0.1	0.0001	0.014704
0.2	0.0002	2.01949
0.3	0.0003	4.04082

0.4	0.0004	6.06246	
0.5	0.0005	8.08443	
0.6	0.0006	10.1067	
0.7	0.0007	12.1293	
0.8	0.0008	14.1523	
0.9	0.0009	16.1755	
1	0.001	18.1991	

Deflection (in)	offset	Load (lbf)	
0		0	
0.003		0.441117	Slope
0.003477	0	10	20215.72
0.006	0.002523	60.5847	
0.009	0.005523	121.2246	
0.012	0.008523	181.8738	
0.015	0.011523	242.5329	
0.018	0.014523	303.201	
0.021	0.017523	363.879	
0.024	0.020523	424.569	
0.027	0.023523	485.265	
0.03	0.026523	545.973	

For estimated E as 1.54 Msi, slope is 10782 lb/in

	FEA 1.54	
time	Deflection (in)	Load (lbf)
0	0	0
0.1	0.0001	0.015096
0.2	0.0002	2.07334
0.3	0.0003	4.14857
0.4	0.0004	6.22413
0.5	0.0005	8.30001
0.6	0.0006	10.3762
0.7	0.0007	12.4528
0.8	0.0008	14.5297
0.9	0.0009	16.6069
1	0.001	18.6845

Deflection (in)	offset	Load (lbf)	
0		0	
0.003		0.45288	Slope
0.003464	-0.00045	10	20754.84
0.006	0.002087	62.2002	
0.009	0.005087	124.4571	
0.012	0.008087	186.7239	
0.015	0.011087	249.0003	

0.018	0.014087	311.286
0.021	0.017087	373.584
0.024	0.020087	435.891
0.027	0.023087	498.207
0.03	0.026087	560.535

APPENDIX E.

EXPERIMENTAL RAW DATA FOR LOAD VS DEFLECTION FOR Control-1(C1)

ASTM 2344 Short Beam Shear with specimen ID.msm		Test Method		
Glass		Sample I. D.		
C1		Specimen Number		
Extension (in)	Offset Extension	Load (lbf)	SBS (Psi)	E (msi)
-0.049		0	0	#DIV/0!
-0.049		0	0	#DIV/0!
-0.049		0	0	#DIV/0!
-0.049		0	0	#DIV/0!
-0.049		0	0	#DIV/0!
-0.049		0	0	#DIV/0!
-0.049		0	0	#DIV/0!
-0.049		0	0	#DIV/0!
-0.049		0	0	#DIV/0!
-0.049		0	0	#DIV/0!
-0.049		0	0	#DIV/0!
-0.049		0	0	#DIV/0!
-0.049		0	0	#DIV/0!
-0.049		0	0	#DIV/0!
-0.049		0	0	#DIV/0!
-0.049		0	0	#DIV/0!

-0.049		0	0	#DIV/0!
-0.049		0	0	#DIV/0!
-0.048		0	0	#DIV/0!
-0.048		0	0	#DIV/0!
-0.048		0	0	#DIV/0!
-0.048		0	0	#DIV/0!
-0.048		0	0	#DIV/0!
-0.048		0	0	#DIV/0!
-0.048		0	0	#DIV/0!
-0.048		0	0	#DIV/0!
-0.048		0	0	#DIV/0!
-0.048		0	0	#DIV/0!
-0.048		0	0	#DIV/0!
-0.048		0	0	#DIV/0!
-0.048		0	0	#DIV/0!
-0.047		0	0	#DIV/0!
-0.047		0	0	#DIV/0!
-0.047		0	0	#DIV/0!
-0.047		0	0	#DIV/0!
-0.047		0	0	#DIV/0!
-0.047		0	0	#DIV/0!
-0.047		0	0	#DIV/0!
-0.047		0	0	#DIV/0!
-0.047		0	0	#DIV/0!
-0.047		0	0	#DIV/0!
-0.047		0	0	#DIV/0!
-0.047		0	0	#DIV/0!
-0.046		0	0	#DIV/0!

-0.046		0	0	#DIV/0!
-0.046		0	0	#DIV/0!
-0.046		0	0	#DIV/0!
-0.046		0	0	#DIV/0!
-0.046		0	0	#DIV/0!
-0.046		0	0	#DIV/0!
-0.046		0	0	#DIV/0!
-0.046		0	0	#DIV/0!
-0.046		0	0	#DIV/0!
-0.046		0	0	#DIV/0!
-0.046		0	0	#DIV/0!
-0.045		0	0	#DIV/0!
-0.045		0	0	#DIV/0!
-0.045		0	0	#DIV/0!
-0.045		0	0	#DIV/0!
-0.045		0	0	#DIV/0!
-0.045		0	0	#DIV/0!
-0.045		0	0	#DIV/0!
-0.045		0	0	#DIV/0!
-0.045		0	0	#DIV/0!
-0.045		0	0	#DIV/0!
-0.045		0	0	#DIV/0!
-0.045		0	0	#DIV/0!
-0.044		0	0	#DIV/0!
-0.044		0	0	#DIV/0!
-0.044		0	0	#DIV/0!
-0.044		0	0	#DIV/0!

-0.044		0	0	#DIV/0!
-0.044		0	0	#DIV/0!
-0.044		0	0	#DIV/0!
-0.044		0	0	#DIV/0!
-0.044		0	0	#DIV/0!
-0.044		0	0	#DIV/0!
-0.044		0	0	#DIV/0!
-0.044		0	0	#DIV/0!
-0.043		0	0	#DIV/0!
-0.043		0	0	#DIV/0!
-0.043		0	0	#DIV/0!
-0.043		0	0	#DIV/0!
-0.043		0	0	#DIV/0!
-0.043		0	0	#DIV/0!
-0.043		0	0	#DIV/0!
-0.043		0	0	#DIV/0!
-0.043		0	0	#DIV/0!
-0.043		0	0	#DIV/0!
-0.043		0	0	#DIV/0!
-0.043		0	0	#DIV/0!
-0.043		0	0	#DIV/0!
-0.042		0	0	#DIV/0!
-0.042		0	0	#DIV/0!
-0.042		0	0	#DIV/0!
-0.042		0	0	#DIV/0!
-0.042		0	0	#DIV/0!
-0.042		0	0	#DIV/0!
-0.042		0	0	#DIV/0!

-0.042		0	0	#DIV/0!
-0.042		0	0	#DIV/0!
-0.042		0	0	#DIV/0!
-0.042		0	0	#DIV/0!
-0.042		0	0	#DIV/0!
-0.041		0	0	#DIV/0!
-0.041		0	0	#DIV/0!
-0.041		0	0	#DIV/0!
-0.041		0	0	#DIV/0!
-0.041		0	0	#DIV/0!
-0.041		0	0	#DIV/0!
-0.041		0	0	#DIV/0!
-0.041		0	0	#DIV/0!
-0.041		0	0	#DIV/0!
-0.041		0	0	#DIV/0!
-0.041		0	0	#DIV/0!
-0.041		0	0	#DIV/0!
-0.041		0	0	#DIV/0!
-0.04		0	0	#DIV/0!
-0.04		0	0	#DIV/0!
-0.04		0	0	#DIV/0!
-0.04		0	0	#DIV/0!
-0.04		0	0	#DIV/0!
-0.04		0	0	#DIV/0!
-0.04		0	0	#DIV/0!
-0.04		0	0	#DIV/0!
-0.04		0	0	#DIV/0!
-0.04		0	0	#DIV/0!

-0.04		0	0	#DIV/0!
-0.04		0	0	#DIV/0!
-0.04		0	0	#DIV/0!
-0.039		0	0	#DIV/0!
-0.039		0	0	#DIV/0!
-0.039		0	0	#DIV/0!
-0.039		0	0	#DIV/0!
-0.039		0	0	#DIV/0!
-0.039		0	0	#DIV/0!
-0.039		0	0	#DIV/0!
-0.039		0	0	#DIV/0!
-0.039		0	0	#DIV/0!
-0.039		0	0	#DIV/0!
-0.039		0	0	#DIV/0!
-0.039		0	0	#DIV/0!
-0.038		0	0	#DIV/0!
-0.038		0	0	#DIV/0!
-0.038		0	0	#DIV/0!
-0.038		0	0	#DIV/0!
-0.038		0	0	#DIV/0!
-0.038		0	0	#DIV/0!
-0.038		0	0	#DIV/0!
-0.038		0	0	#DIV/0!
-0.038		0	0	#DIV/0!
-0.038		0	0	#DIV/0!
-0.038		0	0	#DIV/0!
-0.038		0	0	#DIV/0!
-0.038		0	0	#DIV/0!

-0.037		0	0	#DIV/0!
-0.037		0	0	#DIV/0!
-0.037		0	0	#DIV/0!
-0.037		0	0	#DIV/0!
-0.037		0	0	#DIV/0!
-0.037		0	0	#DIV/0!
-0.037		0	0	#DIV/0!
-0.037		0	0	#DIV/0!
-0.037		0	0	#DIV/0!
-0.037		0	0	#DIV/0!
-0.037		0	0	#DIV/0!
-0.037		0	0	#DIV/0!
-0.037		0	0	#DIV/0!
-0.036		0	0	#DIV/0!
-0.036		0	0	#DIV/0!
-0.036		0	0	#DIV/0!
-0.036		0	0	#DIV/0!
-0.036		0	0	#DIV/0!
-0.036		0	0	#DIV/0!
-0.036		0	0	#DIV/0!
-0.036		0	0	#DIV/0!
-0.036		0	0	#DIV/0!
-0.036		0	0	#DIV/0!
-0.036		0	0	#DIV/0!
-0.036		0	0	#DIV/0!
-0.035		0	0	#DIV/0!
-0.035		0	0	#DIV/0!
-0.035		0	0	#DIV/0!

-0.035		0	0	#DIV/0!
-0.035		0	0	#DIV/0!
-0.035		0	0	#DIV/0!
-0.035		0	0	#DIV/0!
-0.035		0	0	#DIV/0!
-0.035		0	0	#DIV/0!
-0.035		0	0	#DIV/0!
-0.035		0	0	#DIV/0!
-0.035		0	0	#DIV/0!
-0.034		0	0	#DIV/0!
-0.034		0	0	#DIV/0!
-0.034		0	0	#DIV/0!
-0.034		0	0	#DIV/0!
-0.034		0	0	#DIV/0!
-0.034		0	0	#DIV/0!
-0.034		0	0	#DIV/0!
-0.034		0	0	#DIV/0!
-0.034		0	0	#DIV/0!
-0.034		0	0	#DIV/0!
-0.034		0	0	#DIV/0!
-0.034		0	0	#DIV/0!
-0.033		0	0	#DIV/0!
-0.033		0	0	#DIV/0!
-0.033		0	0	#DIV/0!
-0.033		0	0	#DIV/0!
-0.033		0	0	#DIV/0!
-0.033		0	0	#DIV/0!

-0.033		0	0	#DIV/0!
-0.033		0	0	#DIV/0!
-0.033		0	0	#DIV/0!
-0.033		0	0	#DIV/0!
-0.033		0	0	#DIV/0!
-0.033		0	0	#DIV/0!
-0.032		0	0	#DIV/0!
-0.032		0	0	#DIV/0!
-0.032		0	0	#DIV/0!
-0.032		0	0	#DIV/0!
-0.032		0	0	#DIV/0!
-0.032		0	0	#DIV/0!
-0.032		0	0	#DIV/0!
-0.032		0	0	#DIV/0!
-0.032		0	0	#DIV/0!
-0.032		0	0	#DIV/0!
-0.032		0	0	#DIV/0!
-0.032		0	0	#DIV/0!
-0.032		0	0	#DIV/0!
-0.031		0	0	#DIV/0!
-0.031		0	0	#DIV/0!
-0.031		0	0	#DIV/0!
-0.031		0	0	#DIV/0!
-0.031		0	0	#DIV/0!
-0.031		0	0	#DIV/0!
-0.031		0	0	#DIV/0!
-0.031		0	0	#DIV/0!
-0.031		0	0	#DIV/0!

-0.031		0	0	#DIV/0!
-0.031		0	0	#DIV/0!
-0.031		0	0	#DIV/0!
-0.03		0	0	#DIV/0!
-0.03		0	0	#DIV/0!
-0.03		0	0	#DIV/0!
-0.03		0	0	#DIV/0!
-0.03		0	0	#DIV/0!
-0.03		0	0	#DIV/0!
-0.03		0	0	#DIV/0!
-0.03		0	0	#DIV/0!
-0.03		0	0	#DIV/0!
-0.03		0	0	#DIV/0!
-0.03		0	0	#DIV/0!
-0.03		0	0	#DIV/0!
-0.03		0	0	#DIV/0!
-0.029		0	0	#DIV/0!
-0.029		0	0	#DIV/0!
-0.029		0	0	#DIV/0!
-0.029		0	0	#DIV/0!
-0.029		0	0	#DIV/0!
-0.029		0	0	#DIV/0!
-0.029		0	0	#DIV/0!
-0.029		0	0	#DIV/0!
-0.029		0	0	#DIV/0!
-0.029		0	0	#DIV/0!
-0.029		0	0	#DIV/0!
-0.029		0	0	#DIV/0!

-0.028		0	0	#DIV/0!
-0.028		0	0	#DIV/0!
-0.028		0	0	#DIV/0!
-0.028		0	0	#DIV/0!
-0.028		0	0	#DIV/0!
-0.028		0	0	#DIV/0!
-0.028		0	0	#DIV/0!
-0.028		0	0	#DIV/0!
-0.028		0	0	#DIV/0!
-0.028		0	0	#DIV/0!
-0.028		0	0	#DIV/0!
-0.028		0	0	#DIV/0!
-0.028		0	0	#DIV/0!
-0.027		0	0	#DIV/0!
-0.027		0	0	#DIV/0!
-0.027		0	0	#DIV/0!
-0.027		0	0	#DIV/0!
-0.027		0	0	#DIV/0!
-0.027		0	0	#DIV/0!
-0.027		0	0	#DIV/0!
-0.027		0	0	#DIV/0!
-0.027		0	0	#DIV/0!
-0.027		0	0	#DIV/0!
-0.027		0	0	#DIV/0!
-0.027		0	0	#DIV/0!
-0.026		0	0	#DIV/0!
-0.026		0	0	#DIV/0!
-0.026		0	0	#DIV/0!

-0.026		0	0	#DIV/0!
-0.026		0	0	#DIV/0!
-0.026		0	0	#DIV/0!
-0.026		0	0	#DIV/0!
-0.026		0	0	#DIV/0!
-0.026		0	0	#DIV/0!
-0.026		0	0	#DIV/0!
-0.026		0	0	#DIV/0!
-0.026		0	0	#DIV/0!
-0.025		0	0	#DIV/0!
-0.025		0	0	#DIV/0!
-0.025		0	0	#DIV/0!
-0.025		0	0	#DIV/0!
-0.025		0	0	#DIV/0!
-0.025		0	0	#DIV/0!
-0.025		0	0	#DIV/0!
-0.025		0	0	#DIV/0!
-0.025		0	0	#DIV/0!
-0.025		0	0	#DIV/0!
-0.025		0	0	#DIV/0!
-0.025		0	0	#DIV/0!
-0.024		0	0	#DIV/0!
-0.024		0	0	#DIV/0!
-0.024		0	0	#DIV/0!
-0.024		0	0	#DIV/0!
-0.024		0	0	#DIV/0!
-0.024		0	0	#DIV/0!

-0.024		0	0	#DIV/0!
-0.024		0	0	#DIV/0!
-0.024		0	0	#DIV/0!
-0.024		0	0	#DIV/0!
-0.024		0	0	#DIV/0!
-0.024		0	0	#DIV/0!
-0.023		0	0	#DIV/0!
-0.023		0	0	#DIV/0!
-0.023		0	0	#DIV/0!
-0.023		0	0	#DIV/0!
-0.023		0	0	#DIV/0!
-0.023		0	0	#DIV/0!
-0.023		0	0	#DIV/0!
-0.023		0	0	#DIV/0!
-0.023		0	0	#DIV/0!
-0.023		0	0	#DIV/0!
-0.023		0	0	#DIV/0!
-0.023		0	0	#DIV/0!
-0.023		0	0	#DIV/0!
-0.022		0	0	#DIV/0!
-0.022		0	0	#DIV/0!
-0.022		0	0	#DIV/0!
-0.022		0	0	#DIV/0!
-0.022		0	0	#DIV/0!
-0.022		0	0	#DIV/0!
-0.022		0	0	#DIV/0!
-0.022		0	0	#DIV/0!
-0.022		0	0	#DIV/0!

-0.022		0	0	#DIV/0!
-0.022		0	0	#DIV/0!
-0.022		0	0	#DIV/0!
-0.021		0	0	#DIV/0!
-0.021		0	0	#DIV/0!
-0.021		0	0	#DIV/0!
-0.021		0	0	#DIV/0!
-0.021		0	0	#DIV/0!
-0.021		0	0	#DIV/0!
-0.021		0	0	#DIV/0!
-0.021		0	0	#DIV/0!
-0.021		0	0	#DIV/0!
-0.021		0	0	#DIV/0!
-0.021		0	0	#DIV/0!
-0.021		0	0	#DIV/0!
-0.021		0	0	#DIV/0!
-0.02		0	0	#DIV/0!
-0.02		0	0	#DIV/0!
-0.02		0	0	#DIV/0!
-0.02		0	0	#DIV/0!
-0.02		0	0	#DIV/0!
-0.02		0	0	#DIV/0!
-0.02		0	0	#DIV/0!
-0.02		0	0	#DIV/0!
-0.02		0.1	2.362055933	#DIV/0!
-0.02		0.1	2.362055933	#DIV/0!
-0.02		0.2	4.724111867	#DIV/0!
-0.02		0.3	7.0861678	#DIV/0!

-0.019		0.4	9.448223734	#DIV/0!
-0.019		0.6	14.1723356	#DIV/0!
-0.019		0.8	18.89644747	#DIV/0!
-0.019		1.2	28.3446712	#DIV/0!
-0.019		1.6	37.79289494	#DIV/0!
-0.019		1.8	42.5170068	#DIV/0!
-0.019		2.2	51.96523054	#DIV/0!
-0.019		2.6	61.41345427	#DIV/0!
-0.019		2.9	68.49962207	#DIV/0!
-0.019		3.2	75.58578987	#DIV/0!
-0.019		3.5	82.67195767	#DIV/0!
-0.019		3.9	92.12018141	#DIV/0!
-0.018		4.1	96.84429327	#DIV/0!
-0.018		4.5	106.292517	#DIV/0!
-0.018		4.5	106.292517	#DIV/0!
-0.018		4.7	111.0166289	#DIV/0!
-0.018		4.9	115.7407407	#DIV/0!
-0.018		5	118.1027967	#DIV/0!
-0.018		5.2	122.8269085	#DIV/0!
-0.018		5.4	127.5510204	#DIV/0!
-0.018		5.6	132.2751323	#DIV/0!
-0.018		5.6	132.2751323	#DIV/0!
-0.018		5.6	132.2751323	#DIV/0!
-0.018		5.7	134.6371882	#DIV/0!
-0.017		5.7	134.6371882	#DIV/0!
-0.017		5.8	136.9992441	#DIV/0!
-0.017		5.7	134.6371882	#DIV/0!

-0.017		5.7	134.6371882	#DIV/0!
-0.017		5.8	136.9992441	#DIV/0!
-0.017		5.8	136.9992441	#DIV/0!
-0.017		5.8	136.9992441	#DIV/0!
-0.017		5.8	136.9992441	#DIV/0!
-0.017		5.8	136.9992441	#DIV/0!
-0.017		5.8	136.9992441	#DIV/0!
-0.017		5.8	136.9992441	#DIV/0!
-0.017		5.8	136.9992441	#DIV/0!
-0.016		5.8	136.9992441	#DIV/0!
-0.016		5.8	136.9992441	#DIV/0!
-0.016		5.8	136.9992441	#DIV/0!
-0.016		5.8	136.9992441	#DIV/0!
-0.016		5.8	136.9992441	#DIV/0!
-0.016		5.8	136.9992441	#DIV/0!
-0.016		5.8	136.9992441	#DIV/0!
-0.016		5.8	136.9992441	#DIV/0!
-0.016		5.8	136.9992441	#DIV/0!
-0.016		5.8	136.9992441	#DIV/0!
-0.016		5.8	136.9992441	#DIV/0!
-0.016		5.8	136.9992441	#DIV/0!
-0.015		5.7	134.6371882	#DIV/0!
-0.015		5.8	136.9992441	#DIV/0!
-0.015		5.8	136.9992441	#DIV/0!
-0.015		5.8	136.9992441	#DIV/0!
-0.015		5.8	136.9992441	#DIV/0!
-0.015		5.7	134.6371882	#DIV/0!

-0.015		5.7	134.6371882	#DIV/0!
-0.015		5.8	136.9992441	#DIV/0!
-0.015		5.8	136.9992441	#DIV/0!
-0.015		5.7	134.6371882	#DIV/0!
-0.015		5.7	134.6371882	#DIV/0!
-0.015		5.7	134.6371882	#DIV/0!
-0.014		5.7	134.6371882	#DIV/0!
-0.014		5.8	136.9992441	#DIV/0!
-0.014		5.7	134.6371882	#DIV/0!
-0.014		5.7	134.6371882	#DIV/0!
-0.014		5.8	136.9992441	#DIV/0!
-0.014		5.7	134.6371882	#DIV/0!
-0.014		5.7	134.6371882	#DIV/0!
-0.014		5.8	136.9992441	#DIV/0!
-0.014		5.8	136.9992441	#DIV/0!
-0.014		5.8	136.9992441	#DIV/0!
-0.014		5.8	136.9992441	#DIV/0!
-0.014		5.8	136.9992441	#DIV/0!
-0.014		5.8	136.9992441	#DIV/0!
-0.013		5.8	136.9992441	#DIV/0!
-0.013		5.7	134.6371882	#DIV/0!
-0.013		5.7	134.6371882	#DIV/0!
-0.013		5.8	136.9992441	#DIV/0!
-0.013		5.8	136.9992441	#DIV/0!
-0.013		5.8	136.9992441	#DIV/0!
-0.013		5.7	134.6371882	#DIV/0!
-0.013		5.8	136.9992441	#DIV/0!
-0.013		5.8	136.9992441	#DIV/0!

-0.013		5.8	136.9992441	#DIV/0!
-0.013		5.8	136.9992441	#DIV/0!
-0.013		5.7	134.6371882	#DIV/0!
-0.012		5.8	136.9992441	#DIV/0!
-0.012		5.8	136.9992441	#DIV/0!
-0.012		5.7	134.6371882	#DIV/0!
-0.012		5.7	134.6371882	#DIV/0!
-0.012		5.8	136.9992441	#DIV/0!
-0.012		5.8	136.9992441	#DIV/0!
-0.012		5.8	136.9992441	#DIV/0!
-0.012		5.7	134.6371882	#DIV/0!
-0.012		5.7	134.6371882	#DIV/0!
-0.012		5.8	136.9992441	#DIV/0!
-0.012		5.8	136.9992441	#DIV/0!
-0.012		5.8	136.9992441	#DIV/0!
-0.011		5.7	134.6371882	#DIV/0!
-0.011		5.8	136.9992441	#DIV/0!
-0.011		5.7	134.6371882	#DIV/0!
-0.011		5.8	136.9992441	#DIV/0!
-0.011		5.7	134.6371882	#DIV/0!
-0.011		5.7	134.6371882	#DIV/0!
-0.011		5.7	134.6371882	#DIV/0!
-0.011		5.8	136.9992441	#DIV/0!
-0.011		5.8	136.9992441	#DIV/0!
-0.011		5.7	134.6371882	#DIV/0!
-0.011		5.7	134.6371882	#DIV/0!
-0.011		5.8	136.9992441	#DIV/0!

-0.01		5.8	136.9992441	#DIV/0!
-0.01		5.7	134.6371882	#DIV/0!
-0.01		5.8	136.9992441	#DIV/0!
-0.01		5.8	136.9992441	#DIV/0!
-0.01		5.7	134.6371882	#DIV/0!
-0.01		5.7	134.6371882	#DIV/0!
-0.01		5.8	136.9992441	#DIV/0!
-0.01		5.8	136.9992441	#DIV/0!
-0.01		5.8	136.9992441	#DIV/0!
-0.01		5.8	136.9992441	#DIV/0!
-0.01		5.8	136.9992441	#DIV/0!
-0.01		5.8	136.9992441	#DIV/0!
-0.01		5.8	136.9992441	#DIV/0!
-0.009		5.8	136.9992441	#DIV/0!
-0.009		5.8	136.9992441	#DIV/0!
-0.009		5.8	136.9992441	#DIV/0!
-0.009		5.9	139.3613001	#DIV/0!
-0.009		6	141.723356	#DIV/0!
-0.009		5.9	139.3613001	#DIV/0!
-0.009		6	141.723356	#DIV/0!
-0.009		5.9	139.3613001	#DIV/0!
-0.009		6	141.723356	#DIV/0!
-0.009		6	141.723356	#DIV/0!
-0.009		6	141.723356	#DIV/0!
-0.008		6	141.723356	#DIV/0!
-0.008		6	141.723356	#DIV/0!
-0.008		6	141.723356	#DIV/0!

-0.008		6	141.723356	#DIV/0!
-0.008		6	141.723356	#DIV/0!
-0.008		6	141.723356	#DIV/0!
-0.008		6	141.723356	#DIV/0!
-0.008		6	141.723356	#DIV/0!
-0.008		6	141.723356	#DIV/0!
-0.008		6	141.723356	#DIV/0!
-0.008		6	141.723356	#DIV/0!
-0.008		6	141.723356	#DIV/0!
-0.007		6.1	144.0854119	#DIV/0!
-0.007		6.1	144.0854119	#DIV/0!
-0.007		6.1	144.0854119	#DIV/0!
-0.007		6.1	144.0854119	#DIV/0!
-0.007		6.1	144.0854119	#DIV/0!
-0.007		6.1	144.0854119	#DIV/0!
-0.007		6.1	144.0854119	#DIV/0!
-0.007		6.1	144.0854119	#DIV/0!
-0.007		6.1	144.0854119	#DIV/0!
-0.007		6.2	146.4474679	#DIV/0!
-0.007		6.2	146.4474679	#DIV/0!
-0.007		6.1	144.0854119	#DIV/0!
-0.007		6.1	144.0854119	#DIV/0!
-0.006		6.1	144.0854119	#DIV/0!
-0.006		6.1	144.0854119	#DIV/0!
-0.006		6.1	144.0854119	#DIV/0!
-0.006		6.1	144.0854119	#DIV/0!
-0.006		6.1	144.0854119	#DIV/0!

-0.006		6.1	144.0854119	#DIV/0!
-0.006		6.1	144.0854119	#DIV/0!
-0.006		6.1	144.0854119	#DIV/0!
-0.006		6.2	146.4474679	#DIV/0!
-0.006		6.2	146.4474679	#DIV/0!
-0.006		6.1	144.0854119	#DIV/0!
-0.005		6.2	146.4474679	#DIV/0!
-0.005		6.1	144.0854119	#DIV/0!
-0.005		6.1	144.0854119	#DIV/0!
-0.005		6.2	146.4474679	#DIV/0!
-0.005		6.1	144.0854119	#DIV/0!
-0.005		6.1	144.0854119	#DIV/0!
-0.005		6.2	146.4474679	#DIV/0!
-0.005		6.1	144.0854119	#DIV/0!
-0.005		6.1	144.0854119	#DIV/0!
-0.005		6.2	146.4474679	#DIV/0!
-0.005		6.1	144.0854119	#DIV/0!
-0.005		6.1	144.0854119	#DIV/0!
-0.004		6.1	144.0854119	#DIV/0!
-0.004		6.1	144.0854119	#DIV/0!
-0.004		6.1	144.0854119	#DIV/0!
-0.004		6.1	144.0854119	#DIV/0!
-0.004		6.1	144.0854119	#DIV/0!
-0.004		6.1	144.0854119	#DIV/0!
-0.004		6.1	144.0854119	#DIV/0!
-0.004		6.1	144.0854119	#DIV/0!
-0.004		6.1	144.0854119	#DIV/0!

-0.004		6.1	144.0854119	#DIV/0!
-0.004		6.1	144.0854119	#DIV/0!
-0.004		6.2	146.4474679	#DIV/0!
-0.003		6.2	146.4474679	#DIV/0!
-0.003		6.2	146.4474679	#DIV/0!
-0.003		6.2	146.4474679	#DIV/0!
-0.003		6.1	144.0854119	#DIV/0!
-0.003		6.2	146.4474679	#DIV/0!
-0.003		6.1	144.0854119	#DIV/0!
-0.003		6.2	146.4474679	#DIV/0!
-0.003		6.1	144.0854119	#DIV/0!
-0.003		6.2	146.4474679	#DIV/0!
-0.003		6.2	146.4474679	#DIV/0!
-0.003		6.1	144.0854119	#DIV/0!
-0.003		6.2	146.4474679	#DIV/0!
-0.002		6.2	146.4474679	#DIV/0!
-0.002		6.1	144.0854119	#DIV/0!
-0.002		6.1	144.0854119	#DIV/0!
-0.002		6.6	155.8956916	#DIV/0!
-0.002		7.3	172.4300831	#DIV/0!
-0.002		8.3	196.0506425	#DIV/0!
-0.002		9.3	219.6712018	#DIV/0!
-0.002	0	10.4	245.6538171	#DIV/0!
-0.002	0	11.8	278.7226002	#DIV/0!
-0.002	0	12.6	297.6190476	#DIV/0!
-0.002	0	13.4	316.5154951	#DIV/0!
-0.002	0	14.2	335.4119426	#DIV/0!

-0.001	0.001	15.1	356.670446	0.954940711
-0.001	0.001	16.1	380.2910053	1.018181818
-0.001	0.001	17.2	406.2736206	1.087747036
-0.001	0.001	18.3	432.2562358	1.157312253
-0.001	0.001	19.5	460.600907	1.233201581
-0.001	0.001	20.6	486.5835223	1.302766798
-0.001	0.001	21.6	510.2040816	1.366007905
-0.001	0.001	22.6	533.824641	1.429249012
-0.001	0.001	23.6	557.4452003	1.492490119
-0.001	0.001	24.7	583.4278156	1.562055336
-0.001	0.001	25.9	611.7724868	1.637944664
-0.001	0.001	27.3	644.8412698	1.726482213
0	0.002	28.5	673.185941	0.901185771
0	0.002	30.4	718.0650038	0.961264822
0	0.002	31.1	734.5993953	0.983399209
0	0.002	32.2	760.5820106	1.018181818
0	0.002	33.4	788.9266818	1.056126482
0	0.002	34.5	814.9092971	1.090909091
0	0.002	35.6	840.8919123	1.1256917
0	0.002	36.9	871.5986395	1.166798419
0	0.002	38.4	907.0294785	1.214229249
0	0.002	40	944.8223734	1.264822134
0	0.002	42	992.0634921	1.328063241
0	0.002	43	1015.684051	1.359683794
0.001	0.003	44.2	1044.028723	0.931752306
0.001	0.003	45.4	1072.373394	0.957048748
0.001	0.003	46.7	1103.080121	0.984453228

0.001	0.003	48.1	1136.148904	1.013965744
0.001	0.003	49.7	1173.941799	1.047694335
0.001	0.003	51.3	1211.734694	1.081422925
0.001	0.003	53.1	1254.251701	1.119367589
0.001	0.003	54.5	1287.320484	1.148880105
0.001	0.003	55.9	1320.389267	1.178392622
0.001	0.003	57.3	1353.45805	1.207905138
0.001	0.003	58.7	1386.526833	1.237417655
0.001	0.003	60.1	1419.595616	1.266930171
0.002	0.004	61.8	1459.750567	0.977075099
0.002	0.004	63.5	1499.905518	1.003952569
0.002	0.004	65.3	1542.422525	1.032411067
0.002	0.004	67.8	1601.473923	1.071936759
0.002	0.004	68.8	1625.094482	1.087747036
0.002	0.004	70.2	1658.163265	1.109881423
0.002	0.004	71.9	1698.318216	1.136758893
0.002	0.004	73.4	1733.749055	1.160474308
0.002	0.004	75	1771.54195	1.185770751
0.002	0.004	76.7	1811.696901	1.212648221
0.002	0.004	78.8	1861.300076	1.245849802
0.002	0.004	80.8	1908.541194	1.277470356
0.003	0.005	83.2	1965.230537	1.052332016
0.003	0.005	84.8	2003.023432	1.07256917
0.003	0.005	86.2	2036.092215	1.09027668
0.003	0.005	87.8	2073.88511	1.110513834
0.003	0.005	89.4	2111.678005	1.130750988
0.003	0.005	91.3	2156.557067	1.154782609

0.003	0.005	93.4	2206.160242	1.181343874
0.003	0.005	95.6	2258.125472	1.20916996
0.003	0.005	98.1	2317.176871	1.240790514
0.003	0.005	99.6	2352.60771	1.259762846
0.003	0.005	101.3	2392.762661	1.281264822
0.003	0.005	103.2	2437.641723	1.305296443
0.004	0.006	104.9	2477.796674	1.105665349
0.004	0.006	106.7	2520.313681	1.124637681
0.004	0.006	108.7	2567.5548	1.14571805
0.004	0.006	111	2621.882086	1.169960474
0.004	0.006	113.1	2671.485261	1.192094862
0.004	0.006	116.3	2747.071051	1.225823452
0.004	0.006	117.4	2773.053666	1.237417655
0.004	0.006	119	2810.846561	1.25428195
0.004	0.006	120.9	2855.725624	1.2743083
0.004	0.006	122.7	2898.24263	1.293280632
0.004	0.006	124.6	2943.121693	1.313306983
0.004	0.006	126.8	2995.086924	1.336495389
0.005	0.007	129.2	3051.776266	1.167250141
0.005	0.007	131.6	3108.465608	1.188932806
0.005	0.007	134.1	3167.517007	1.211518916
0.005	0.007	135.9	3210.034014	1.227780915
0.005	0.007	137.6	3250.188964	1.243139469
0.005	0.007	139.4	3292.705971	1.259401468
0.005	0.007	141.2	3335.222978	1.275663467
0.005	0.007	143.3	3384.826153	1.294635799
0.005	0.007	145.6	3439.153439	1.31541502

0.005	0.007	147.8	3491.11867	1.335290796
0.005	0.007	150.5	3554.89418	1.359683794
0.005	0.007	152.1	3592.687075	1.374138905
0.006	0.008	154	3637.566138	1.217391304
0.006	0.008	156	3684.807256	1.233201581
0.006	0.008	158	3732.048375	1.249011858
0.006	0.008	159.9	3776.927438	1.264031621
0.006	0.008	162.1	3828.892668	1.281422925
0.006	0.008	164.4	3883.219955	1.299604743
0.006	0.008	166.7	3937.547241	1.317786561
0.006	0.008	170.1	4017.857143	1.344664032
0.006	0.008	171.2	4043.839758	1.353359684
0.006	0.008	172.8	4081.632653	1.366007905
0.006	0.008	174.8	4128.873772	1.381818182
0.006	0.008	176.7	4173.752834	1.396837945
0.007	0.009	178.5	4216.269841	1.25428195
0.007	0.009	180.8	4270.597128	1.270443566
0.007	0.009	183.3	4329.648526	1.28801054
0.007	0.009	185.8	4388.699924	1.305577514
0.007	0.009	188.5	4452.475435	1.324549846
0.007	0.009	190.3	4494.992441	1.337198068
0.007	0.009	192.1	4537.509448	1.349846289
0.007	0.009	193.8	4577.664399	1.361791831
0.007	0.009	195.7	4622.543462	1.375142732
0.007	0.009	197.8	4672.146636	1.38989899
0.007	0.009	200.3	4731.198035	1.407465964
0.007	0.009	202.6	4785.525321	1.42362758

0.008	0.01	205.4	4851.662887	1.298972332
0.008	0.01	206.7	4882.369615	1.307193676
0.008	0.01	208.5	4924.886621	1.318577075
0.008	0.01	210.5	4972.12774	1.331225296
0.008	0.01	212.4	5017.006803	1.343241107
0.008	0.01	214.3	5061.885865	1.355256917
0.008	0.01	216.6	5116.213152	1.369802372
0.008	0.01	219	5172.902494	1.384980237
0.008	0.01	221.3	5227.229781	1.399525692
0.008	0.01	224.7	5307.539683	1.421027668
0.008	0.01	225.8	5333.522298	1.42798419
0.008	0.01	227.4	5371.315193	1.438102767
0.009	0.011	229.4	5418.556311	1.318864535
0.009	0.011	231.3	5463.435374	1.329787999
0.009	0.011	233.2	5508.314437	1.340711462
0.009	0.011	235.3	5557.917611	1.352784765
0.009	0.011	237.8	5616.96901	1.367157743
0.009	0.011	240.3	5676.020408	1.381530722
0.009	0.011	242.8	5735.071807	1.395903701
0.009	0.011	244.6	5777.588813	1.406252246
0.009	0.011	246.3	5817.743764	1.416025871
0.009	0.011	248	5857.898715	1.425799497
0.009	0.011	249.8	5900.415722	1.436148042
0.009	0.011	251.9	5950.018896	1.448221344
0.01	0.012	254.3	6006.708239	1.340184453
0.01	0.012	256.6	6061.035525	1.352305665
0.01	0.012	259.6	6131.897203	1.368115942

0.01	0.012	260.8	6160.241875	1.374440053
0.01	0.012	262.5	6200.396825	1.383399209
0.01	0.012	264.4	6245.275888	1.393412385
0.01	0.012	266.2	6287.792895	1.402898551
0.01	0.012	268	6330.309902	1.412384717
0.01	0.012	270.2	6382.275132	1.42397892
0.01	0.012	272.5	6436.602419	1.436100132
0.01	0.012	274.8	6490.929705	1.448221344
0.01	0.012	278.4	6575.963719	1.467193676
0.011	0.013	279.3	6597.222222	1.358710854
0.011	0.013	280.7	6630.291005	1.365521435
0.011	0.013	282.6	6675.170068	1.374764366
0.011	0.013	284.3	6715.325019	1.383034357
0.011	0.013	286	6755.47997	1.391304348
0.011	0.013	288.2	6807.4452	1.402006689
0.011	0.013	290.5	6861.772487	1.4131955
0.011	0.013	293	6920.823885	1.425357251
0.011	0.013	295.5	6979.875283	1.437519003
0.011	0.013	297.2	7020.030234	1.445788994
0.011	0.013	298.7	7055.461073	1.453086044
0.011	0.013	300.3	7093.253968	1.460869565
0.012	0.014	302	7133.408919	1.364201016
0.012	0.014	304	7180.650038	1.37323546
0.012	0.014	306.2	7232.615268	1.383173348
0.012	0.014	308.3	7282.218443	1.392659514
0.012	0.014	311.4	7355.442177	1.406662902
0.012	0.014	312.3	7376.70068	1.410728402

0.012	0.014	313.8	7412.131519	1.417504235
0.012	0.014	315.6	7454.648526	1.425635234
0.012	0.014	317.4	7497.165533	1.433766234
0.012	0.014	319.1	7537.320484	1.441445511
0.012	0.014	321	7582.199546	1.450028233
0.012	0.014	323.1	7631.802721	1.459514399
0.013	0.015	325.3	7683.767952	1.371488801
0.013	0.015	328.5	7759.353741	1.384980237
0.013	0.015	329.2	7775.888133	1.387931489
0.013	0.015	330.6	7808.956916	1.393833992
0.013	0.015	332.2	7846.749811	1.40057971
0.013	0.015	333.8	7884.542706	1.407325428
0.013	0.015	335.3	7919.973545	1.413649539
0.013	0.015	337.3	7967.214664	1.422081686
0.013	0.015	339.6	8021.54195	1.431778656
0.013	0.015	341.8	8073.507181	1.441054018
0.013	0.015	344.2	8130.196523	1.451172596
0.013	0.015	345.6	8163.265306	1.457075099
0.014	0.016	347	8196.334089	1.371541502
0.014	0.016	348.3	8227.040816	1.376679842
0.014	0.016	349.7	8260.109599	1.382213439
0.014	0.016	351.7	8307.350718	1.390118577
0.014	0.016	353.8	8356.953893	1.398418972
0.014	0.016	355.7	8401.832955	1.405928854
0.014	0.016	358.7	8472.694633	1.417786561
0.014	0.016	359.1	8482.142857	1.419367589
0.014	0.016	360.2	8508.125472	1.423715415

0.014	0.016	361.7	8543.556311	1.429644269
0.014	0.016	363.1	8576.625094	1.435177866
0.014	0.016	364.7	8614.417989	1.441501976
0.014	0.016	366.5	8656.934996	1.448616601
0.015	0.017	368.3	8699.452003	1.370099977
0.015	0.017	370.1	8741.96901	1.376796094
0.015	0.017	373.1	8812.830688	1.387956289
0.015	0.017	373.6	8824.640967	1.389816322
0.015	0.017	374.7	8850.623583	1.393908393
0.015	0.017	376	8881.33031	1.398744478
0.015	0.017	377.3	8912.037037	1.403580563
0.015	0.017	378.6	8942.743764	1.408416647
0.015	0.017	380.3	8982.898715	1.414740758
0.015	0.017	382.3	9030.139834	1.422180888
0.015	0.017	384.2	9075.018896	1.429249012
0.016	0.018	385.6	9108.08768	1.354765042
0.016	0.018	386.6	9131.708239	1.358278437
0.016	0.018	387.5	9152.966742	1.361440492
0.016	0.018	388.3	9171.86319	1.364251208
0.016	0.018	389.2	9193.121693	1.367413263
0.016	0.018	390.5	9223.82842	1.371980676
0.016	0.018	391.6	9249.811036	1.375845411
0.016	0.018	392.9	9280.517763	1.380412824
0.016	0.018	395.4	9339.569161	1.389196311
0.016	0.018	395.3	9337.207105	1.388844971
0.016	0.018	395.8	9349.017385	1.390601669
0.016	0.018	396.8	9372.637944	1.394115064

0.016	0.018	397.8	9396.258503	1.397628458
0.017	0.019	398.7	9417.517007	1.327064697
0.017	0.019	400.1	9450.58579	1.331724568
0.017	0.019	401.4	9481.292517	1.336051591
0.017	0.019	402.8	9514.3613	1.340711462
0.017	0.019	405.2	9571.050642	1.348699813
0.017	0.019	405	9566.326531	1.348034117
0.017	0.019	405.3	9573.412698	1.349032661
0.017	0.019	406	9589.94709	1.351362596
0.017	0.019	406.4	9599.395314	1.352693988
0.017	0.019	406.8	9608.843537	1.35402538
0.017	0.019	407.6	9627.739985	1.356688163
0.017	0.019	408.3	9644.274376	1.359018099
0.018	0.02	408.3	9644.274376	1.291067194
0.018	0.02	177.9	4202.097506	0.562529644